AD-A035 928 NAVAL RESEARCH LAB WASHINGTON D C F/G 11/4
HIGH PERFORMANCE COMPOSITES AND ADHESIVES FOR V/STOL AIRCRAFT.(U)
DEC 76 W D BASCOM, L B LOCKHART

UNCLASSIFIED NRL-MR-3433 NL

1 OF 2
AD
AD35928

NRL Memorandum Report 3433

# High Performance Composites and Adhesives for V/STOL Aircraft

## First Annual Report

WILLARD D. BASCOM AND LUTHER B. LOCKHART, JR.
Editors

*Polymeric Materials Branch*
*Chemistry Division*

December 1976



NAVAL RESEARCH LABORATORY
Washington, D.C.

SECURITY CLASSIFICATION OF THIS PAGE (When Data Entered)

## REPORT DOCUMENTATION PAGE

READ INSTRUCTIONS BEFORE COMPLETING FORM

| | |
|---|---|
| 1. REPORT NUMBER<br>NRL ~~Memorandum Report~~ -MR- 3433 | 2. GOVT ACCESSION NO. |
| 3. RECIPIENT'S CATALOG NUMBER<br>Rept. no. 1 (Annual), |
| 4. TITLE (and Subtitle)<br>HIGH PERFORMANCE COMPOSITES AND ADHESIVES FOR V/STOL AIRCRAFT – FIRST ANNUAL REPORT | 5. TYPE OF REPORT & PERIOD COVERED<br>~~Progress report~~<br>1 July 1975 – 1 September 1976 |
| | 6. PERFORMING ORG. REPORT NUMBER |
| 7. AUTHOR(s)<br>Willard D. Bascom and Luther B. Lockhart, Jr., Editors | 8. CONTRACT OR GRANT NUMBER(s) |
| 9. PERFORMING ORGANIZATION NAME AND ADDRESS<br>Naval Research Laboratory<br>Washington, D.C. 20375 | 10. PROGRAM ELEMENT, PROJECT, TASK AREA & WORK UNIT NUMBERS<br>NRL Problem C04-10<br>PE62761 N; F54593201 |
| 11. CONTROLLING OFFICE NAME AND ADDRESS<br>Naval Air Systems Command<br>Washington, D.C. 20361 | 12. REPORT DATE<br>December 1976<br>13. NUMBER OF PAGES<br>127 (128 p.) |
| 14. MONITORING AGENCY NAME & ADDRESS (if different from Controlling Office)<br>Naval Air Development Center<br>Warminster, Pennsylvania 18974 | 15. SECURITY CLASS. (of this report)<br>UNCLASSIFIED<br>15a. DECLASSIFICATION/DOWNGRADING SCHEDULE |
| 16. DISTRIBUTION STATEMENT (of this Report)<br>Approved for public release; distribution unlimited. | (16) F54593<br>(17) WF54593201 |
| 17. DISTRIBUTION STATEMENT (of the abstract entered in Block 20, if different from Report) | |
| 18. SUPPLEMENTARY NOTES | |

19. KEY WORDS (Continue on reverse side if necessary and identify by block number)

| | |
|---|---|
| V/STOL aircraft | Fracture |
| Composites | Polymer characterization |
| Adhesives | Design optimization |
| Polymer synthesis | Radiation curing |

20. ABSTRACT (Continue on reverse side if necessary and identify by block number)

An interdisciplinary program has been undertaken to address the composite and adhesive materials requirements of V/STOL aircraft. The primary tasks are to develop and characterize high modulus, high toughness resins with use temperatures of 350°F to 450°F or higher, to develop fabrication technology for newly developed resin matrices for graphite-fiber reinforced composites, to develop composite failure criteria for design optimization and to establish appropriate quality control parameters. This report is the first annual review of the program, covering the period 1 July 1975 to 1 September 1976. The principal accomplishments to date have been to demonstrate (a) the

(Continues) → next page

DD FORM 1 JAN 73 1473 EDITION OF 1 NOV 65 IS OBSOLETE
S/N 0102-014-6601



SECURITY CLASSIFICATION OF THIS PAGE (When Data Entered)

251 950

6 pg

20. Abstract (Continued)

variation in mechanical properties obtainable by the molecular tailoring of polyphthalocyanine resins, (b) the effectiveness of NMR spectroscopy for chemical characterization of resins of complex composition, (c) the viability of resin cure using ionizing radiation, and (d) the development of a unique approach to determining failure criteria for flaw growth in resin matrix composites.

## CONTENTS



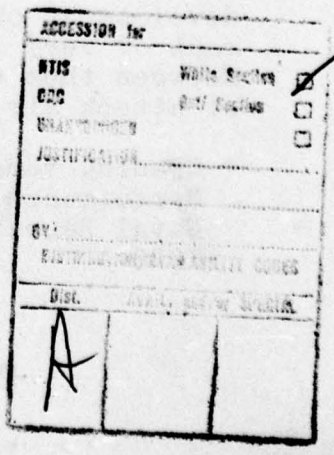

# PREFACE*

Alan Berman
Director of Research
Naval Research Laboratory

As Director of Research at NRL I seem to spend a great deal of my time either welcoming people to symposia or attending studies relative to the future of the Navy. The U. S. Navy seems to be going through an identity crisis in the attempt to discover how the future Navy should be configured. I have recently come back from a study which was given some guide lines which went roughly as follows:

Given the ensemble of military and political events on a worldwide basis which might involve the Navy during the next twenty-five years, and given the ensemble of technological advances which might take place in the next twenty-five years, how should we configure the Navy for the year 2000? Questions of this sort are probably unanswerable. When one attempts to resolve them, two overwhelming factors inevitably come out. One is that there is no way in which a future Navy can survive without performing all of the functions that are now subsumed under the title of Tactical Air. Currently, Tactical Airpower is provided to the Navy largely by carrier-based aircraft. On the other hand, all studies indicate that there is an ever growing problem with aircraft carriers in the future. Neglecting questions of possible vulnerability, carriers, their aircraft and accompanying support ships are extremely expensive. A carrier and its auxiliary support costs about 4 billion dollars. For the United States to have as many as 12 active carrier groups will cost 50 billion dollars.

It is clear that the Nation cannot afford many additional carrier task groups and even if carriers could be protected from hostile action other approaches must be discovered. There is a going perception that two alternatives exist to perform the functions currently assigned to carrier-based tactical aircraft. One is the development of V/STOL aircraft. The other is the development of very long endurance - long range aircraft. Between them they could in principle perform the functions of attack air, ASW, AEW, Electronic Support, etc.

* Opening remarks at the First Annual Review on High Performance Composites and Adhesives for V/STOL Aircraft, Naval Research Laboratory, Washington, D. C., September 8, 1976.

Both V/STOL and long range aircraft suffer from the fact that they are weight-limited systems. The endurance of an aircraft is typically a function of just three things: the lift-drag ratio, the thrust of the engines and the logarithm of the ratio of the take-off weight and the landing weight. The lighter one can make the empty airframe of an aircraft, the better the performance will be. Indeed, as one reduces the weight of an aircraft, its range or its endurance increases exponentially. We at NRL believe that a major opportunity exists to affect the future of the U. S. Navy. We recognize that there is a major need for weight reduction in the structural components of V/STOL aircraft to compensate for the increased weight of the propulsion system. The severe limitations in payload and range resulting from the high power demands of the V/STOL can be restored by a 30% reduction in V/STOL structural weight.

The replacement of metal structures with fiber-reinforced composites and the use of adhesive bonding techniques can, in principle, achieve the necessary weight savings. Unfortunately, present day composites and adhesives, which have a 250-300$^{o}$F maximum service temperature limit, are inadequate for the underbody of the V/STOL, which may experience transient skin temperatures in the 400-600$^{o}$F range from heat reflected during take-off and landing. In addition to the service temperature ceiling, other major problem areas of high performance polymers which require attention are their brittleness, their behavior in the presence of moisture, and their engineering reliability.

The purpose of our program is to carry to the point of production readiness one or more high-strength adhesive and graphite-fiber reinforced composite systems with a temperature capability in excess of 450$^{o}$F for V/STOL applications.

Our work will involve the selection and pilot-plant synthesis of commercial or in-house resin systems which offer promise of meeting the V/STOL temperature requirements. We will undertake composition analysis, adhesive formulation and testing, and graphite-reinforced composites fabrication and testing. In addition, we want to develop characterization procedures that are suitable for procurement and for the quality control of composite and adhesive materials in production. We want to establish failure criteria for these materials using an automated (computer) process. Finally, we hope to incorporate all

data in an automated closed-loop system for both materials and structural design optimization.

Hopefully, the operation of the process will be demonstrated by the design and construction of one or more simple V/STOL structural elements.

The effort that faces us must clearly be a community effort. It will involve major industrial participation, it will involve personnel from many in-house laboratories, it will involve aircraft structure people, and it will involve chemists, chemical engineers and aerodynamicists. I believe that it is an interesting, challenging program. If we are successful, this program will have a very high payoff for the Navy. I am sure you will find today's presentations interesting and provocative.

I note on the cover of your program that this meeting is entitled "The First Annual Review on High Performance Composites and Adhesives for V/STOL Aircraft". Being the first annual meeting provokes an image of a second annual, a third annual and a fourth annual meeting, and so on into the distant future. I have an image of all of you growing old together and developing an adhesives and composites "marching and chowder society". I really hope that you won't do that. I hope that by the time the third or fourth annual review comes around, the problems will be solved. Indeed the problems are much too important for you to let them go unresolved for more than a few more years. Good luck!

# HIGH PERFORMANCE COMPOSITES AND ADHESIVES FOR V/STOL AIRCRAFT

## First Annual Report

### INTRODUCTION

This Nation's limited capacity to deploy large aircraft carriers and their increasing vulnerability to enemy countermeasures (sea/sea and air/sea ballistic missiles and torpedoes) suggests that the future Navy must rely on a larger fleet of smaller, less costly carriers or other ships capable of deploying combat aircraft. The ability to do this effectively depends on the development of V/STOL aircraft having the combat effectiveness, range and payload of conventional carrier aircraft.

Today's military and civilian aircraft are making use of fiber-reinforced composite materials as a substitute for metals both because of the weight savings and the cost effectiveness of these new structural materials. This weight savings is even more critical to the successful development and deployment of V/STOL aircraft to compensate for the larger and heavier turbine engine required.

The program described in this report is designed to provide the performance and design data on graphite fiber-reinforced composite materials and on improved adhesives needed for their optimum use as structural materials for Navy V/STOL aircraft. Basically, the requirements are for materials that will operate in a higher temperature regime than state-of-the-art composites and will resist degradation by the marine environment.

An integrated approach is used in this program to bring into play the key elements of materials properties, fabricability and processability, quality control and design optimization. Interaction between these elements provides feedback for resin modifications leading to improved materials for adhesives and as the matrix for fiber-reinforced composites.

The major program tasks and their responsibilities are:

Resin Synthesis - Make chemical modifications to phthalocyanine resins to provide optimum thermomechanical properties; develop commercial source of promising materials.

Thermomechanical Characterization - Evaluate behavior of commercial and experimental resins under mechanical and thermal stress; provide feedback on structure/property relationships.

Note: Manuscript submitted December 10, 1976.

Chemical Characterization - Develop techniques for analysis of resin systems for purposes of identification and quality control, and evaluation of cure state.

Radiation Curing of Resins - Evaluate potential of electron-beam curing of selected resin systems to provide strain-free adhesive joints.

Composites Fabrication - Develop procedures for obtaining reproducible, low void composites for design optimization studies.

Design Optimization - Develop failure criteria for crack propagation in composites; demonstrate validity of criteria in predicting defect growth in a typical structural subcomponent; incorporate data in an automated closed loop system for optimized design of the component.

The initial portion of this program has been carried out primarily in-house. However, the program is entering the stage where outside, commercial enterprises need to be involved, namely in scaled-up syntheses of resins for composites and adhesives, in manufacture of graphite fiber or fabric prepreg materials using the new resin systems, and in developing fabrication technology. It is planned that at the end of this program the necessary technology transfer to industry will have taken place so that resin production, prepreg manufacture and composites fabrication capabilities will be available from commercial sources.

## SUMMARY

This report covers the progress and accomplishments of the major tasks of this Program from July 1975 through September 1976. The essential results and plans are outlined in this section with separate, detailed accounts given in the individual Task Reports.

### Resin Synthesis

A number of resins have been synthesized which can be cross-linked through the reaction of aromatic orthodinitrile groups to produce polymers containing the thermally stable phthalocyanine group. The modulus, toughness and Tg of the polymers can be controlled through structural modification of the basic resin system. The polymer based on the C-10 diamide resin has mechanical properties equivalent to conventional epoxies and comparable fabricability, but with much greater thermal stability and higher Tg. A commercial source for these resins has been developed.

Current work is being directed toward the synthesis of resins which will provide the optimum in mechanical performance without sacrificing the ease of processability and the resistance to degradation by heat or moisture shown by the C-10 phthalocyanine material.

### Thermomechanical Characterization

Several polyphthalocyanine resins have been evaluated for modulus and fracture energy and it has been shown that the properties of these resins are capable of three-fold variation by deliberate changes in molecular structure. However, an increase in one property usually occurs at some sacrifice in the other. Tests of commercial resins indicate that all have similar moduli and toughness despite major differences in chemical structure. Thermal soak tests (up to 480 hrs at 288°C) of the $C_{10}$-polyphthalocyanine and Hexcel F-178 produced considerable advancement of the resin cure accompanied by increased modulus and qualitative evidence of loss in fracture toughness.

An exploratory study of the effect of a low modulus, elastomeric interlayer on graphite fibers to enhance composite toughness indicates that the effects are too marginal to permit judgement to be made on the viability of the concept.

Measurements of the modulus and fracture toughness of a variety of commercial and in-house resins will be continued with in-depth evaluation of the more promising candidates. This effort will include the effect of absorbed water on the resin Tg and modulus. Work will begin on the formulation of high toughness (high peel strength) adhesives for use at 232°C (450°F).

## Chemical Characterization

Various chemical separation and spectroscopy techniques have been used to analyze and characterize resins of interest to this Program. The baseline resin, Narmco 5208, and two polyimide resins, Hexcel F-178 and Kerimid 601, have been successfully analyzed for their principal and minor components. The proposed structure of the diamide precursor of the $C_{10}$-polyphthalocyanines has been confirmed.

Nuclear magnetic resonance spectra of a number of epoxy resin systems and components have been obtained and are included in a catalog now being prepared for publication.

Analyses of candidate resins and adhesives are continuing and will include measurements of resin aging in composites prepreg materials.

## Radiation Curing

A vinyl-terminated bisphenol A (epoxy-like) polymer has been formulated with reactive monomers to give resins curable by ionizing radiation and which have good strength retention to 150°C. A radiation-curable resin formulation with strength retention above 200°C has been developed based on the polyimide Hexcel F-178 and N-vinyl-2-pyrrolidone. These and similar resin systems will be optimized for cure conditions, ultimate mechanical and thermal properties, and use as matrix resins in graphite fiber composites.

## Composites Fabrication

Fabrication procedures for T-300/5208 composites have been optimized and 16-ply laminates prepared with $[\pm 15^{\circ}]$ to quasi-isotropic fiber orientations. The high quality of these laminates was established by determining void content, elastic mechanical properties and fiber orientation. Fabrication procedures are being established for T-300 composites with $C_{10}$-polyphthalocyanine and Hexcel F-178.

## Design Optimization

A computer controlled in-plane loader has been used to obtain failure criteria for T-300/5208 composites as a function of fiber angle. It has been demonstrated that failure under combined loads is uniquely defined by an abrupt rise in the dissipative energy with increasing displacement. The data define smooth failure surfaces in three-dimensional space (tension, shear and bending) for each fiber orientation. The three-dimensional results have been analytically recast into a two-parameter form by J-integral analysis. Plots of the tensile ($J_x$) vs shear ($J_y$) J-integrals give straight lines characteristic for each fiber angle. Similar in-plane load

tests of adhesive/aluminum specimens give a failure surface in three dimensional deformation space which reveals a strong dependence of flaw growth resistance on the combination of loading modes.

Future work will include a broader range of in-plane loads for both composites and adhesive bonds, evaluation of composites of T-300 graphite with other resin matrices and testing at elevated temperatures.

# TASK A. RESIN SYNTHESIS

J. R. Griffith and J. G. O'Rear
Organic Chemistry Branch
Chemistry Division

## INTRODUCTION

In recent publications (1,2,3,4) we have reported a resin system in which polymerization is made to occur through aromatic orthodinitrile groups. Evidence indicates that the process involves the formation of the highly stable phthalocyanine nucleus. The resin monomers are synthesized from 4-aminophthalonitrile and aliphatic diacid chlorides to give diamides of the following structure:

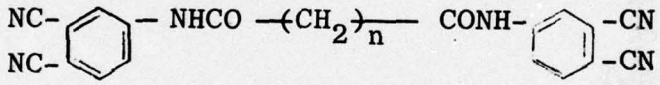

Polymerization proceeds through a "B" stage and the cure (at about 200°C) to give intensely green resins which solidify, gel and develop strength. The result is a network of stable phthalocyanine nuclei crosslinked through aliphatic diamide linkages. Polymerization of the resin monomers can be enhanced by the presence of selected metallic powders, although a metal is not required for cure. The polymerization can be represented as shown in Table I.

Our previous Progress Report (5) covered the synthesis of five phthalonitrile resin monomers which were designed to give large variations in the length of the connecting diamide moiety. Their structures are:

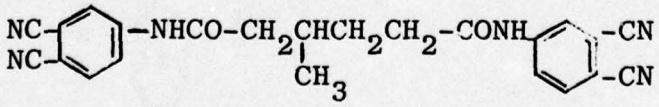

and

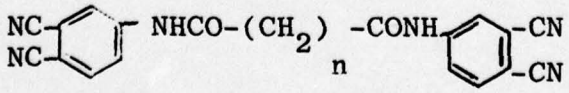

where n = 7, 8, 11 and 20

Table I

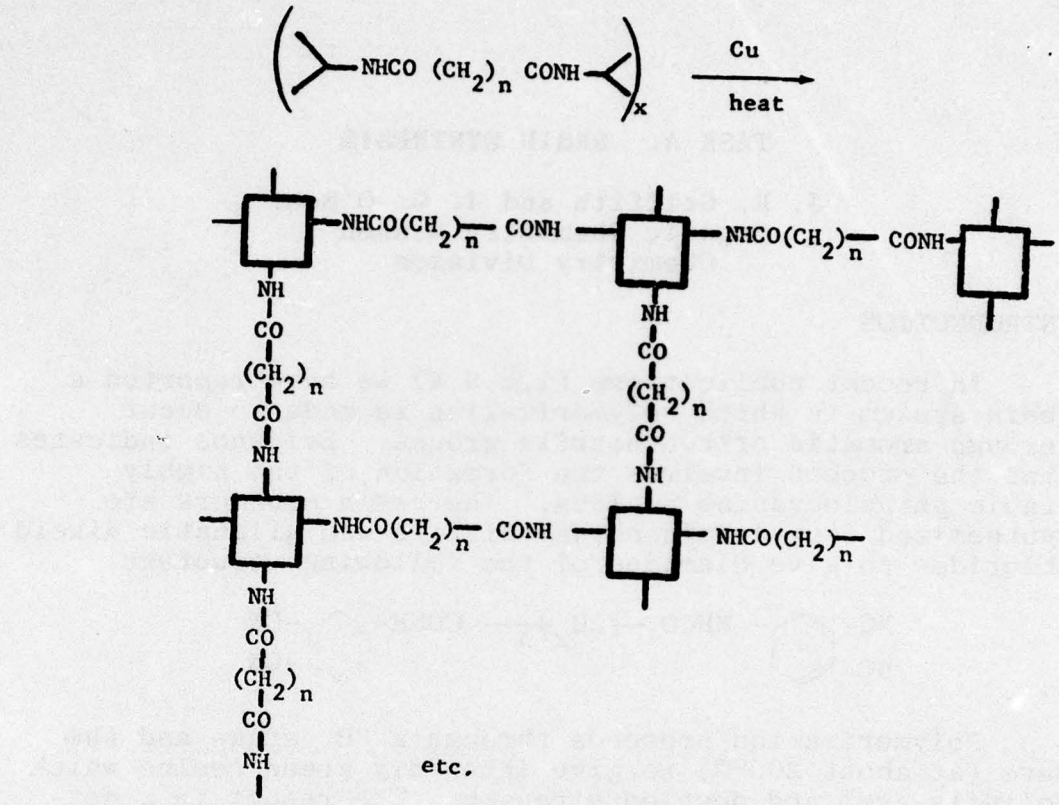


where

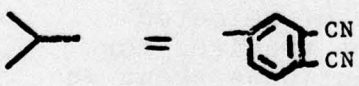


and

= Cu phthalocyanine nucleus

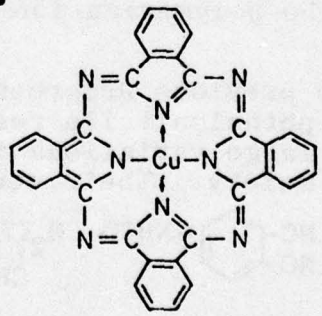

Nomenclature of the five N,N'-bis(3,4-dicyanophenyl) alkane diamides is cumbersome. Abbreviated names have been adopted to identify these compounds. The respective examples illustrate the abbreviations: Me-$C_6$ Diamide, $C_9$ Diamide, $C_{10}$ Diamide, $C_{13}$ Diamide and $C_{22}$ Diamide.

Diamide formation was accomplished by a modification of the Schotten-Bauman reaction (3):

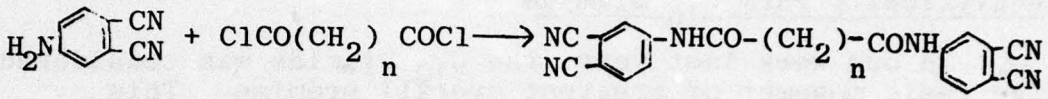

The required 4-aminophthalonitrile was prepared initially in 1 lb. quantities by methods developed at NRL (2,3) using the reaction sequence

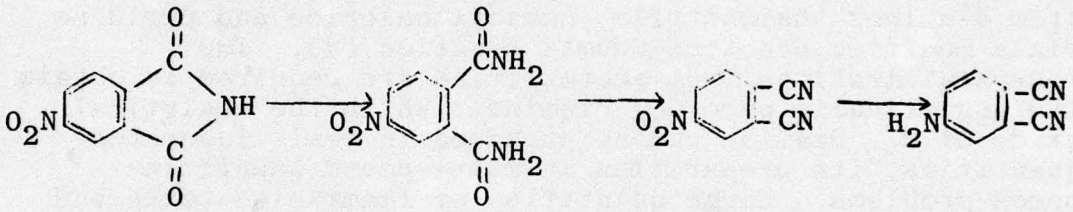

The required diacid chlorides were synthesized by standard procedures, with the exception of azelaoyl chloride and sebacyl chloride, which were purchased from Eastman Kodak Co.

Several recrystallizations from appropriate solvents led to the analytical monomers reported in Table II.

Table II

| Monomer | Melting Point (°C) | Recrysl. Solvent | Yield (%) |
|---|---|---|---|
| Me-$C_6$ Diamide | 204-206* | MeOH | 60.1 |
| $C_9$ Diamide | 181-183 | MeOH | 63 |
| $C_{10}$ Diamide | 192-194 | $CH_3CN$ | 64.4 |
| $C_{13}$ Diamide | 178-181 | $CH_3CN$ | 71 |
| $C_{22}$ Diamide | 150-152 | EtOH | 49.4 |

*The $C_6$ Diamide melts at 320-323° and is difficult to "B" stage (2,3)

## PROGRESS

The present reporting period covers progress made in the scaled-up production of the $C_{10}$ Diamide, the preparation of certain "B" staged phthalocyanine resins derived from mixtures of the $C_{10}$ and $C_{22}$ Diamides, and the mixed Dianil-Diamide resins of improved high temperature properties.

### Analytically Pure $C_{10}$ Diamide

In our work last year, the $C_{10}$ Diamide was considered the resin monomer of greatest overall promise. This preference was based on considerations such as modulus, cure versatility, cost and ease of fabrication in composites. During that period only analytically pure $C_{10}$ Diamide was employed in this program. The diamide is made from 4-aminophthalonitrile, sebacyl chloride and pyridine via a modified Schotten-Bouman reaction (3). Two recrystallizations from acetonitrile are required to obtain the analytically pure $C_{10}$ Diamide. While the analytical grade of $C_{10}$ Diamide can be prepared in small laboratory quantities, its preparation in multi-pound quantities poses problems. Large quantities of flammable, toxic and expensive acetonitrile are required. Moreover, complete solvent removal is difficult to achieve.

### Practical Grade $C_{10}$ Diamide

Current work in this task has been aimed at simplifying and scaling up the production of a "practical" grade of the $C_{10}$ Diamide. Considerable effort has been made to accomplish the purification by avoiding the two recrystallization steps. Our efforts in this direction have been prompted by obvious economic advantages, an available supply (28.6 lbs.) of 4-aminophthalonitrile procured under contract with Eastman Kodak Co., and a recently purchased 12-liter reaction vessel.

An acceptable quality of the practical grade $C_{10}$ Diamide has been achieved. The purification procedure uses an efficient water and alcohol wash. The latter step requires contacting the dry, pulverized, water-washed product with boiling ethyl alcohol, chilling the resulting mixture to -5°C, collecting and drying the insoluble solids. This procedure leads to the practical grade $C_{10}$ Diamide; mp 188-191°; 78% yield. To date we have produced 4 lbs of the practical grade $C_{10}$ Diamide. This quality of $C_{10}$ Diamide cures normally in the presence or absence of metals and is being evaluated for both

thermomechanical properties and fiber reinforcement applications.

## "B" Staged Phthalocyanine Resins for Toughness Experiments

One synthetic effort has been aimed at improving the toughness of the Zn-$C_{10}$ phthalocyanine polymer. This approach uses the "B" staged resin derived from the $C_{22}$ Diamide and zinc as the toughening component for the corresponding "B" staged resin derived from the $C_{10}$ Diamide and zinc. Samples of the mixed resins have been submitted for evaluation in the Thermomechanical Characterization Task.

## Dianil-Diamide Resins

Some applications demand further stiffening of the final cross-linked phthalocyanine polymer. One approach to this problem is the copolymerization of the $C_{10}$ Diamide with a dianil-linked phthalonitrile, e.g., N,N'-(1,4-phenylenedimethylidyne)bis-(3,4-dicyonoaniline). The latter compound has been designated as p-Dianil. Methods have been devised by us for synthesizing two isomeric Dianils (6). These Dianils have a completely conjugated structure.

The preferred preparative procedure is to react equivalent molecular quantities of the appropriate aromatic aldehyde with 4-aminophthalonitrile in refluxing toluene, while removing the water of reaction azeotropically. The reaction is catalyst dependent, and the preferred catalyst is p-toluene-sulfonic acid (0.01 to 0.05% by wt.). The Dianil precipitates as yellow crystals which can be isolated from hot toluene in high yields (85-95%). The preparative method for the p-Dianil is shown schematically:

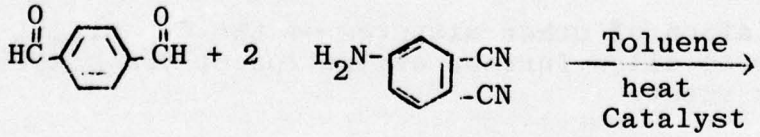


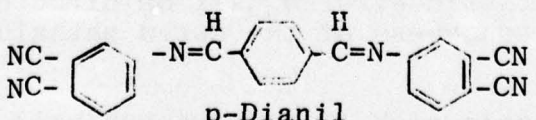


p-Dianil
mp 273-275°C (recrystallized from acetonitrile)

The isomeric m-Dianil is prepared similarly by substituting m-phthalaldehyde for p-phthalaldehyde. The m-Dianil can be recrystallized from a toluene: pyridine mixture (50:50 vol. %); mp 253-257°C.

In efforts to improve the stiffness of the cured phthalocyanine polymer, we have prepared the following physical mixtures: (a) 20.0 g 75 mole % $C_{10}$ Diamide plus 25 mole % p-Dianil, and (b) 20.0 g 75 mole % $C_{10}$ Diamide plus 25 mole % p-Dianil, mixed with copper powder (1.0 atom Cu/2 moles of the combination). Polymers derived from the above mixtures are being evaluated for modulus and toughness in the Thermomechanical Characterization Task. The prospect for further improvement by this method has prompted the synthesis of an additional quantity of the p-Dianil.

## FUTURE WORK

It has recently been brought to our attention that exceptionally high thermal stability (in excess of 450°F) probably will not be required for most V/STOL applications. This gives considerable flexibility to our synthesis projections, allowing us to give more weight to such properties as processability, resistance to water effects, modulus (stiffness), fracture energy (toughness) and economics. For example, work on the effect of the aliphatic chain length on fracture energy and water resistance is anticipated.

Two chemical approaches will be tried for improving the modulus of the cured phthalocyanine polymers:

(a) Synthesis of additional Me-$C_6$ Diamide to be cured either alone or as a modifier for longer chain Diamides.

(b) Formulation of other mixtures of the $C_{10}$ Dianil and $C_{10}$ Diamide to allow further evaluation of the Dianil as a stiffening agent.

Three synthetic efforts will be directed toward improving the toughness of the cured phthalocyanine polymers:

(a) Synthesis of N-(3,4-dicyanophenyl) stearamide.

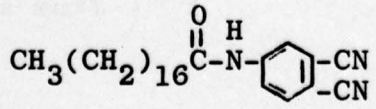

This structure is designed to act as a chain stopper in copolymerizations with conventional Diamides. In this role it is expected to reduce the degree of cross-linking, while entanglement of the long alkyl substituent may provide a mechanism for energy absorption.

(b) Synthesis of Diamide monomers derived from Empol Dimer acids sold commercially by Emergy Industries, Inc. The dimer acids are produced by [redacted] polymerization of unsaturated $C_{18}$ acids (e.g., linoleic acid) via the Diels-Alder reaction. The pure dimer is a $C_{36}$ aliphatic dibasic acid. Essentially it is a long-chain dicarboxylic acid with two or more alkyl side chains. These features assure the lengthening of the diamide moiety, known to improve toughness, and introduce pendant alkyl groups capable of entanglement in the cured phthalocyanine polymer.

(c) Synthesis of additional quantities of the $C_{22}$ Diamide. This will permit further evaluation of the fracture-toughening potential of this material.

The delivery of 34 lbs. of $C_{10}$ Diamide from Eastman Kodak Co. is expected momentarily. This material should assure a significant scale-up in the formulation of castings, composites and adhesives.

REFERENCES


1. "Resin Systems Cured Through Aromatic Ortho Dinitrile Groups", J. R. Griffith and T. R. Walton, Polymer Preprints 15, No. 1, p. 787 (April 1974), Los Angeles ACS National Meeting.

2. "Phthalocyanine Resins. A New Class of Thermally Stable Resins for Adhesives", T. R. Walton, J. R. Griffith and J. G. O'Rear, Organic Coatings and Plastic Preprints 34, No. 2, p. 446 (September 1974), Atlantic City ACS National Meeting.

3. "Phthalonitrile Resins", T. R. Walton, J. R. Griffith and J. G. O'Rear, Advances in Chemistry Series 142, p. 458 (1975).

4. "The Thermal Stability of Phthalocyanine and Polymeric Phthalocyanine in Air", T. R. Walton and J. R. Griffith, Coatings and Plastics Preprints 35, No. 2, p. 574 (April 1975), Philadelphia ACS National Meeting.

5. NRL Memorandum Report 3223, High Performance Composites and Adhesives for V/STOL Aircraft, Progress Report 1 July - 31 December 1975, Willard B. Bascom and Luther B. Lockhart, Jr., Editors, February 1976.

6. Resin Research at NRL - Fluoroepoxies and Phthalocyanines, J. R. Griffith, Technology in Transition, 20, 582 (1975), 20th National SAMPE Symposium and Exhibition..

## TASK B. THERMOMECHANICAL CHARACTERIZATION

W. D. Bascom, R. L. Cottington, J. L. Bitner
and J. Oroshnik
Surface Chemistry Branch
Chemistry Division

### INTRODUCTION

The mechanical property requirements of the matrix resins of composites for advanced V/STOL aircraft are primarily stiffness (high modulus) and toughness (high fracture energy). It is the purpose of this task to determine the effect of temperature, moisture exposure and heat soak on these properties for a variety of candidate resins. The basis for resin selection is that the candidate be a potential matrix resin with use temperature to at least 350°F but preferably higher. Cost, availability, potential fabrication problems and quality control are not considered in this task, although they affect how extensively a resin is evaluated.

Joining composite structural elements, to themselves or to metals, is most effectively done by adhesive bonding. At present there are no high peel strength (high fracture energy) structural adhesives available for use above 350°F. There are also design problems associated with the adhesive bonding of composites in that there is a need to develop failure criteria both for normal load bearing applications and for stress corrosion conditions. These problems are being worked on in this Task. Work on increasing the toughness of 450°F resins by incorporating a dispersed, elastomeric (rubber) phase to give acceptable peel strengths begins in FY 77. This effort will be informally coordinated with similar work underway at DoD or industrial laboratories. The mechanisms involved in obtaining a dispersed, elastomeric phase in the resin are so complex that an empirical approach must be taken.

Adhesive bond failure criteria are being developed in cooperation with the Design Optimization Task, and initial results are presented elsewhere in this report. It is the responsibility of the Thermomechanical Characterization Task to select adhesive resins and prepare specimens for fracture testing under in-plane load conditions.

The high toughness that elastomers can impart to resins to give high adhesive peel strength does not translate into composite toughness when the same elastomer-resin composition is used as the matrix. However,

there is both theoretical and experimental evidence that the application of a thin elastomer layer to the reinforcing fiber can significantly improve composite toughness. The magnitude of this effect is being determined under this Task.

PROGRESS

Matrix Resin Modulus and Toughness

The candidate matrix resins are tested using a torsion pendulum (1) for shear modulus (G) and log decrement damping factor ($\Delta$). The resin toughness is determined by measuring opening mode fracture energy ($\mathcal{G}_{Ic}$) using a method in which the resin is held as an adhesive layer between two metal double cantilever beams (2).

The G and $\mathcal{G}_{Ic}$ values at 25°C for the candidate resins tested thus far are listed in Table I. As previously noted (3), the polyphthalocyanines offer a range of moduli and toughness depending on the aliphatic chain length. Note that the $C_{10}$-polyphthalocyanine cured without a metal catalyst had essentially the same properties as the Zn-cured $C_{10}$-polymer. The slightly higher values for the latter could be due to a stiffening and toughening action of the unreacted Zn metal particles.

It should be noted that the resins listed in Table I have been cured to different extents and that this will affect the magnitude (but not the direction) of their different properties. To aid in making comparisons and for later discussion the various cure conditions are listed in Table II. The property most influenced by the cure is the glass transition temperature (Tg) and some of the resins in Table I were incompletely cured. In these instances the Tg is followed by (i) to indicate incomplete cure.

Fracture energy values for the Hexcel F-178 polyimide resin could not be obtained using the double cantilever beam specimen. Large voids were produced in the resin layer because of volatilization of the reactive diluent (triallylisocyanurate) during the heat cure. The $\mathcal{G}_{Ic}$ value for this resin will be determined by casting the resin as compact tension specimens (see below).

Shear modulus vs temperature (T) curves are given in Figure 1 for three polyphthalocyanines, Narmco-5208 (the reference matrix resin) and Hexcel F-178. These results differ somewhat from those presented in an earlier report (3). It was found that the torsion pendulum specimens had been too thick, much greater than the requisite 0.03 to 0.04 in. thickness for stiff materials (4). The principal effect of the reduction in specimen thickness was to increase G values below 25°C.

The polyphthalocyanine data in Figure 1 illustrate the range in modulus available through a change in aliphatic chain length. The $C_{10}$-polyphthalocyanine, the Narmco 5208, the F-178 polyimide and, in

fact, all of the commercial resins listed in Table I fall within a relatively narrow G vs T range bracketed by the $C_{22}$- and $MeC_6$-polyphthalocyanines.

A study is underway to increase the modulus of the $C_{10}$-polyphthalocyanine resin without any sacrifice in fracture energy. Accordingly, a dianil-based phthalocyanine was synthesized (Task Report A) in which the dianil structure replaces a portion of the straight chain segment of the aliphatic-based polyphthalocyanines. The rigidity of the dianil moiety should markedly enhance the resin modulus. A mixture of 75 mole % $C_{10}$-diamide and 25%-dianil phthalocyanine was cured (without metal) and tested for shear modulus. As indicated in Table I, a 30% increase in modulus at 25°C was achieved over the $C_{10}$-polythalocyanine alone. The G vs T torsion pendulum results showed that this improvement in modulus was never less than 20% (below 25°C) and increasing to as much as 75% at 250°C. It remains to be determined what effect the p-dianil additive has on fracture energy.

The effect of heat soaking at 288°C (550°F) on the modulus and loss decrement of the $C_{10}$-Zn cured polyphthalocyanine is shown in Figures 2 and 3. There is an increase in modulus with exposure indicating a gradual advancement of the cure. The maximum Tg ($\sim$ 375°C) was essentially reached after 24 hr with some overall increase in modulus with further heat soaking. This thermal treatment was embrittling the resin as evidenced by micro-crack formation. Samples soaked for longer than 250 hr were too brittle to test.

The damping factor results for the 288°C heat soak of the $C_{10}$-resin are given in Figure 3. The low temperature peak at about -150°C is attributed to the aliphatic chain. The peak at -50 to -75°C is presumably due to ice on the specimen and possibly absorbed water picked up from the $N_2$ gas used for purging the test chamber. The peak at 200°C for the initial sample is a quasi-glass transition temperature appearing well below the ultimate Tg this polymer attains, i.e. $\sim$ 360°C. The low temperature of this peak suggests the molecular network is poorly consolidated and under cured. The heat soak caused this peak to be shifted to above 350°C. There is also a change in the aliphatic damping peak (-150°C) with the thermal treatment. After 120hr and 240hr a double peak develops and is probably due to thermal decomposition of the $C_{10}$-aliphatic chain.

A similar thermal treatment of the Hexcel F-178 polyimide was conducted, and the G vs T and $\Delta$ vs T results are presented in Figures 4 and 5. The modulus curve indicates that the ultimate Tg of $\sim$ 350°C is essentially reached after 24hr at 288°C. A general increase in modulus occurred up to 120hr, but with little change thereafter (up to 480hr); however, the 240hr and 480hr specimens suffered notable shrinkage and micro-cracking. The damping factor vs temperature results for the F-178 polyimide are given in Figure 5. The polymer structural units responsible for the various peaks have not been identified (except for

the ice peak at -50 to -75°C). The most that can be said is that the cure is gradually advanced to a constant Tg of ∿ 350°C. The low magnitude of the log decrement in this region for the 120hr and 240hr specimens (also for the 480hr data not included here) indicates that the material has a very high crosslink density and is incapable of significant mechanical damping even above Tg.

The Narmco-5208 resin could not withstand more than 8hr at the 288°C heat soak temperature. This resin is an epoxy polymer and is not expected to have useful service life above 177°C (350°F). The torsion pendulum results in Figure 6 indicate a severe loss in modulus and a decrease in Tg even after only 8hr at 288°C (550°F). In these tests it was noted that if the specimens were cooled from 288°C by removing from the hot oven into a room temperature (∿ 25°C) receptacle (quenched specimen), the decrease in modulus was greater than if they were brought to 25°C in a slowly (24hr) cooled oven (annealed specimen). This effect is due to extra free volume (internal enthalpy) in the rapidly cooled material (5,6). A similar effect would be expected to occur in rapid heating and cooling (thermal spike) of resin matrix composites and should be considered in studying thermal spike effects in the presence of water.

These thermal soak results do not of themselves gauge the thermal degradation of the resins. The increase in modulus indicates progressive crosslinking but not degradation. The only evidence of degradation was the change in the aliphatic peak of the $C_{10}$-polyphthalocyanine. The decline in modulus of the Narmco-5208 occurred under conditions excessively severe for this resin. For the results to be meaningful, thermal aging should be done at about 50°C above the expected use temperature.

Nevertheless, there was certainly qualitative evidence of degradation in the embrittlement and shrinkage of the polyphthalocyanine and polyimide specimens. An effort will be made to establish quantitatively whether embrittlement is occurring by fracture testing heat-soaked specimens. Certainly, the progressive advance of the cure evident from the torsion pendulum results would lead to less capacity for yielding and hence lower fracture energy. This advancing cure probably offsets (in terms of modulus) thermal degradation. Indeed, these competing processes, crosslinking *vs* degradation, probably account for some of the thermal stability of high temperature resins, especially since the initial resins are considerably undercured.

The fracture energy ($\mathcal{G}_{Ic}$) *vs* temperature results for the Zn-cured $C_{10}$-polyphthalocyanine and the Narmco-5208 are given in Figure 7. As noted previously (3), the rise in fracture energy with decrease in temperature for the polyphthalocyanine and the maximum for the Narmco-5208 at ∿ 100°C are probably related to damping peaks in the log decrement curves. However, such associations must be considered tentative.

The data in Figure 7 were obtained using tapered double cantilever beam specimens in which the resin is held as a bonding layer between metal beams. As long as failure is center-of-bond through the resin layer the test gives a good measure of the resin fracture energy. This condition was met using aluminum beams, and these data correspond to the filled symbols in Figure 7. An attempt was made to use titanium beams in order to test at temperatures above which aluminum could not be used. However, failure of the titanium specimens was consistently along the resin/metal boundary. The titanium specimen data are represented by the open symbols in Figure 9 and are consistently lower than the aluminum specimen data. Evidently, the acid-phosphate etch used to clean the titanium was insufficient to overcome the normally poor bondability of titanium.

The steep rise in $\mathcal{G}_{Ic}$ for the Narmco 5208 is expected for the temperature region at 200°C near the resin Tg. The data were obtained using titanium beams, and so the actual rise in $\mathcal{G}_{Ic}$ may be even steeper.

These problems with titanium, the difficulties in obtaining fracture data for the Hexcel F-178 and other problems dictate against the continued use of metal cantilever beam specimens for $\mathcal{G}_{Ic}$ testing. In future work, plates or discs of neat resin will be cast or cut into compact tension specimens (or other geometry) for bulk fracture testing. The principal advantage of the metal cantilever beam method was that it is conservative on the amount of resin required. However, at this stage of the program, the resins of interest are available in sufficient quantity for bulk testing.

Elastomeric Interlayer for Improved Composite Toughness

The purpose of this subtask is to examine the concept of increasing the fracture resistance of resin-matrix composites by applying an elastomeric interlayer between resin and fiber. Bench-scale winding equipment has been constructed, and a schematic is given in Figure 8. Presently, NOL rings are being fabricated using diglycidyl-ether bisphenol A epoxy resin (DER 332) and hexahydrophthalic anhydride (HHPA) with benzyldimethylamine (BDMA) catalyst. Resin impregnation is done using a "vacuum release" technique (7) to obtain void-free composites. The NOL rings are cut into segments for interlaminar shear (ILS) testing (8), and for a three-point-load fracture testing. The latter involves a machined V-notch in the center of the concave side of an ILS specimen and loading in three-point bending to failure at the notch tip.

A preliminary study has been completed in which an Adiprene urethane elastomer (duPont L100) was applied from acetone solution to heat cleaned T-300 graphite (Union Carbide 30%, no twist) with BDMA as catalyst. The solution concentration was varied to give different (but unknown) coating thicknesses. Inspection by light microscopy and SEM indicate the coating (from solutions of < 0.5 wt %) to be uniform with little welding of filaments. The treated yarn was then fabricated into

NOL ring anhydride-epoxy resin composites, as described above and in reference 7.

The ILS results are given in Figure 9. There are two important points to be made. First, the heat cleaning of the T-300 yarn very seriously damaged the fibers as far as interlaminar shear strength (ILSS) is concerned. (Compare the filled points in Figure 9.) Part of this degradation may have been due to oxidation since air was not excluded from the heating column. Secondly, the effect of the coating was to restore the ILSS to that of the as-received fiber. At this point, it is problematical whether the effect of the coating was simply to replace the original finish (a B-staged epoxy resin) removed during heat cleaning or whether the urethane coating has an effect of its own which, superimposed on the epoxy finish, would enhance the ILSS of the as-received fiber composite.

The notched ring segment test results are presented in Figure 10. As with the ILSS results, the effect of the urethane coating was a maximum in the notched specimen strength for treatment from a 0.1 - 0.3 wt % solution. In this test, the heat cleaning did not degrade the notch strength as much as in the ILS test. The low values at concentration > 0.5 wt % in both Figures 11 and 12 are probably due to the coating bonding filaments together and preventing good resin penetration into the yarn. The urethane treatment at the optimum solution concentration gave a significant improvement (20%) over the heat-cleaned and over the as-received fiber specimens. Assuming that this test is actually measuring composite fracture toughness, this strength improvement translates into a toughness improvement of about 44% ($\mathcal{G}_c = f(\text{load})^2$). The failure mode was not always crack initiation from the notch tip but inter-laminar shear failure away from the tip. Possibly, the data in Figures 9 and 10 are measuring the same failure mode.

Mixed-Mode Adhesive Fracture

It has been observed (3) that in scarf-joint adhesive fracture tests there is a strong dependence of fracture energy (mixed-mode strain energy release rate, $\mathcal{G}_{(I,II)c}$) on bond angle ($\phi$) with a maximum at $\phi = 45°$. It was thought that this stress angle dependence might translate into the flaw growth in composites with different fiber or ply orientation. However, recent work has established that the scarf angle dependence is due to differences in the interaction of crack propagation with adherend surface roughness. Although this effect may play a small role in composite fracture, it is probably a second or third-order effect. Indeed, the results presented in Task Report F (Figure 9) indicate a linear increase in fracture energy (J) with ply angle and no evidence of a maximum at 45°. The mixed-mode results are not, however, without significance to the subject of adhesive joint performance, but continued work on the problem cannot be justified in this Program. The current tests will be completed and a manuscript prepared for publication.

FUTURE PLANS

Additional commercial resins will be evaluated for modulus, damping factor and fracture energy at ambient (25°C, 50% RH) conditions in an effort to characterize the principal state-of-the-art resins for high performance composites and, hopefully, to identify resins with one or more outstanding properties. These resins will include representatives of all classes of so-called high temperature resins including thermoplastic polysulfones and polyimides.

These mechanical characterization tests will be supplemented by measurements of the effect of moisture on the resin Tg using a special closed-cell attachment to a differential scanning calorimeter.

Polyphthalocyanine resins will be synthesized by the Resin Synthesis Task and have specific molecular structure designed to give high modulus, toughness and/or moisture resistance. These "molecularly tailored" resins will include (a) mixtures of aliphatic and dianil based phthalocyanines, and (b) end-capped phthalocyanine structures with the end-cap moiety being an aliphatic chain long enough (C-18) to provide molecular entanglements which may enhance toughness to offset the loss in cross-linking but also provide a mechanism for increased toughness via plastic deformation of the entanglements. Also, aliphatic-based resins will be synthesized from acid chlorides based on "dimer-acid" in the hope of obtaining resins at least as tough as the C-22 polyphthalocyanine (Table I) but with a much less costly diacid starting material. Dimer acid-based resins also have unsaturated sites which may allow curing (with reactive diluents) by ionizing radiation (Task D).

Selected resins will be tested for the effect of heat soak on $\mathcal{G}_{Ic}$, modulus, damping factor and $\mathcal{G}_{Ic}$ vs T. The selection will be based on potential as matrix (or adhesive) resins for V/STOL structures.

Work will begin on formulating high toughness adhesives. Initial effort will be to incorporate fibrillated PTFE in $C_{10}$-phthalocyanine, Hexcel F-178 and a fluoroepoxy resin.

Critical experiments are underway to determine the viability of the elastomer interlayer approach to improving composite toughness. A decision on continuing this subtask will be made in FY 77.

Stress corrosion studies of adhesively bonded aluminum and titanium specimens will be started in FY 77. The test procedure will be based on tapered double cantilever beam specimens as described by Mostovoy (9). Tests will begin with a "model" structural adhesive (2) and followed by testing of 450°F adhesives formulated in this Task.

Table I

BULK PROPERTIES OF RESINS

| RESIN | TYPE | SOURCE | SHEAR MODULUS* G', $GN/m^2$ | FRACTURE ENERGY* $\mathcal{G}_{Ic}$, $J/m^2$ | Tg, °C |
|---|---|---|---|---|---|
| 5208 | Tetrafunctional epoxy | Narmco | 1.35 | 82 | 260 |
| Zn-Me $C_6$ - PC | Phthalocyanine | NRL | 1.60 | 56 | 325 (i) |
| Zn-$C_{10}$ - PC | Phthalocyanine | NRL | 1.24 | 124 | 375 |
| Zn-$C_{22}$ - PC | Phthalocyanine | NRL | 0.78 | 362 | 150 (i) |
| $C_{10}$ - PC | Phthalocyanine | NRL | 0.93 | 116 | 375 |
| $C_{10}$/dianil - PC (3:1)‡ | Phthalocyanine | NRL | 1.20 | - | - |
| ECN-1235 | Cresol - Novolac/NMA | Ciba-Geigy | 0.67 | 100 | 180 (i) |
| Xylok-235C | Polybenzyl | Ciba-Geigy | 1.27 | - | 230 (i) |
| F-178 | Polyimide (addition) | Hexcel | 1.49 | | 360 |
| Kerimid 601 | Polyimide (addition) | Rhodia | 1.14 | | - |

* 25°C

‡ see text

i - "initial" ∿Tg for incompletely cured resin

Table II

RESIN CURE SCHEDULE

| RESIN | Temp °C | Time hr | Temp °C | Time hr | Temp °C | Time hr | Temp °C | Time hr | Temp °C | Time hr |
|---|---|---|---|---|---|---|---|---|---|---|
| 5208[a] | 93 | 20 | 121 | 3 | 149 | 2 | 177 | 2 | 200 | 4 |
| Zn -Me $C_6$-PC | 220 | 48 | | | | | | | | |
| Zn-$C_{10}$-PC | 220 | 48 | | | | | | | | |
| Zn-$C_{22}$-PC | 200 | 24 | | | | | | | | |
| $C_{10}$-PC | 260 | 50 | | | | | | | | |
| $C_{10}$/dianil (3:1) | 260 | 72 | | | | | | | | |
| ECN-1235 | 120 | 1 | 150 | 1 | 180 | 12 | 215 | 16 | | |
| Xylok 2356 | 150 | 1 | 200 | 5 | | | | | | |
| F-178 | 235 | 4.5 | | | | | | | | |
| Kerimid 601 | 177 | 1 | 232 | 16 | | | | | | |

[a] See Table I for resin sources and type

REFERENCES

1. Nielsen, L. E., Mechanical Properties of Polymers, Vol. 1, Chap. 4, Dekker, N.Y., 1974.

2. Bascom, W. D., Cottington, R. L., Jones, R. L. and Peyser, P., J. Appl. Polym. Sci. 19, 2545 (1974).

3. NRL Memo Report 3223, High Performance Composites and Adhesives to V/STOL Aircraft, February 1976, W. D. Bascom and L. B. Lockhart, Jr.

4. ASTM Method D2236-70, Dynamic Mechanical Properties of Plastics by Means of a Torsion Pendulum.

5. Jones, G. O., Glass, Wiley, N. Y., 1956.

6. Peyser, P. and Bascom, W. D., The Effect of Filler and Cooling Rate on the Tg of Polymers, in press.

7. Bascom, W. D. and Romans, J. B., I&EC Product Research and Development 7, 172 (1968).

8. ASTM Method D2344-72, Standard Method of Test for Apparent Horizontal Shear Strength of Reinforced Plastics by Short Beam Method.

9. Ripling, E. J., Mostovoy, S., and Corten, H. T., J. Adhesion 3, 107 (1971).

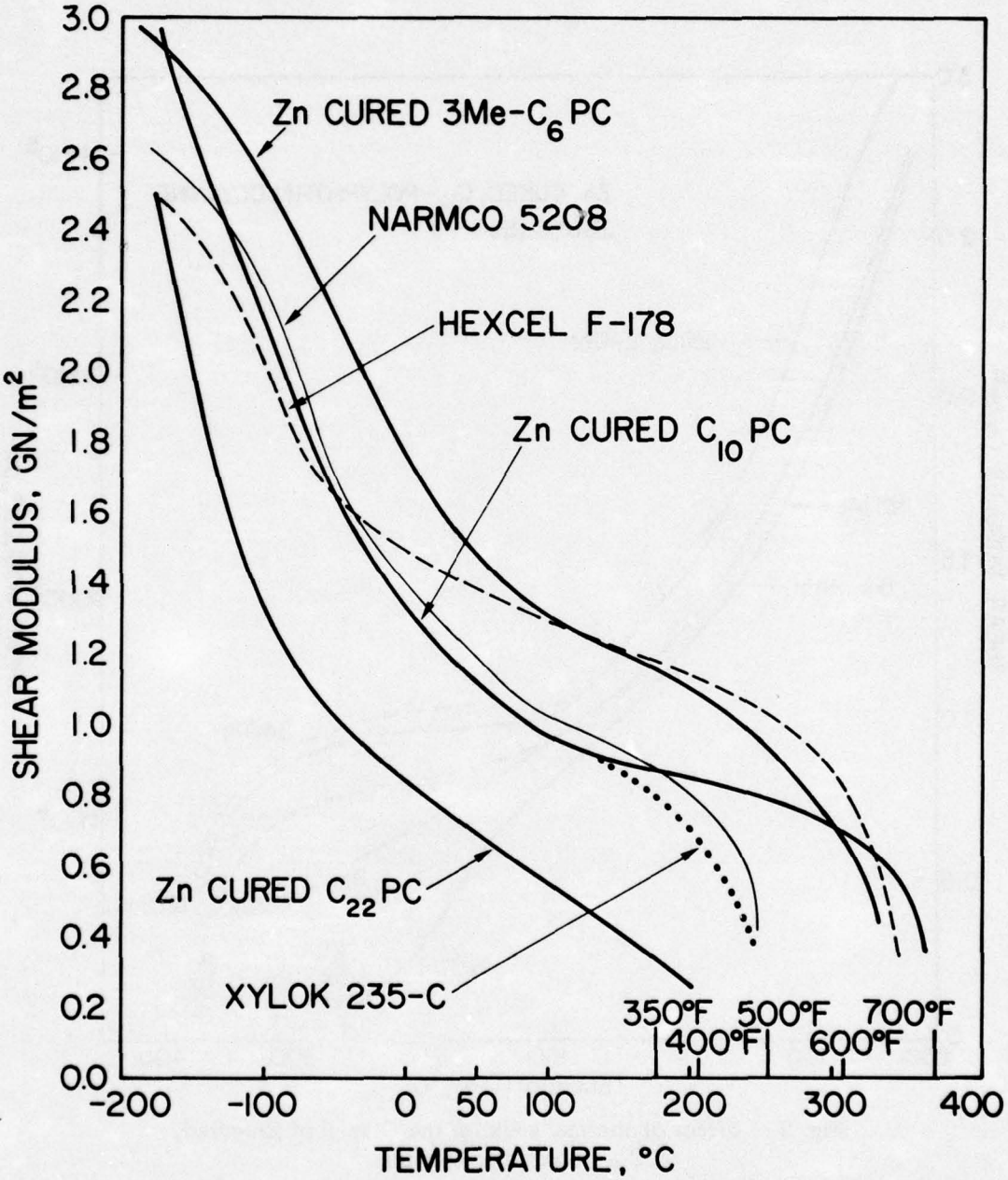


Fig. 1 — Modulus — temperature curves for various high-performance resins

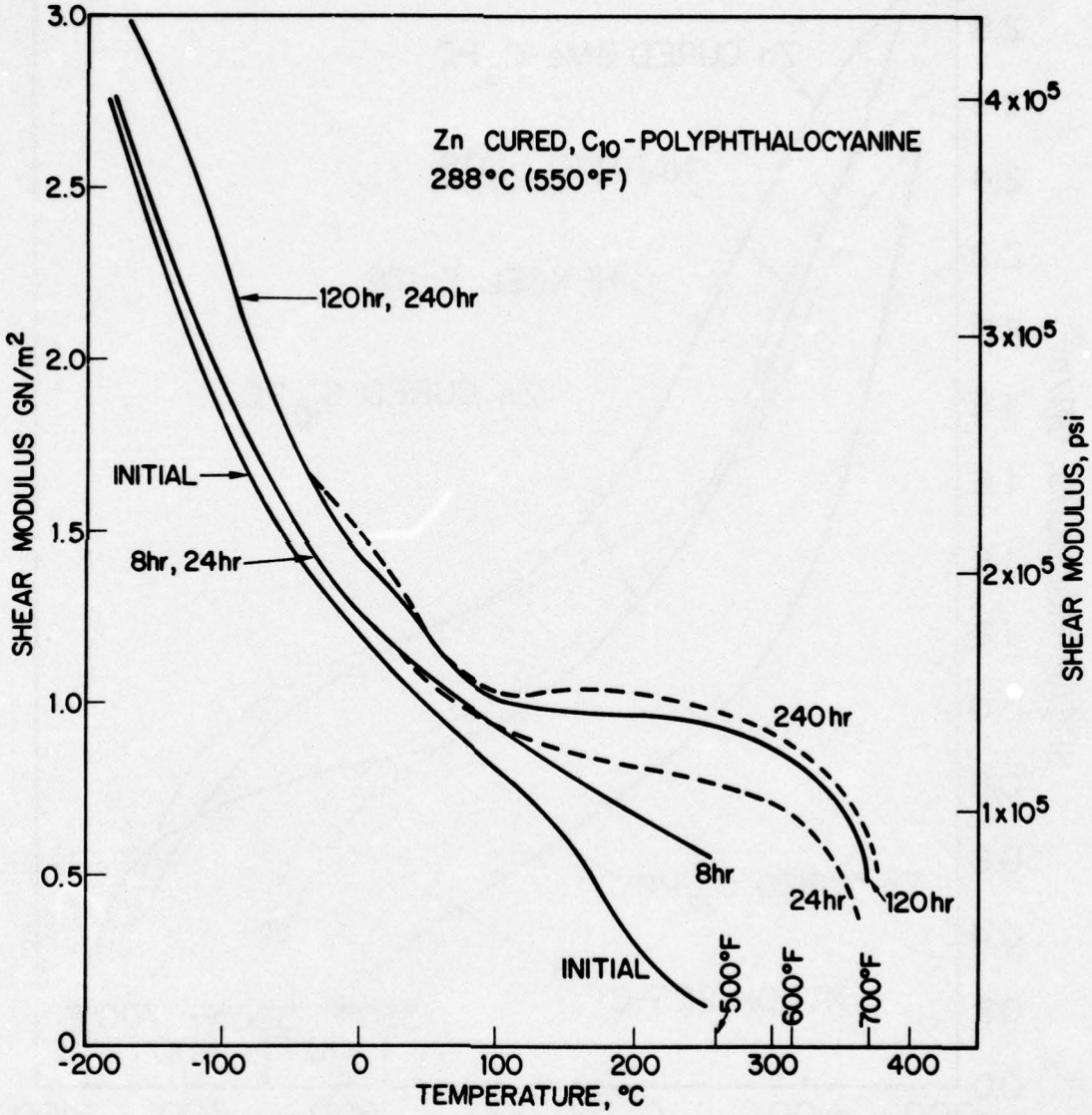


Fig. 2 — Effect of thermal soak on the G vs T of Zn-cured, $C_{10}$-polyphthalocyanine

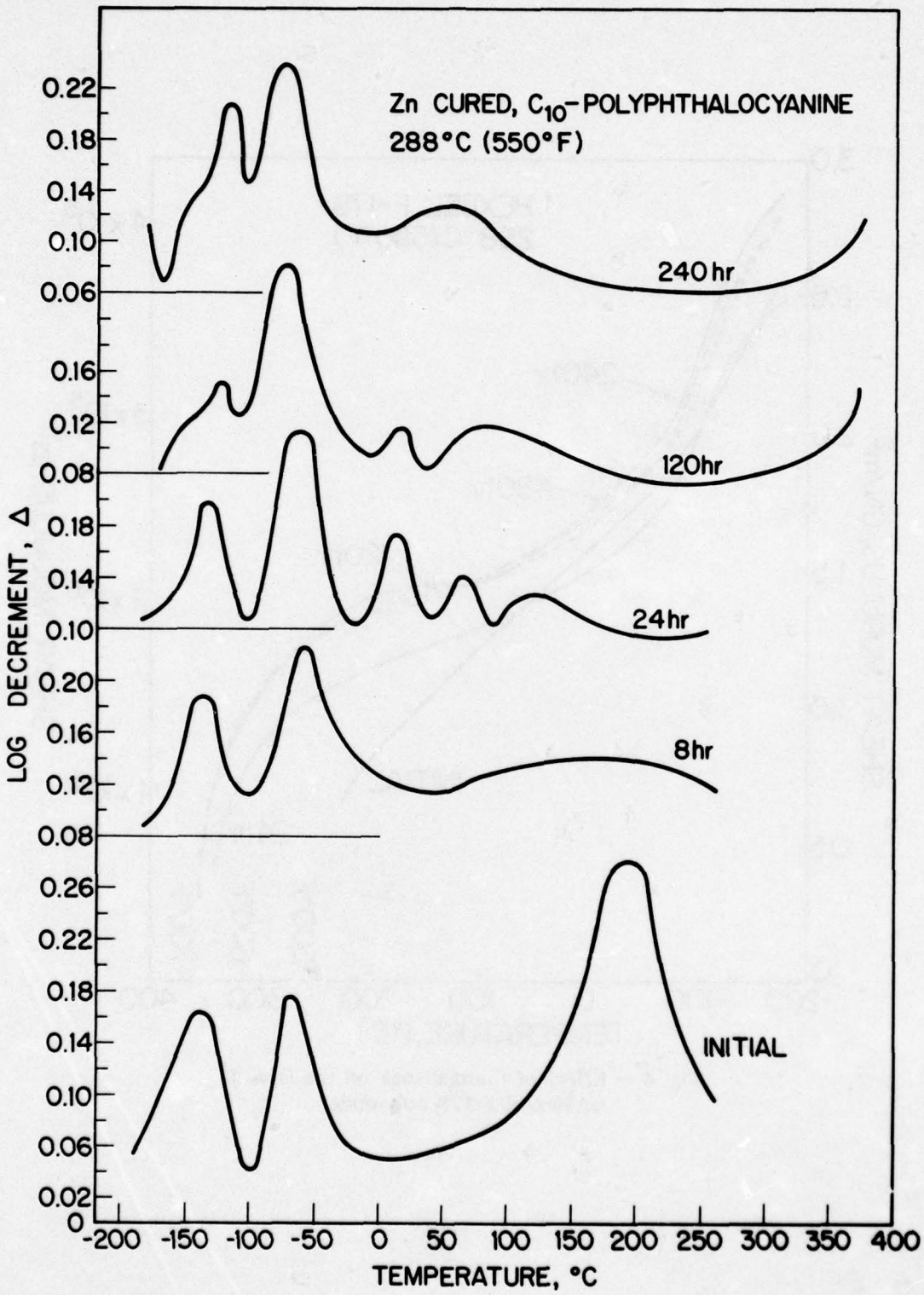


Fig. 3 — Effect of thermal soak on the Δ vs. T of Zn-cured, $C_{10}$-polyphthalocyanine

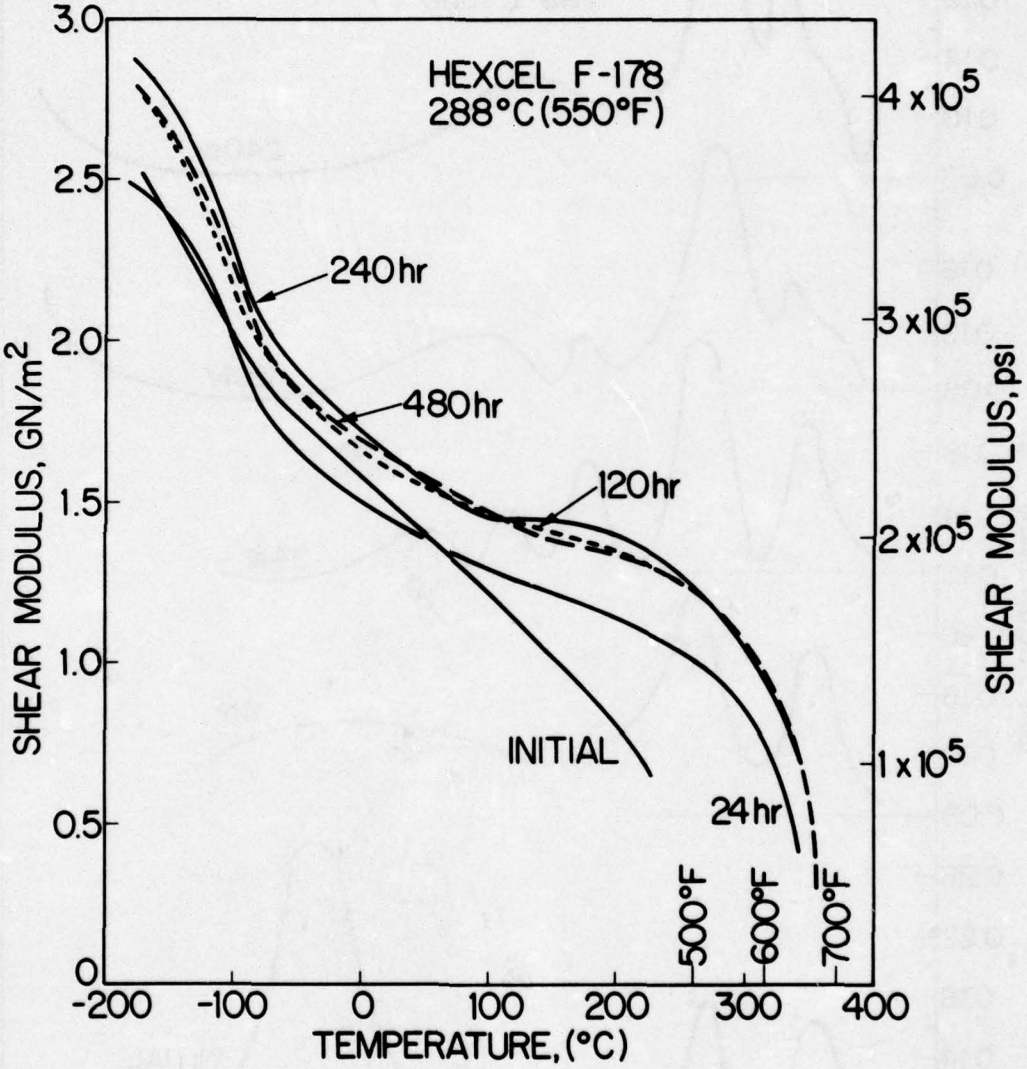


Fig. 4 — Effect of thermal soak on the G vs T of Hexcel F-178 polyimide

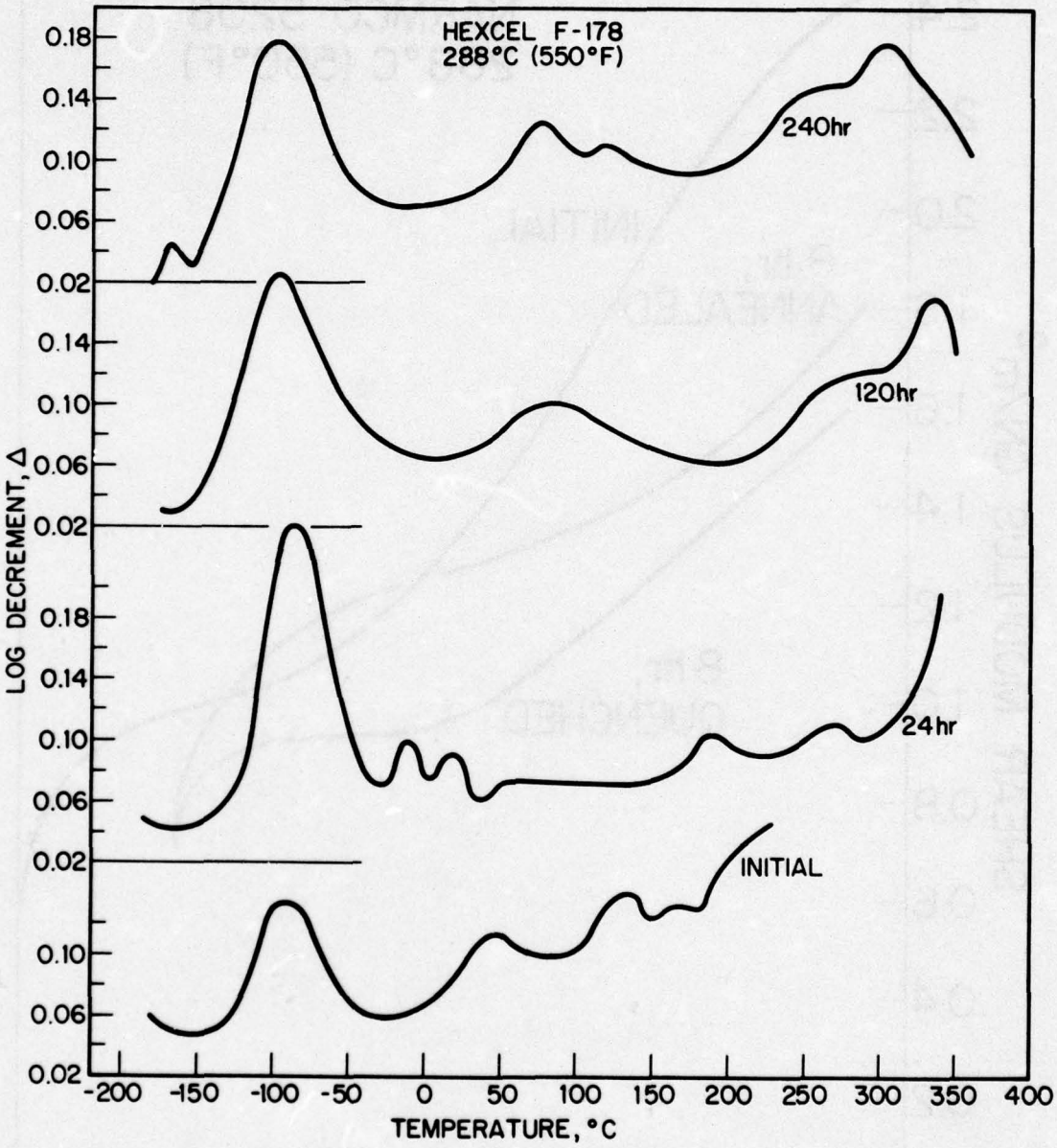


**Fig. 5 — Effect of thermal soak on the Δ vs T of Hexcel F-178 polyimide**

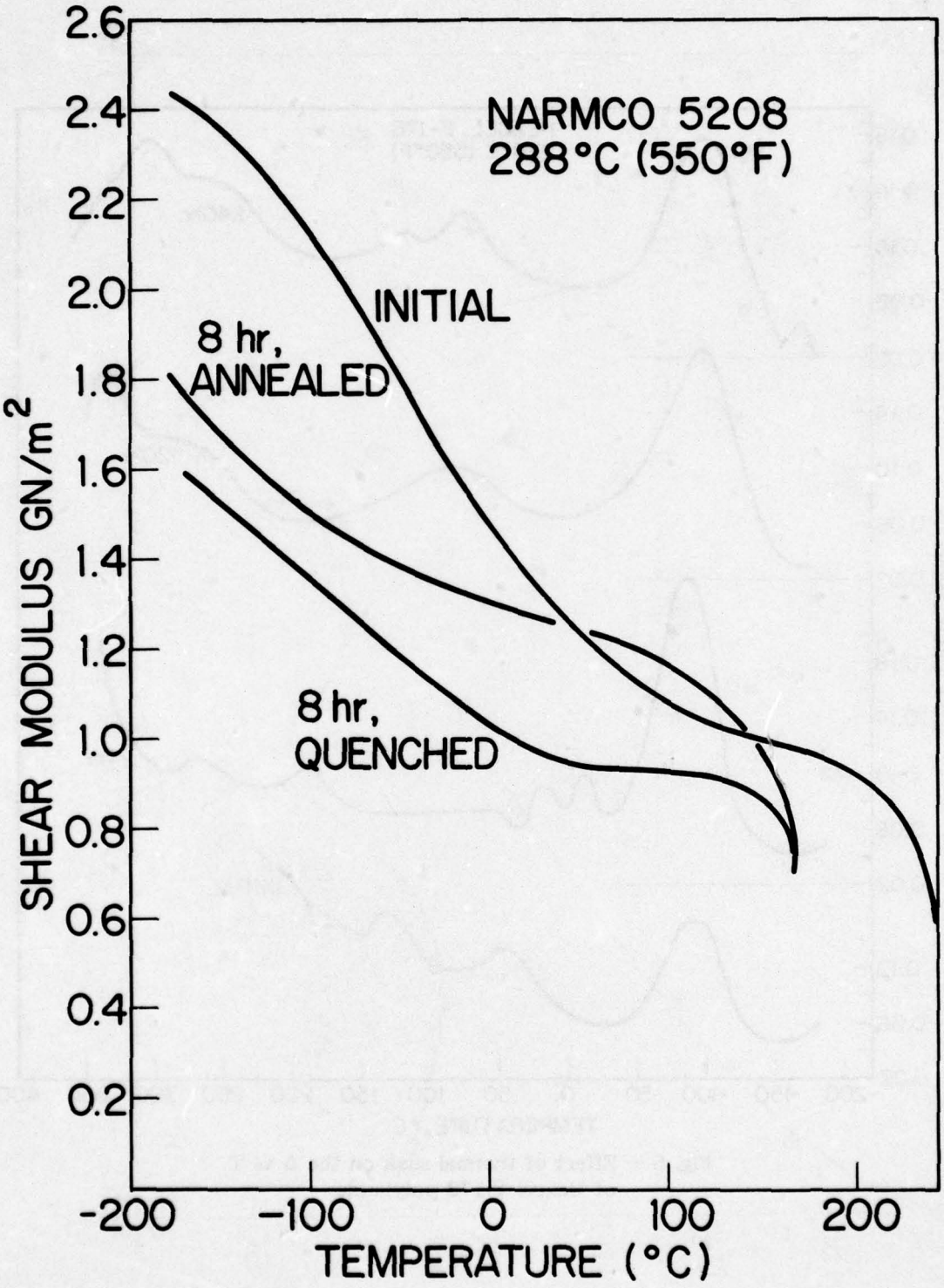


Fig. 6 — Effect of thermal soak on the G vs. T of Narmco 5208 epoxy

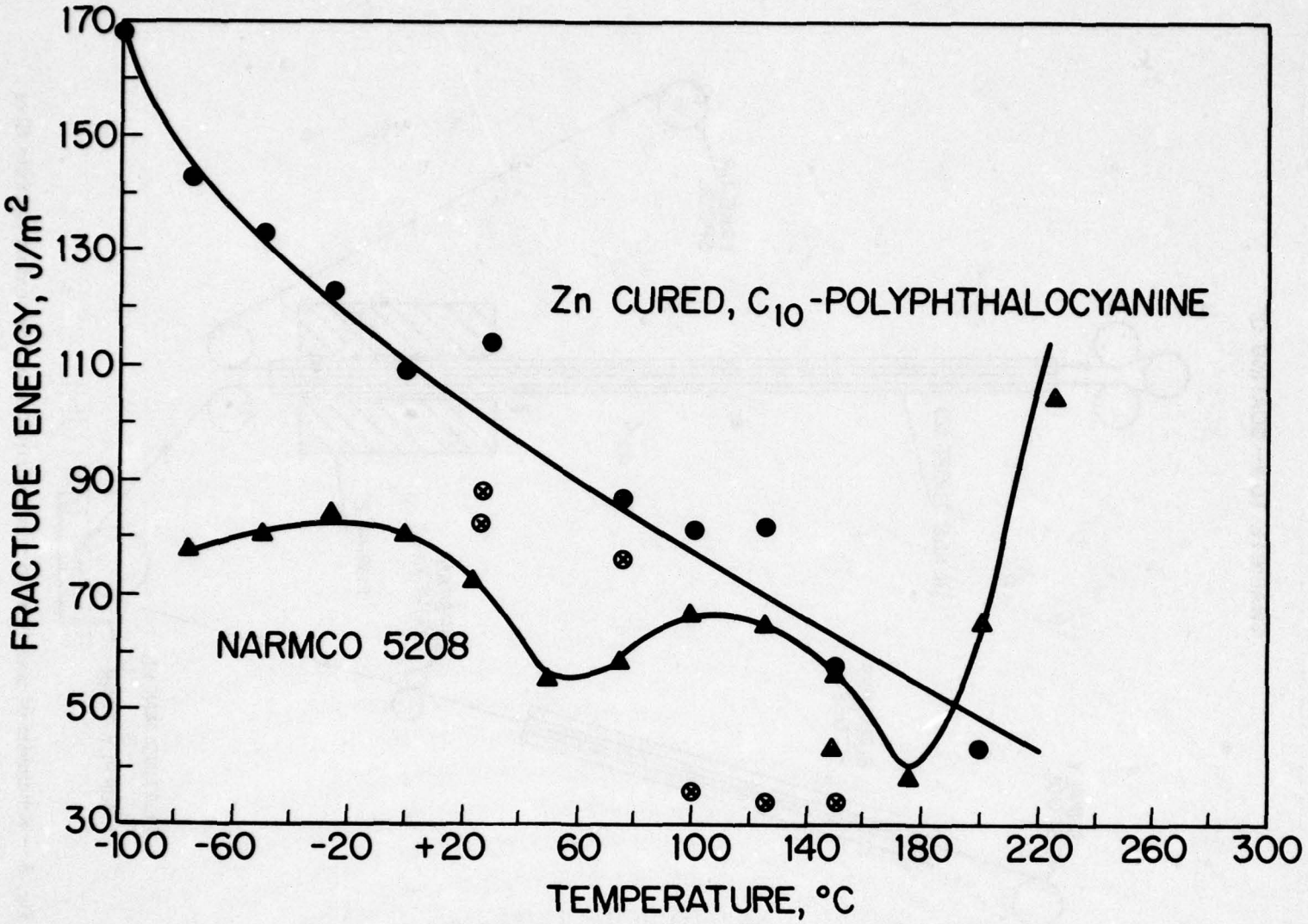


Fig. 7 — Effect of temperature on fracture energy; filled points — aluminum beams, open points — titanium beams

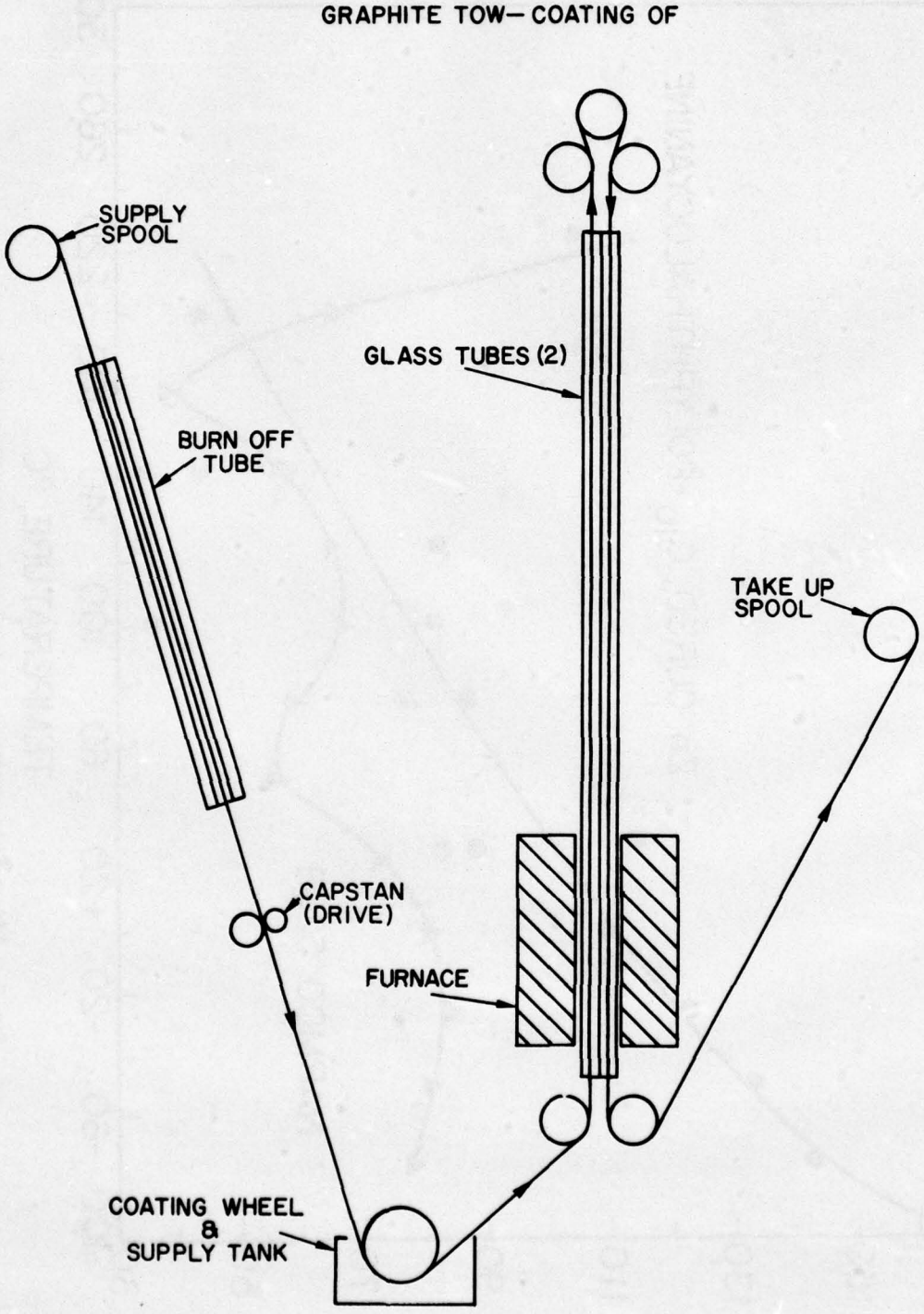


Fig. 8 — Schematic of single-strand winding equipment for coating graphite fiber

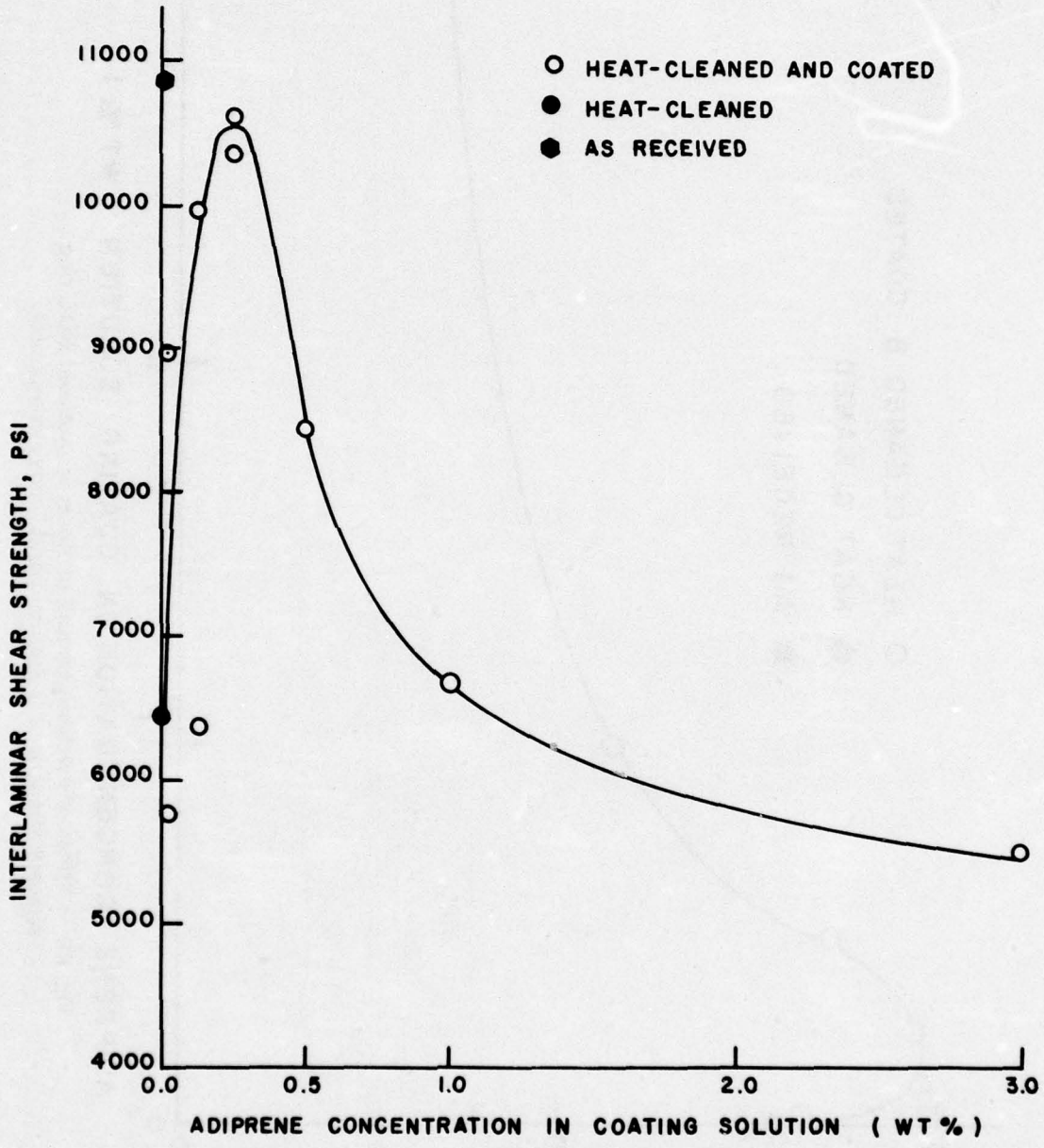


Fig. 9 — Effect of urethane coating of fibers on interlaminar shear strength of T-300 anhydride-epoxy NOL ring composites

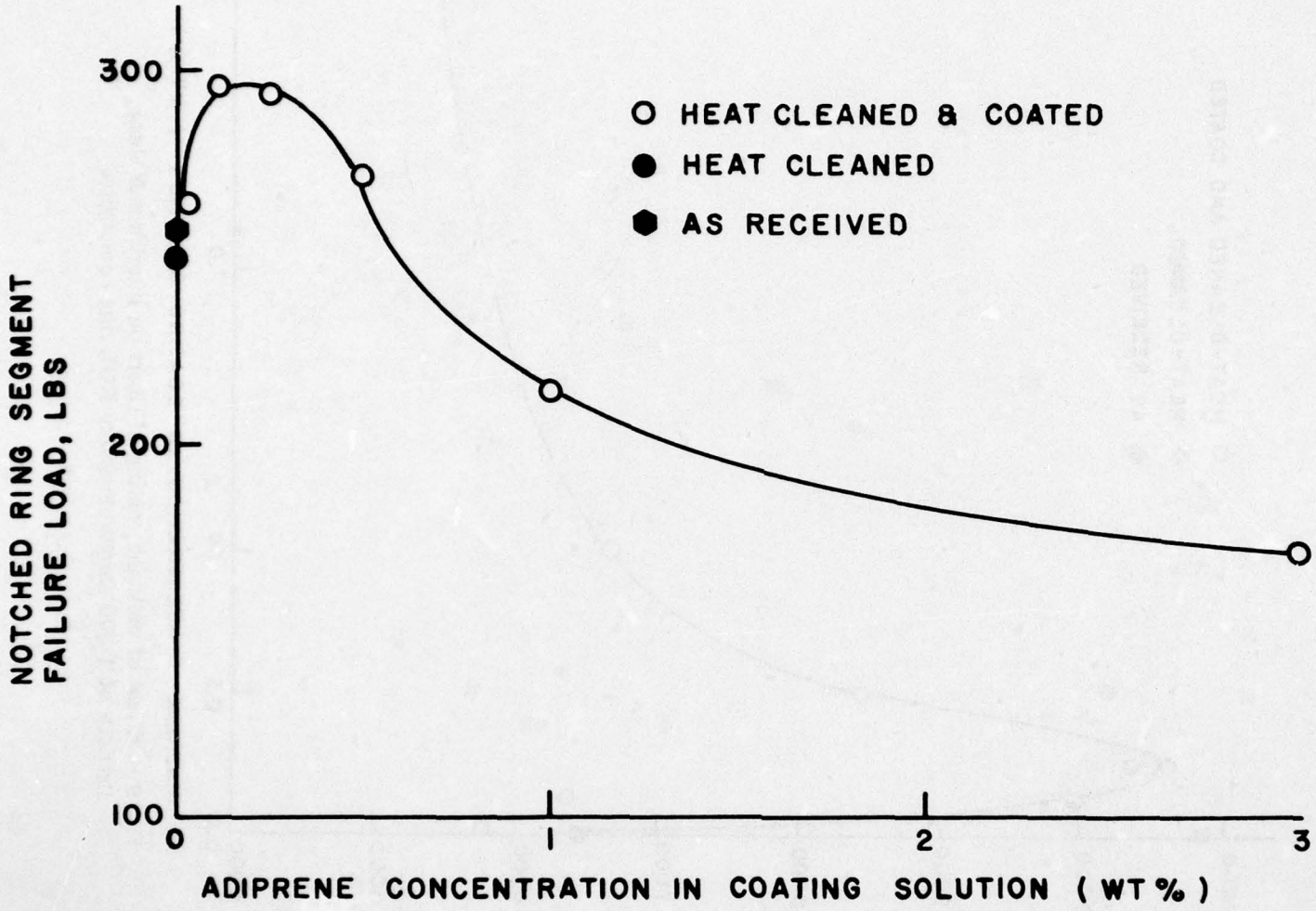


Fig. 10 — Effect of urethane coating of fibers on notched NOL ring segment strength of T-300/anhydride-epoxy composites

# TASK C. CHEMICAL CHARACTERIZATION

C. F. Poranski, Jr. and W. B. Moniz
Organic Chemistry Branch
Chemistry Division

## INTRODUCTION

The high strength-to-weight ratio of structural composites and adhesives cannot be fully exploited because of batch-to-batch variability in engineering properties which frequently exceeds ±25%. The use of such materials in primary structures requires stringent control on reproducibility and reliability. The Chemical Characterization Task helps investigate the relationships between chemical composition and engineering variability. The task determines the identity, purity, and quantity of ingredients in resin systems selected for investigation in the NRL-V/STOL Program. It also develops methodology and specifications to monitor composition so that adverse effects upon engineering properties due to variability in raw materials may be minimized. The chemical results will be correlated with the physical and thermomechanical results obtained in other Tasks to generate meaningful quality control parameters.

The objectives for FY76/FYTQ were (a) analysis of the baseline resin system, Narmco 5208; (b) general characterization of commercial resin systems of interest to this program (continuing); and (c) characterization of phthalocyanine and other NRL formulated resin systems (continuing).

This Task routinely screens candidate materials which enter the NRL-V/STOL Program for evaluation. The screening, usually by carbon-13 and proton nuclear magnetic resonance spectroscopy (C-13 or proton NMR) (1), confirms or establishes the chemical nature of the material. Materials selected for extensive evaluation in the program are studied more intensively by a battery of analytical methods. Finally, a quality assurance scheme based on composition will be developed for the resin system which meets the performance goals of the NRL-V/STOL Program.

PROGRESS

Highlights

The baseline resin system, Narmco 5208, was found to consist principally of the tetraglycidyl ether of methylene dianiline (TGMDA), an epoxide, and diaminodiphenyl sulfone (DDS), the curing agent. The Task showed that the modified epoxy, Celanese SU-8, is also present as a minor constituent.

Two polyimide resin systems, Rhodia Kerimid 601 and Hexcel F-178 were shown to differ markedly in composition. Kerimid 601 is composed principally of the bis-maleimide of methylene dianiline, while Hexcel F-178 contains the reactive plasticizer triallyl isocyanurate as a major constituent in addition to the above bis-maleimide.

The proposed structure of the $C_{10}$ Diamide, a precursor to the NRL-developed phthalocyanine resin, was confirmed by C-13 and proton NMR spectra.

NMR spectra have been obtained for a number of resins, curing agents, etc., to provide reference data for the chemical characterization efforts.

Narmco 5208

Narmco's Rigidite 5208, chosen as a baseline material for the NRL-V/STOL Program, is a graphite-epoxy prepreg material manufactured from Narmco 5208 epoxy resin system and Thornel 300 graphite fiber. It is one of several state-of-the-art high temperature graphite-epoxy systems used in the fabrication of airframe components on a commercial scale.

The Narmco 5208 resin system is based on the tetraglycidyl ether of methylene dianiline (TGMDA) and diaminodiphenyl sulfone (DDS). The structures and C-13 NMR spectra of these compounds are given in Figures 1 and 2, respectively.

Carbon-13 and proton NMR spectra of Narmco 5208 (Figures 3 and 4) readily confirm that the major constituents are TGMDA and DDS. In addition, they indicate the presence of other materials. The C-13 data point to a glycidyl ether type of resin (2). In the proton spectrum of Narmco 5208 the glycidyl ether region is swamped by lines due to the glycidyl amine groups of TGMDA (Figure 4, 2.2-3.8 ppm). However, the 1.6 ppm

region of this spectrum shows lines which are not present in TGMDA, but which closely resemble lines in the proton spectrum of Celanese SU-8. SU-8 is a polymeric epoxy resin of "unique structure" (3). The C-13 spectrum of SU-8 (Figure 5) matches many of the peaks attributed to minor constituent(s) in Narmco 5208. On the basis of the proton and C-13 spectra, we conclude that Celanese SU-8 is a minor constituent of Narmco 5208. This conclusion has been independently reached by two other groups working on characterization of TGMDA/DDS resin systems (4,5).

Besides the determination of qualitative composition of systems like Narmco 5208, we are developing methods for quantitative analysis.

Proton NMR can often be used for quantitative analysis of mixtures. Figure 6 illustrates the approach for a TGMDA/DDS resin system. The proton spectrum of the resin system designated R-33 is the combination of the spectra of the two components, DDS and TGMDA. Since one-half of the aromatic proton spectrum of DDS is well separated, R-33 can be quantitatively analyzed by integration of peak areas. For three synthetic mixtures of DDS and TGMDA containing 10, 20 and 30% by weight of DDS, we obtained, by this method, 10.9%, 20.7% and 29.7% DDS, respectively. Extension of this procedure to Narmco 5208 has been hampered because the aromatic protons of SU-8 overlap those of the DDS and TGMDA. If the structure of SU-8 were known, integration of the peak due to SU-8 at 1.6 ppm in the Narmco 5208 spectrum (Figure 4) would eliminate the problem.

Carpenter (5) has reported quantitative techniques based on infrared spectroscopy and differential scanning calorimetry for these types of resin systems. In his work, also, the presence of other components affects the accuracy of the analyses.

Other TGMDA/DDS resin systems

We have obtained survey spectra of two other TGMDA/DDS resin systems, Hercules 3501-5 and Fiberite 934. The Hercules 3501-5 contains only TGMDA, DDS and about 1% of a boron fluoride ($BF_3$) complex as a catalyst (4). We have not yet confirmed the presence of the $BF_3$ complex by NMR methods, but fluorine-19 NMR should be applicable. The C-13 and proton NMR spectra of Fiberite 934 are more complex. The C-13 spectrum (Figure 7) has additional lines in the 40-70 ppm region and at 165 ppm due to the presence of diglycidyl phthalate.

## Epoxy Novolacs

Epoxy novolac resins combine the temperature stability of phenolic resins with the curing versatility of the epoxide group. The structures and C-13 NMR spectra of two epoxy novolacs are given in Figures 8 and 9. The spectra differ primarily because of the aromatic methyl substituent in the CIBA material (Fig. 9). The C-13 NMR spectra for two higher molecular weight materials, D.E.N. 438 and D.E.N. 439 closely resemble that of D.E.N. 431.

## Phthalocyanines

The Resin Synthesis Task has developed a series of compounds of the general structure, I, which polymerize to form polyphthalocyanines. The Chemical Characterization

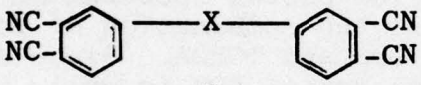


I

Task has run C-13 NMR spectra of several of these compounds. The structure and spectrum of the $C_{10}$ Diamide, where X = $-N(H)-C(=O)-(CH_2)_8-C(=O)-N(H)-$, are given in Figure 10. We have also begun to characterize the dianil- and the polyphenylether-variations of phthalonitrile resins.

## Polyimides

Samples of four addition-type polyimide systems have been received for preliminary investigation. They are CIBA P-13N (varnish), Gulf Thermid 600, Rhodia Kerimid 601 and Hexcel F-178. The Hexcel material has been most thoroughly investigated.

Figures 11 and 12 give, respectively, the C-13 and proton NMR spectra of Kerimid 601 and F-178. The two materials have many spectral features in common, but it is immediately evident that F-178 has at least one other major component. Treatment of F-178 with $CCl_4$ (room temperature stirring or Soxhlet extraction) resulted in the extraction of a colorless liquid whose C-13 and proton NMR spectra account for most of the extra lines in the F-178. We identified this liquid as triallyl isocyanurate by comparison of its infrared and C-13 and proton NMR spectra with those of an authentic sample

(Aldrich Chemical Company #11,423-5, Triallyl-S-triazine-2,4,6 (1H,3H,5H)-trione)).

This result is consistent with the report by Penn, et al, (6) of a component of F-178 which volatilized under vacuum and high temperature. The infrared spectrum they show for this volatile component closely matches the one given for triallyl isocyanurate in the Aldrich IR Spectra Catalog (7).

Current information (6) indicates that the other major component of F-178 is the bis-maleimide of methylene dianiline. We are currently attempting to obtain an authentic sample of this material for confirmation by spectral methods. The NMR spectra also indicate the presence of minor components which we have not yet identified.

Other Epoxy Resin Systems

Since little published data on the C-13 and proton NMR characteristics of DGEBA and cycloaliphatic epoxy systems exist, we have had to obtain survey spectra of a wide variety of these materials. These reference data have helped in the identification of components added to the TGMDA/DDS systems, Narmco 5208 and Fiberite 934. Formulators may add other materials to the resins they use in high temperature epoxy/graphite prepregs in order to improve handling or processing. Some results of our C-13 NMR studies of epoxy resins have been reported (1,2). Because our compilation of spectra may be useful in other polymer characterization laboratories, we are preparing a spectra catalog for publication as an NRL Report. The first volume covers epoxy resin systems.

FUTURE WORK

During FY77, the principal activities to be addressed in the Chemical Characterization Task are to:

1. complete the analysis, including quantitative proton NMR measurements, of Hexcel F-178;

2. produce and distribute Volume 1 of the NMR Spectra Catalog; investigate computerization of catalog information;

3. develop rapid and reliable analytical techniques for the $C_{10}$ diamide and other precursors to phthalocyanine resins;

4. investigate methods for determining compositional changes in prepreg materials due to thermal aging (in cooperation with the Composites Fabrication Task);

5. characterize new materials as received;

6. begin quality control parameter definition of selected resin system(s).

## SUMMARY

The Chemical Characterization Task of the NRL-V/STOL Program has investigated a number of high temperature resin systems and epoxies. The primary analytical tools were C-13 and proton NMR spectroscopy. Detailed analyses were started on Narmco 5208, Hexcel F-178 and NRL's C-10 diamide precursor to polyphthalocyanine resins. Narmco 5208 was found to contain the modified epoxy, SU-8, in addition to the main components, TGMDA and DDS. Hexcel F-178 appears to be a blend of the bismaleimide of methylene dianiline and triallyl isocyanurate and some yet unidentified minor components. Work will continue on F-178 to quantify the major components as well as to identify the minor components. Improved analytical methods must be developed for polyphthalocyanine precursors. The NMR spectral information obtained in this program will be published.

## ACKNOWLEDGEMENTS

We gratefully acknowledge helpful exchanges of information and samples with C. A. May and J. Carpenter. Dr. S. A. Sojka, Mr. John Kopfle and Miss Dale Birkle assisted with some of the experimental work.

## REFERENCES

1. "Carbon-13 Fourier Transform NMR - An Important New Analysis Tool," W. B. Moniz, C. F. Poranski, Jr. and S. A. Sojka, Report of NRL Progress, August 1975.

2. "C-13 NMR Characterization of Epoxy Resins," C. F. Poranski, Jr. and W. B. Moniz, Coatings and Plastic Preprints, 36, No. 2, 139 (1976).

3. Epi-Rez SU-8 Technical Data Sheet, Celanese Resin Systems, no date.

4. C. A. May, private communication (AFML Report in preparation).

5. J. F. Carpenter, Second Quarterly Progress Letter for Contract No. NOOO19-76-C-0138, Quality Control of Structural Nonmetallics, 15 Jan 1976 to 14 Apr 1976.

6. "Characterization of a Polyimide Matrix for Fiber Composites," L. S. Penn, E. T. Mones and T. T. Chiao, SAMPE Quarterly, 7, No. 2 (1976).

7. "The Aldrich Library of Infrared Spectra," 2nd Edition, C. J. Poucherts, Ed., Aldrich Chemical Co., Inc., Milwaukee, WI, 1975, spectrum #427C.

bis(N,N-Di(2,3-epoxypropyl)-4-aminophenyl)methane (TGMDA)

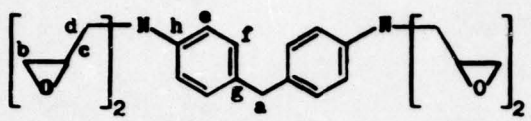


Source: Ciba-Geigy MY720

Solvent: 10% Acetone*

Assignments:

| | | | |
|---|---|---|---|
| a | 39.9t | h | 146.9s |
| b | 45.1t | i | |
| c | 50.5d | j | |
| d | 53.2t | k | |
| e | 112.7d | l | |
| f | 129.5d | m | |
| g | 130.5s | n | |

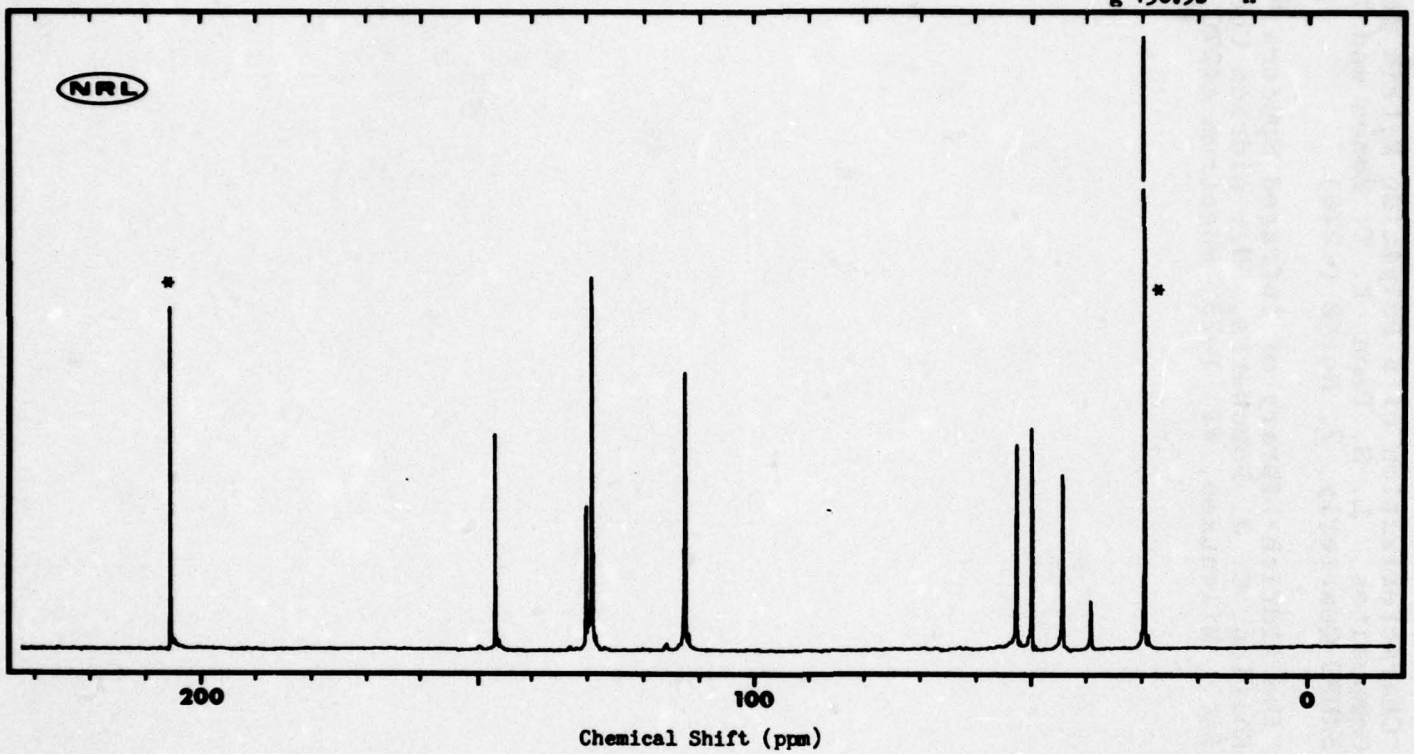


Fig. 1 — Carbon-13 NMR spectrum of bis(N,N-di(2,3-epoxypropyl)-4-aminophenyl)methane

bis(4-Aminophenyl)sulfone (DDS)

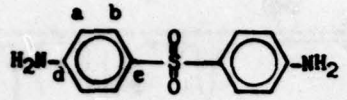


**Source**: Aldrich A7480-7

**Solvent**: 50% Acetone*

| Assignments: | | | |
|---|---|---|---|
| a | 113.6d | h | |
| b | 128.9d | i | |
| c | 129.7s | j | |
| d | 152.3s | k | |
| e | | l | |
| f | | m | |
| g | | n | |

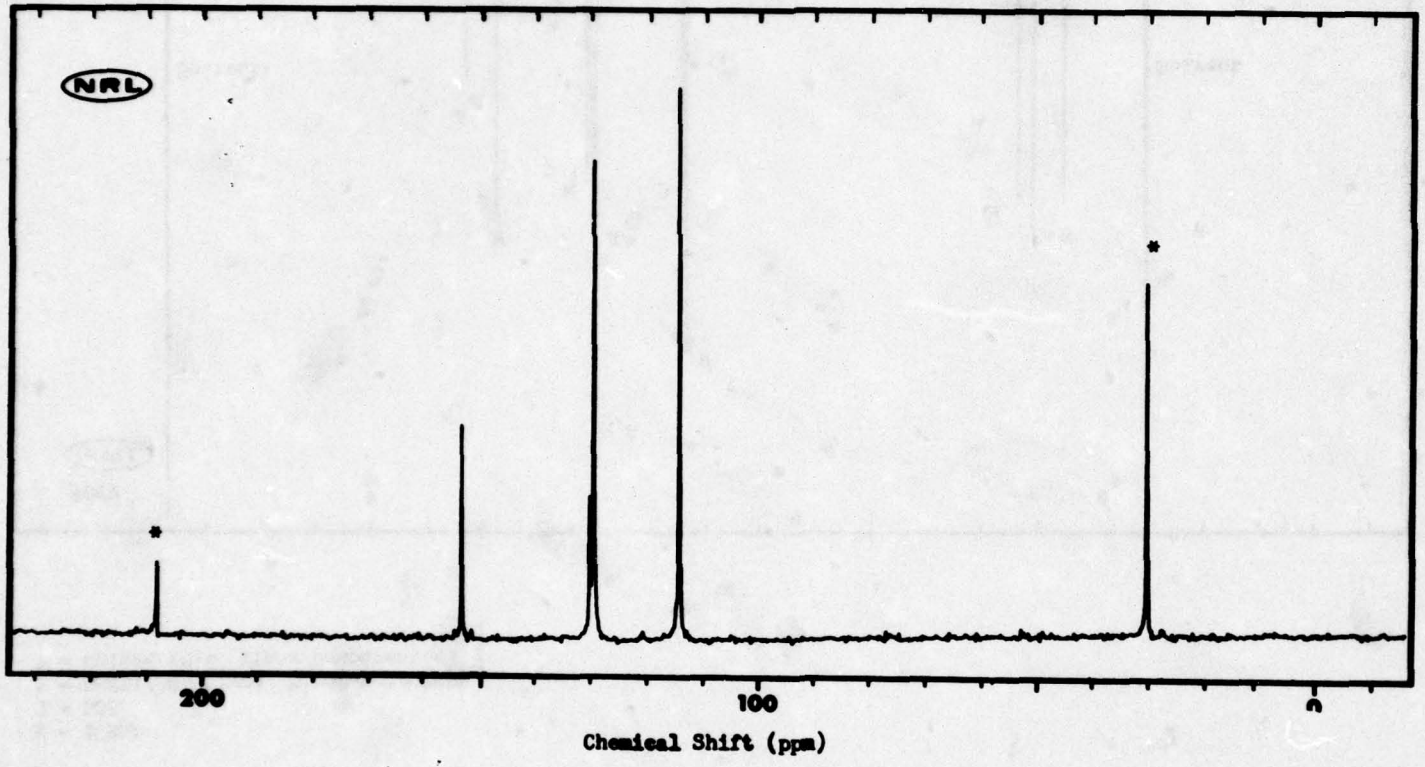


Fig. 2 — Carbon-13 NMR spectrum of bis(4-Aminophenyl)sulfone

Narmco 5208 in Acetone (50%)

M = TGMDA
S = DDS
I = DGEBA/SU-8 Type Minor Component
? = Unidentified Minor Component(s)

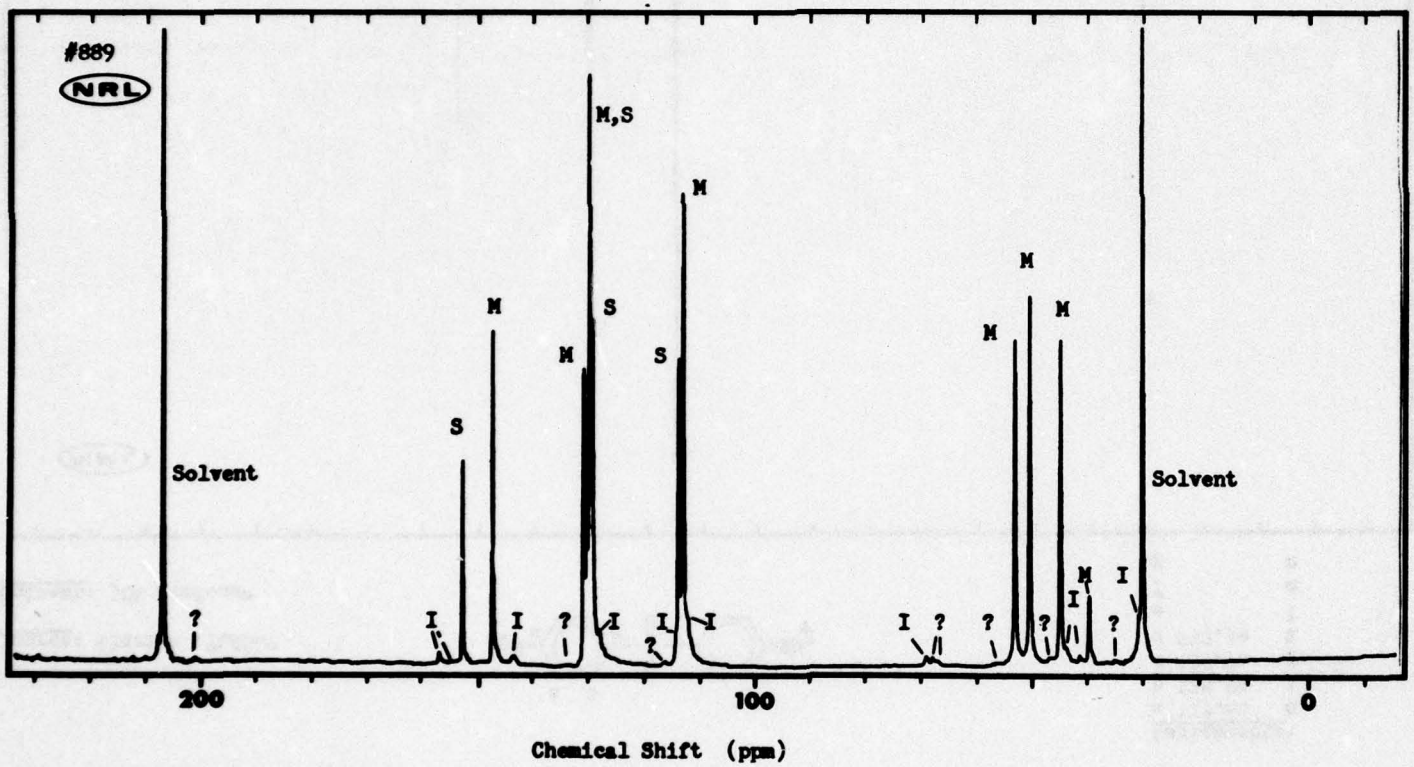


Fig. 3 — Carbon-13 NMR spectrum of Narmco 5208 in acetone

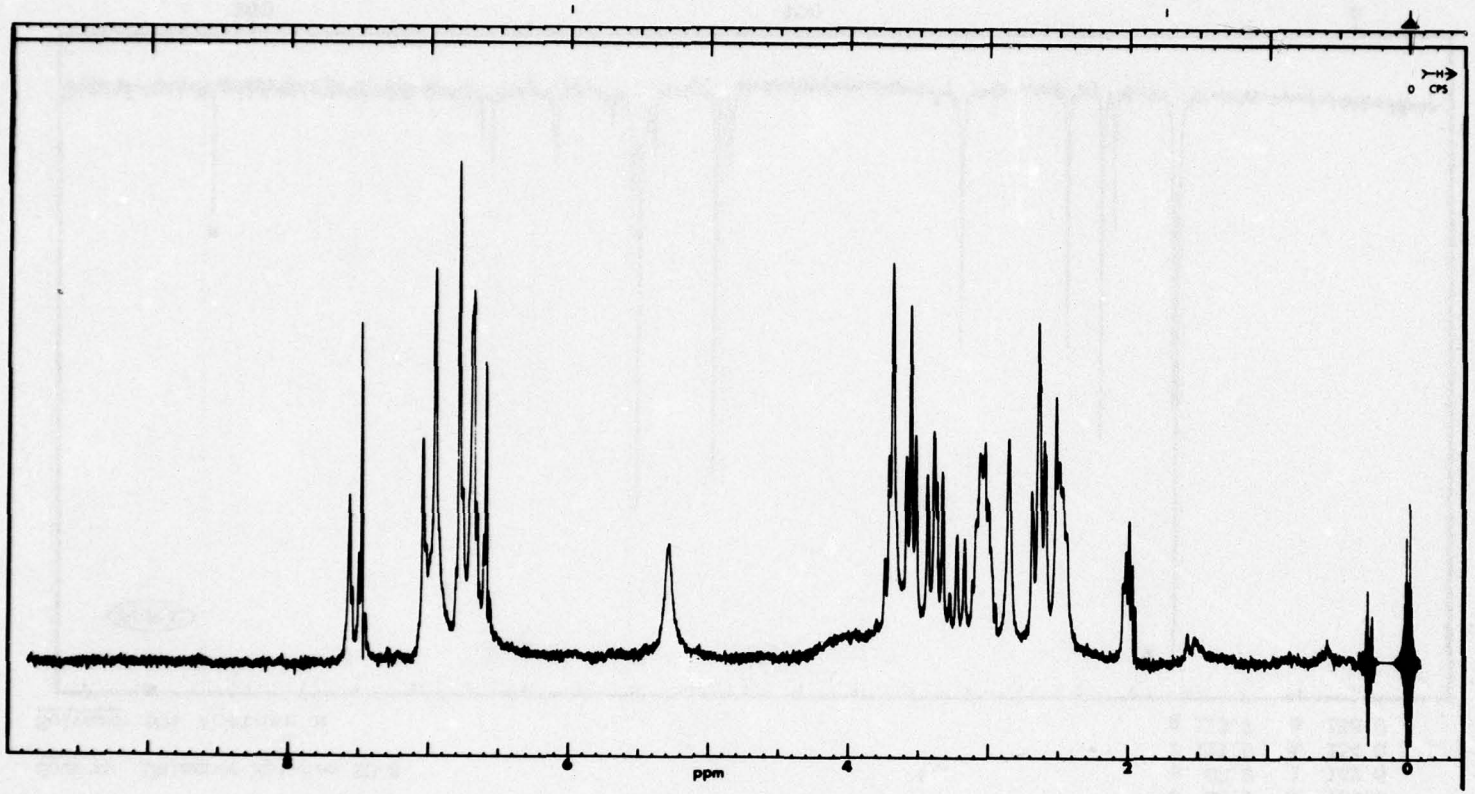


Fig. 4 — Proton NMR spectrum of Narmco 5208 in hexadeutero-acetone.
The multiplet at 2 ppm is due to the solvent.

Epoxy Resin, Polyfunctional

Source: Celanese Epi-Rez SU-8

Solvent: 50% Acetone ×

Assignments:

| | | | |
|---|---|---|---|
| a | 30.9 | h | 124.7 |
| b | 41.6 | i | 127.3 |
| c | 43.9 | j | 128.8 |
| d | 50.0 | k | 134.0 |
| e | 69.2 | l | 142.6 |
| f | 111.0 | m | 154.0 |
| g | 113.7 | n | 156.0 |

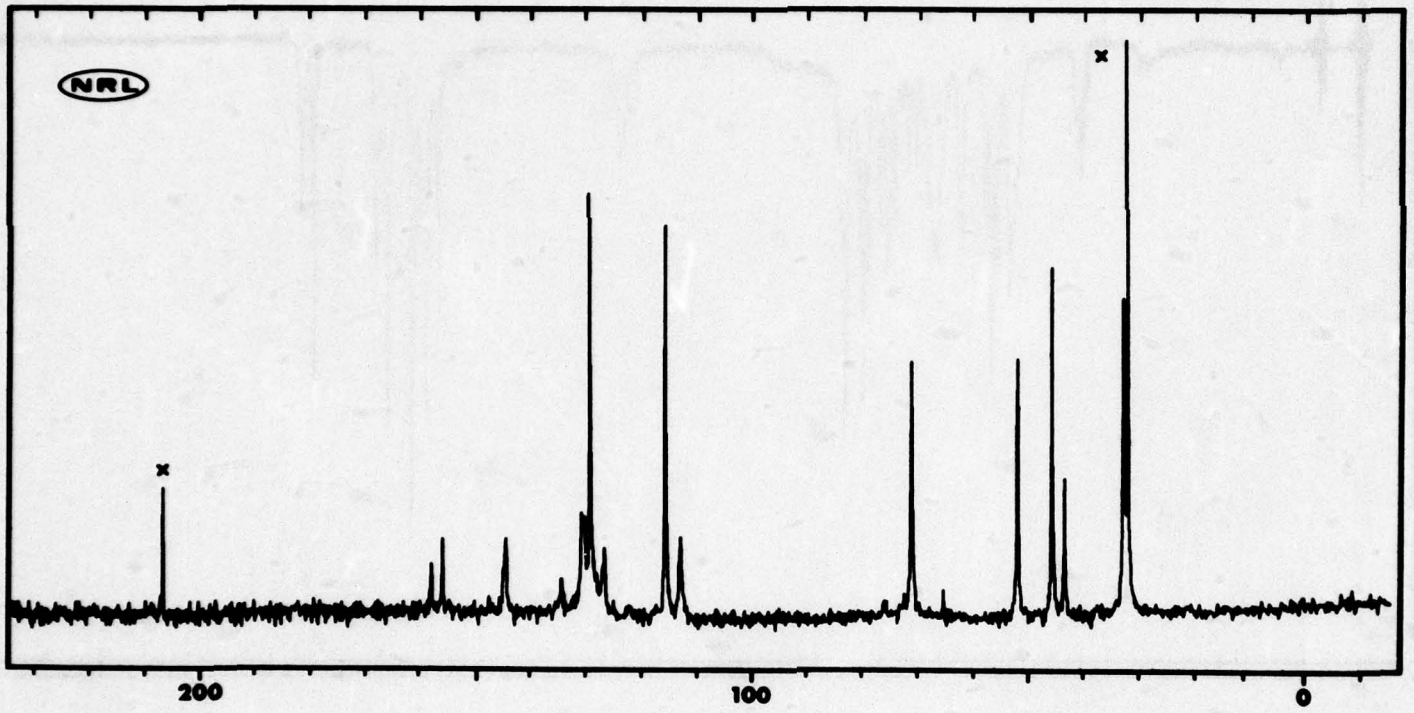


Fig. 5 — Carbon-13 NMR spectrum of SU-8

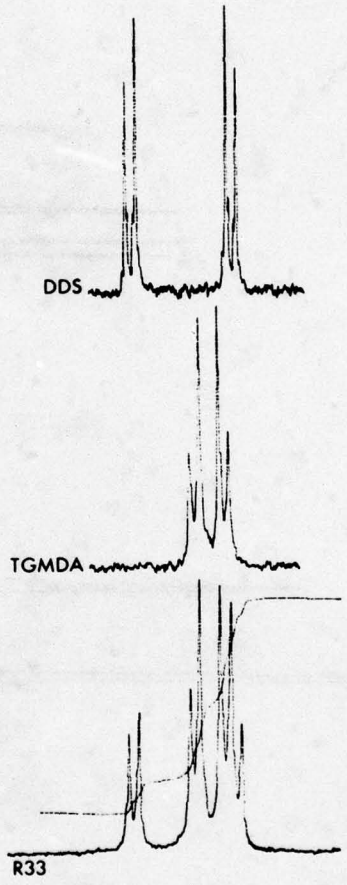


Fig. 6 — Proton NMR spectra of the aromatic regions of DDS (top), TGMDA (middle), and a resin system based on them (bottom). An integral of the resin system spectrum is superposed.

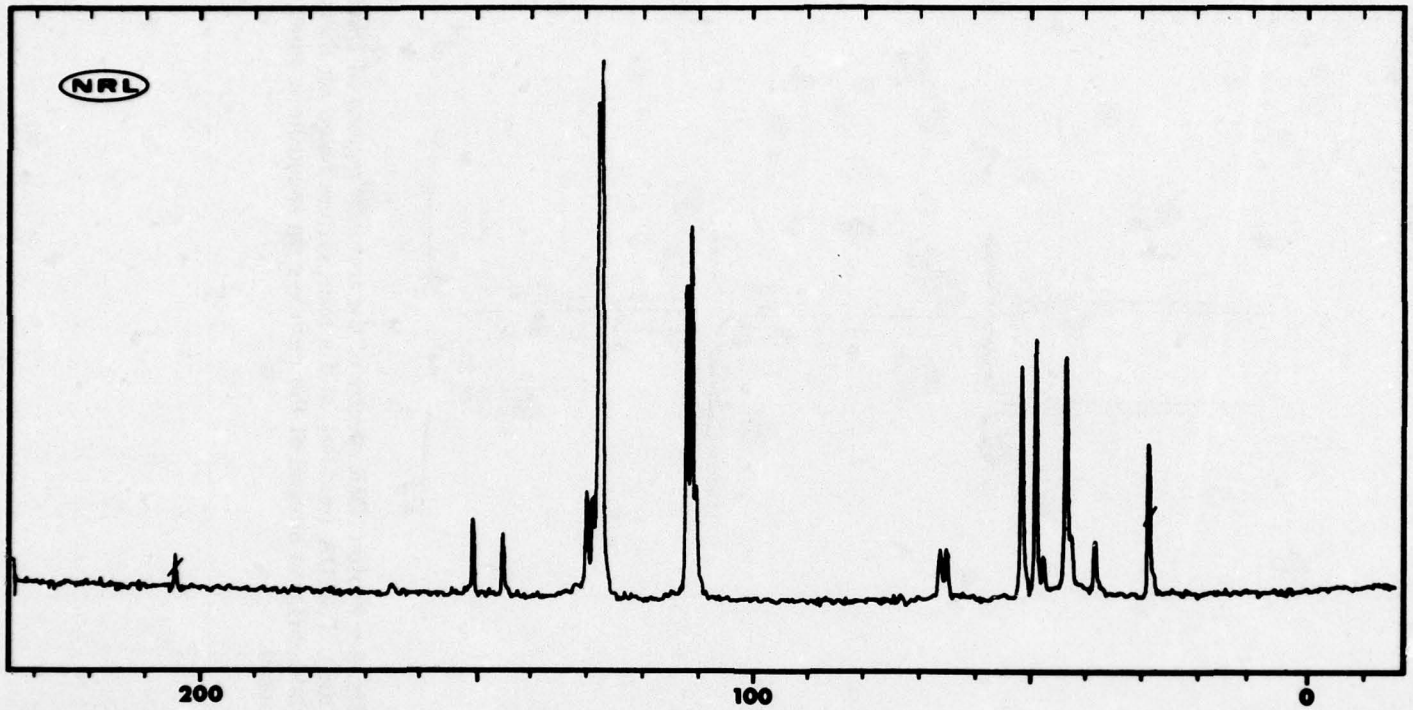


Fig. 7 — Carbon-13 NMR spectrum of Fiberite 934 in acetone.
The solvent peaks are indicated by the slash (/).

Epoxy Novolac Resin

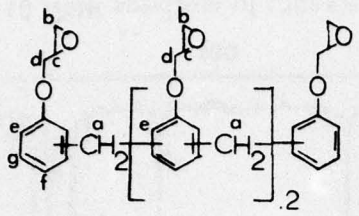

Source: Dow D.E.N. 431

Solvent: 20% $CHCl_3$ ✖

Assignments:

| | | | |
|---|---|---|---|
| a | 29-40 | g | 126-130 |
| b | 43.3 | h | 132.6 |
| c | 49.2 | | 133.2 |
| d | 68.0 | i | 153-156 |
| e | 110.8 | | |
| | 113.6 | | |
| f | 120.1 | | |

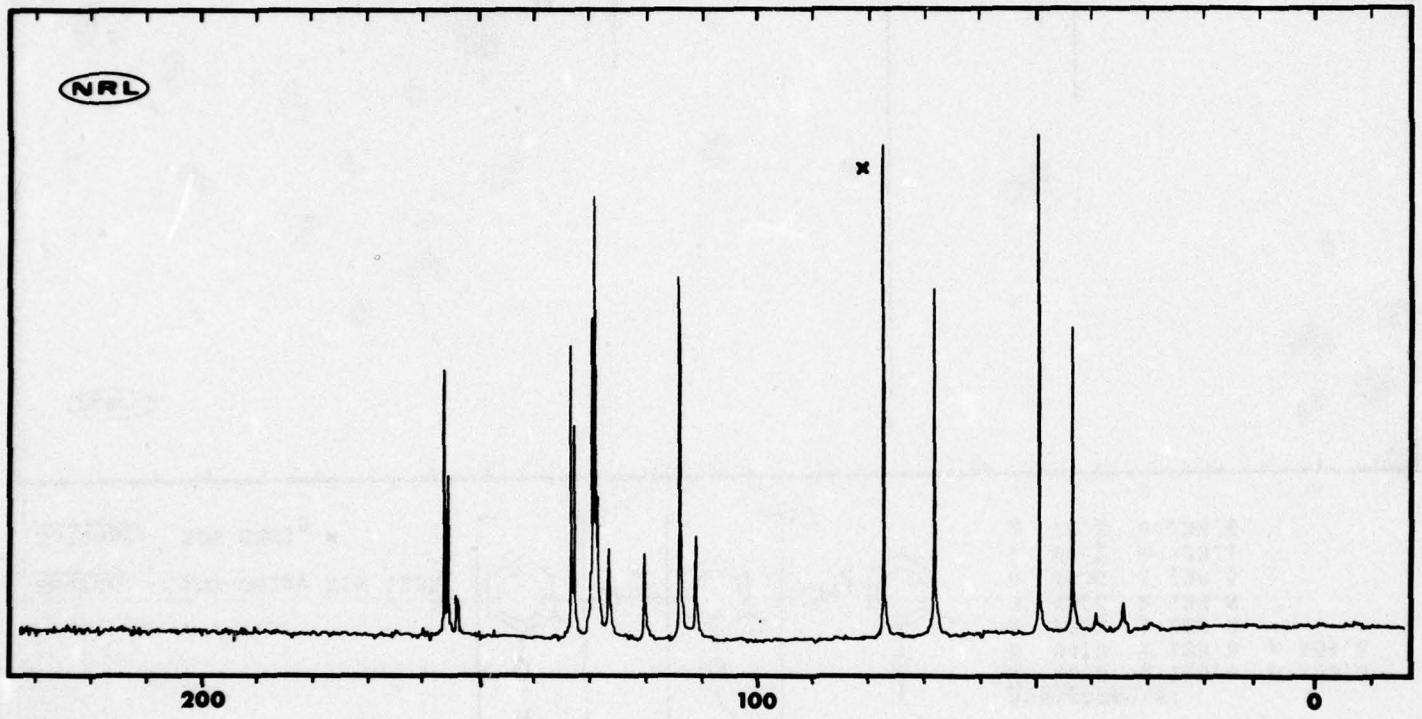


Fig. 8 — Carbon-13 NMR spectrum of Dow D.E.N. 431

Epoxy Novolac Resin

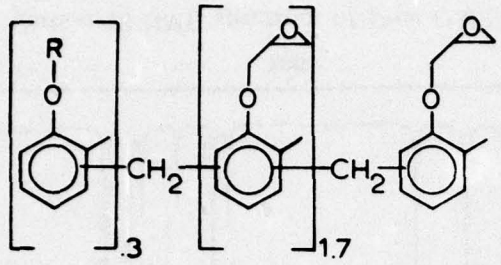


Source: Ciba-Geigy ECN 1235

Solvent: 50% $CHCl_3$ ×

Assignments:

| | | | | | |
|---|---|---|---|---|---|
| a | 15.6 | h | 110.6 | o | 152.6 |
| b | 34.2 | i | 123.3 | p | 154.2 |
| c | 39.4 | j | 126.0 | | |
| d | 43.6 | k | 128.6 | | |
| e | 49.6 | l | 130.5 | | |
| f | 68.2 | m | 133.1 | | |
| g | 72.8 | n | 136.4 | | |

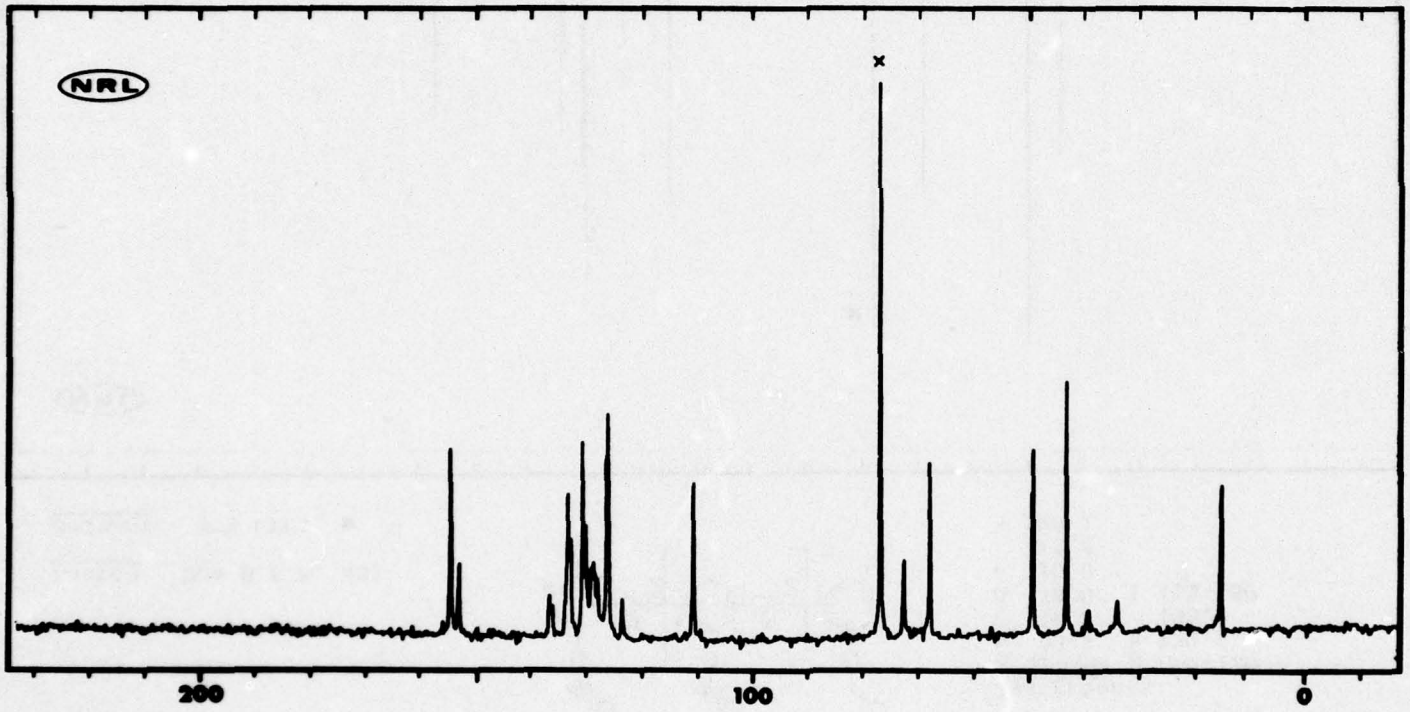


Fig. 9 — Carbon-13 NMR spectrum of Ciba-Geigy ECN 1235

$C_{10}$ Diamide

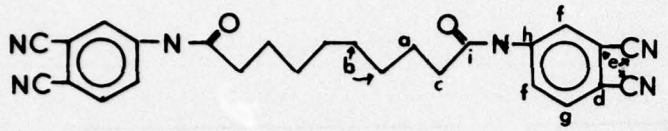


Source: NRL, Code 6120

Solvent: Dimethyl formamide ✖

Assignments:

| | | | |
|---|---|---|---|
| a | 25.6 | g | 135.4 |
| b | 29.8 | h | 144.7 |
| c | 37.6 | i | 173.3 |
| d | 108.5 | | |
| e | 116.4 | | |
| f | 123.4 | | |

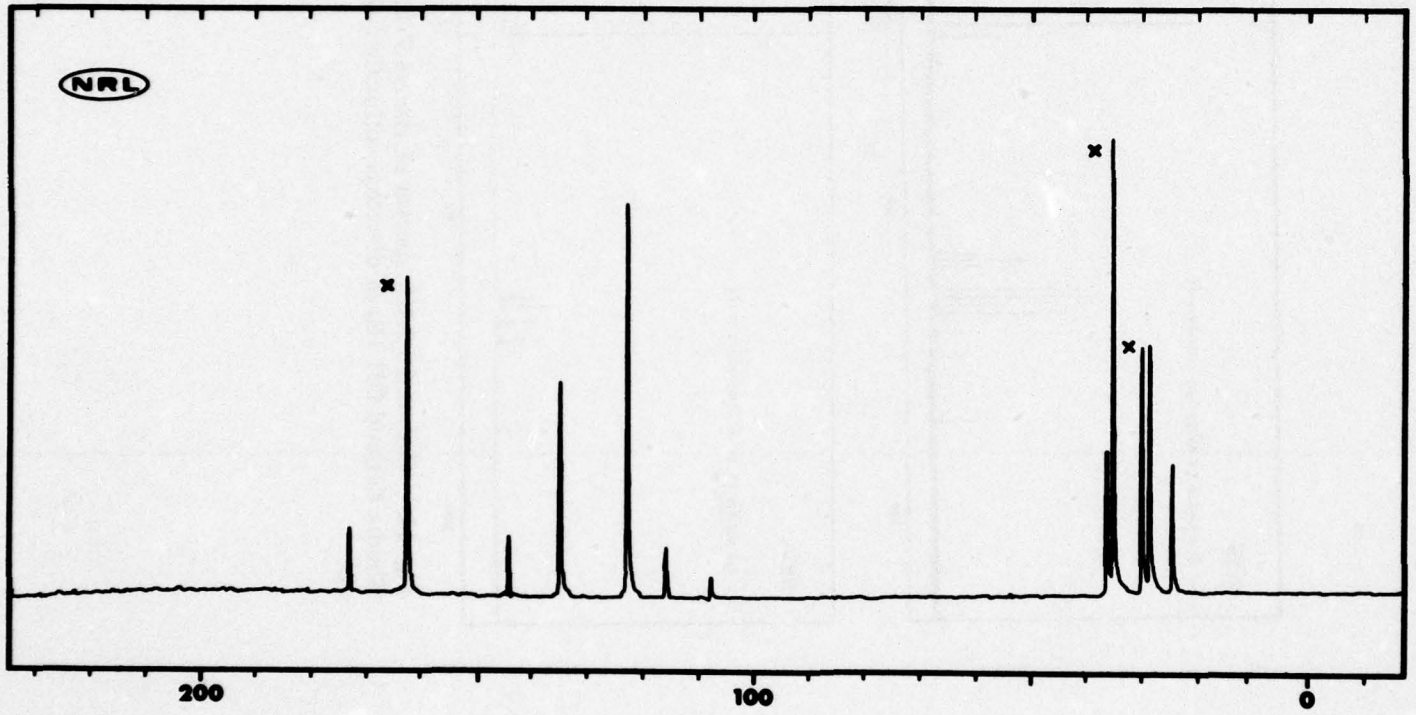


Fig. 10 — Carbon-13 NMR spectrum of $C_{10}$ Diamide

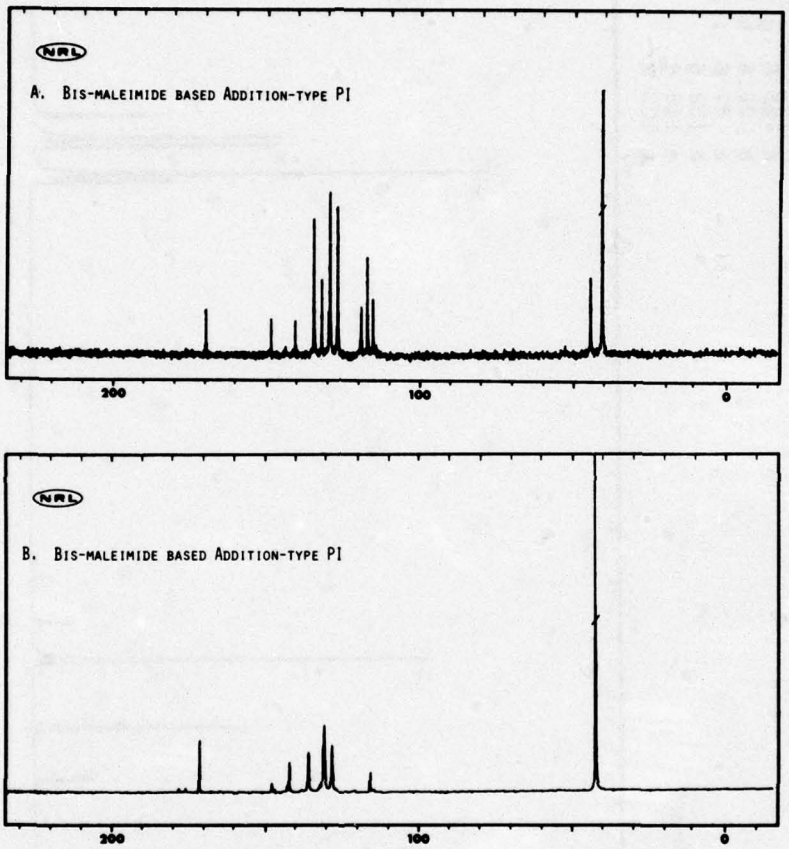


Fig. 11 — Carbon-13 NMR spectra of Hexcel F-178 (A) and Rhodia Kerimid 601 (B) in dimethyl sulfoxide (indicated by /).

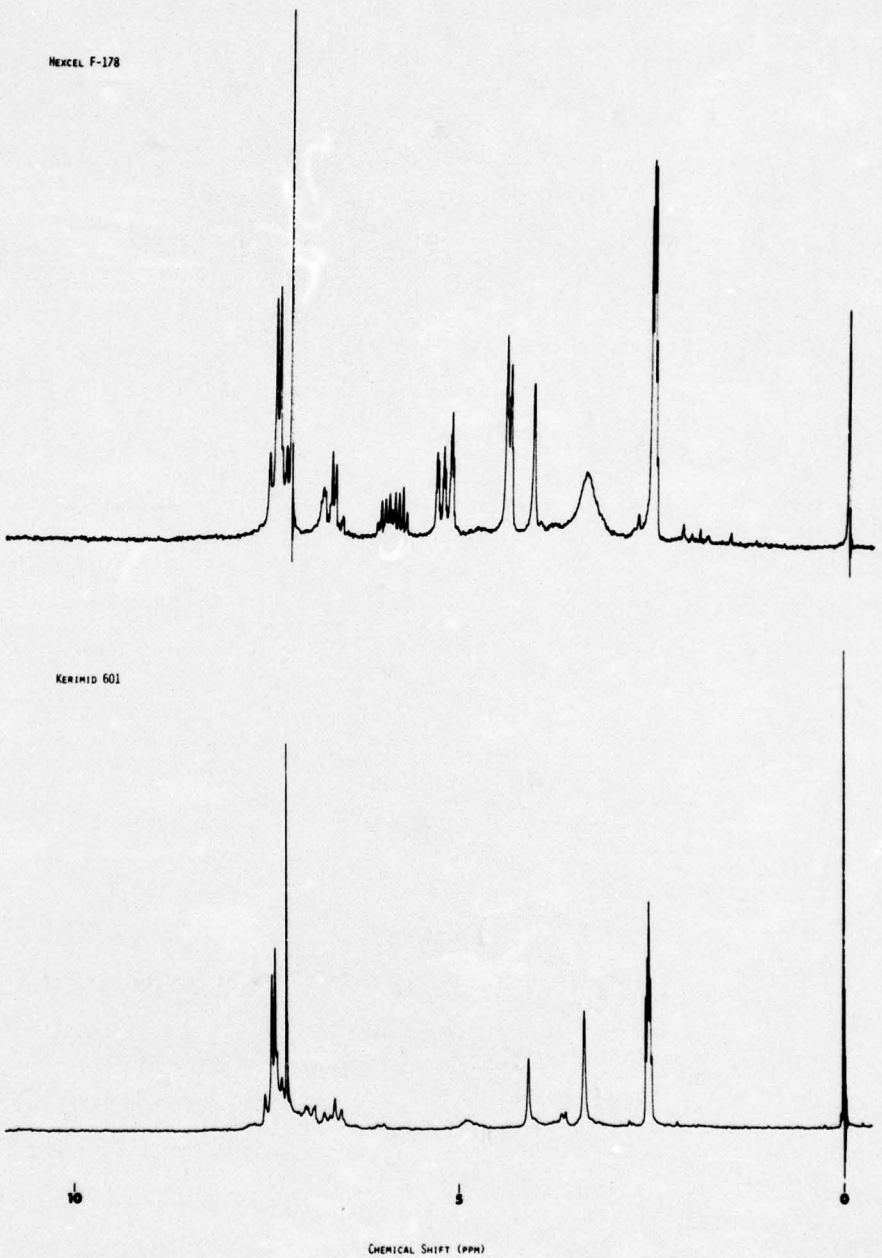


Fig. 12 — Proton NMR spectra of Hexcel F-178 (upper) and Rhodia Kerimid 601 (lower) in hexadeutero-dimethyl sulfoxide, DMSO-$d_6$. In each spectrum the line at 0 ppm is due to the internal reference, tetramethylsilane, and the lines at 2.5 ppm are due to the solvent, DMSO-$d_6$. The line at 3.5 ppm (broad in the F-178 spectrum, narrower in the 601 spectrum) is due to water.

# TASK D. RADIATION CURING

F. J. Campbell, W. Brenner*, L. M. Johnson and M. E. White
Radiation Effects Branch
Radiation Technology Division

## INTRODUCTION

The utilization of industrial electron accelerator equipment for radiation curing of polymeric materials has reached commercial maturity in several areas. Specifically, it has become a cost-effective processing method for cross-linking plastic film, rubber sheet, wire insulation and heat-shrinkable tubing. The objectives of the Radiation Curing Task are to apply this technology to the curing of high performance adhesives and composites for aircraft parts and assemblies and to demonstrate the performance stability of the products. Additional advantages will be detailed in both the versatility and economics of these methods.

A typical example of a commercial application is the vulcanization of sheet rubber by an electron accelerator, replacing the conventional batch autoclaving process. A study made of the comparative energy utilization efficiency gave values of 40% to 60% for an electron accelerator versus 1% to 5% for heat curing systems (1). Figure 1 shows the layout of a typical Dynamitron electron-beam processing facility for the radiation curing of sheet materials. The accelerator equipment is basically the same for all types of product applications, whereas the vault and conveyor system can be varied to accomodate many different products. In the design of radiation curing facilities consideration must be given to the ease of product transport while providing absolute radiation safety to the workers. Because electrons have limited range, one is concerned, not with the direct electron hazard, but rather with the secondary radiation, Bremstrahlung, produced when the electrons are stopped. These X-rays are highly penetrating and, therefore, the heavy shielding of concrete or other dense material is required between the target materials and the personnel area.

*Division of Applied Science, New York University

Some advantages of curing adhesives and composites for aerospace and missile construction with electron beam radiation energy at room temperature are listed in Table I. One of the most important advantages is that materials having different thermal expansion coefficients can be bonded without the introduction of residual heat-shrink stresses that usually result from conventional heat curing techniques, which require heating to temperatures up to 150°C, and sometimes higher. As a result of the high temperatures, residual stresses of unknown magnitude are often left in the polymer adhesives and/or the metal adherends. In some instances these stresses are larger than the ultimate composite strength, especially in transverse directions, and microcracks develop in the resin matrix.

The use of heat cured adhesives may also be prohibitive in certain structures because of the heat distortion or degradation of some components during the curing process. For example, the bonding of graphite fiber-epoxy composite laminates to the aluminum or titanium skins of aircraft presents serious problems because the thermal coefficients of expansion of the composite and the metals differ so radically.

Where adhesives can be used, it is normally necessary to heat the entire assembly in one curing cycle. This requires massive curing ovens for structures such as airplane wings or missile bodies, which wastes quite substantial quantities of energy. When performed by electron beam radiation, the cure can be completed in a much shorter time, and the amount of energy expended to accomplish it is much less. For example, one aircraft manufacturer estimates that a typical sub-assembly requiring a normal autoclaving heat cure cycle which takes 4 hours could be completely cured in about 40 minutes with an industrial electron accelerator (2). Moreover, a completely radiation-cured resin does not contain volatile products, since totally reactive liquid adhesive systems can be used.

Looking into the future, it may be practical to accomplish the adhesive cure on designated spots or seams where a repair patch might be needed on a damaged aircraft or ship component by means of a remote controlled trunnion-mounted accelerator. The Varian Linatron pictured in Figure 2 would be adaptable for this purpose. By removing the X-ray producing element normally installed for radiographic inspection, this unit becomes a 8 to 10 meV electron beam source that can be directed to scan the bond line.

Radiation curing should also be ideal in the new hybrid joining technique of Weld-Bonding because radiation-curable adhesives have the following characteristics in addition to those given above: (1) controlled viscosity for good surface wetting and flow, (2) long pot-life since no catalyst is used, and (3) minimal pre-cure from the heat of the welding step.

## PROGRESS

### Vinyl Ester Resins

The first part of this program consisted of a study to screen a wide variety of commercially available resins which appeared to be most suitable for radiation curing by virtue of their chemical structure. Some of the most readily available and previously characterized types are the vinyl ester-modified epoxy resins. Those contain selected vinyl-terminated high temperature backbone molecules which have been found to be readily cross-linked by typical free-radical addition reactions. Six different products were selected for initial testing based on the manufacturers' claims of high temperature stability and high degree of reactivity.

Of those initially screened, the commercially available Epocryl 12 prepolymer was selected for a comprehensive study of the effects of variations in formulation and radiation dose. The preparation of this resin, which is typical of the reaction between an epoxy and an acrylic acid, proceeds as follows:

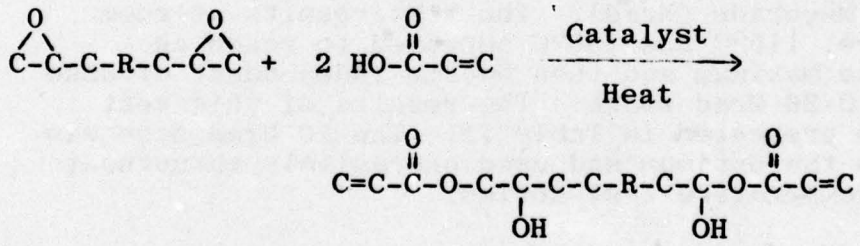


When R is the bisphenol A group, we have

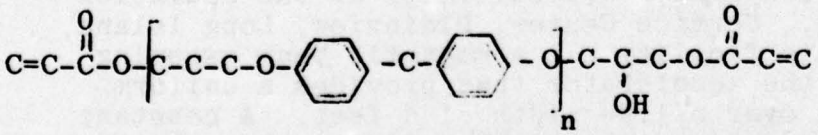

Depending on the size of n, the resulting linear molecules tend to be either high viscosity liquids or solids at room temperature, which inhibits the ease of application as room

temperature radiation curable adhesives. It may also be desirable to enhance the reactivity and the degree of cross-linking. Therefore, by formulating with vinyl functional monomers which are fluid at room temperature or slightly above, solutions can be obtained with viscosities appropriate for adhesive applications or composites fabrication and with more unsaturated sites for reaching higher cross-link densities than the neat Epocryl resin itself.

Figure 3 shows the structural formulas of three such monomers that were utilized in the resin formulation study. The supplier of triallyl cyanurate (TAC) claims that a resin formulated with TAC will retain its high temperature strength in the range of 50 to 120°C higher than the non-TAC modified resin, probably because of its trifunctionality. Other typical monomers that are useful are divinyl benzene (DVB) (which is difunctional) and styrene (which is monofunctional).

Formulations of each of these monomers were prepared with the Epocryl 12 resin and evaluated as adhesives for bonding aluminum to aluminum in single lap-shear test specimens using 7075 aluminum alloy. Surfaces were prepared by an acid-chromate (FPL) etching procedure prior to specimen assembly.

An initial study was conducted to determine the effect of radiation dose on bond strengths of the different formulations. Single lap-shear specimens were prepared and electron-beam irradiated to nominal doses of 8, 10, 20 and 30 megarads (Mrad). The test results at room temperature, 115°C and 150°C appeared to reach an approximate maximum and then became independent of dose over the 10-30 Mrad range. The results of this test series are presented in Table II. The 10 Mrad dose was adopted as the optimum and used exclusively throughout the high temperature test series.

Throughout the Epocryl 12 formulation test series, the electron beam irradiations were performed with the 3-MeV Dynamitron electron accelerator at the Radiation Dynamics, Inc., Service Center, Plainview, Long Island, New York. This facility has a magnetic beam sweeping accessory on the accelerator that provides a uniform electron flux over a line width of 4 feet. A constant speed conveyor system carries the objects through the line of electrons so that uniform, large-area irradiations are obtainable.

The entire facility is similar to that illustrated in Figure 1, except for the difference in the conveyor. At the Service Center the conveyors are flat-bed cars on a continuous moving track. Figure 4 shows one of these cars with a medical unit being sterilized as it passes under the beam-sweeper at a speed of 0.15 m/s. Since the dose per pass at the level of the car platform is nominally 2.5 Mrad for a beam current of 25 ma, the 10 Mrad dose deposited in the adhesive test specimens was obtained in four passes.

Further experiments were conducted on specimens prepared, irradiated and tested in the same manner to obtain a range of bond strength versus temperature data for three different formulations of Epocryl 12 with TAC, DVB and styrene.

The specimens were bonded and irradiated at room temperature with only contact pressure. A comparison was obtained with conventional heat cured specimens which contained 0.5% benzoyl peroxide added to each of the above formulations. These were cured in accordance with the manufacturer's recommendation of 2 hours at 80°C under pressure. Each group of specimens was then tested at room temperature, 115°C, 150°C, 200°C and 260°C. The results of this series are tabulated in Table III and the data points are plotted graphically in Figure 5. The values given are averaged from five specimens each, in which the extreme value ranges were typically in the order of ±15%. The resulting data show that both the Epocryl 12/DVB and the Epocryl 12/TAC adhesive systems can be radiation cured at ambient temperatures and have superior strength retention at 150°C; even at 260°C there is approximately 40% retention of initial strength. The Epocryl 12/styrene system shows significantly greater losses at the elevated temperatures. Radiation curing produced lap-shear strengths which were greater than those of the corresponding heat-peroxide curing in all three systems.

## High Temperature Resin Survey

In addition to the vinyl ester resin survey the program has maintained a forward objective of determining the radiation cross-linkability of other types of resins as well. The selections were governed by the claimed capabilities and availabilities of either commercial or research-grade resins that should have high-temperature or environmental stability, or both. As such, their potential for radiation-induced cross-linking reactions

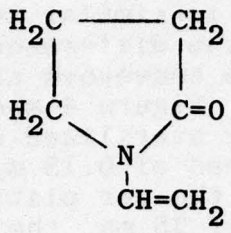

It has been reported to be a radiation crosslinkable monomer that has been used as a reactive diluent in radiation curable coating systems. For the radiation curing experiments described below, mixtures of 1 part VP to 2 parts resin were employed.

$C_{10}$ Diamide/VP

The $C_{10}$-polyphthalocyanine (N,N'-bis-(3,4-dicyanophenyl)decandiamide) is readily soluble in N-vinyl-2-pyrrolidone to give a clear, straw-colored, low viscosity liquid. At a radiation dose of 10 Mrad the solution gelled and became a soft gum, but further doses up to 90 Mrad produced no additional change.

Kerimid 601/VP

The Kerimid 601/VP mixture required heating to about 35°C to form a clear, reddish-brown solution that remained clear on cooling. Initial radiation curing experiments were conducted on the bulk material with gamma-rays at increments of doses from 2 to 30 Mrad. A glassy-state was reached at the 2 Mrad dose. DSC and TMA/P analyses performed using a DuPont 990 Thermal Analyzer System demonstrated that the glass transition temperature increased with dose to a maximum in the 20 to 30-Mrad region. Figure 6 shows scans of the 30-Mrad specimens, indicating a $T_g$ of about 325°C.

F-178/VP

The F-178 resin is of a pasty consistency at room temperature and becomes a clear, dark brown syrup when mixed with VP. As with the Kerimid 601/VP, the DSC and TMA/P analyses showed that about the same increase in cure versus dose occurred until in the region of 25-30 Mrads it reached a maximum. As shown in Figure 7, at 30 Mrad the $T_g$ was about 300°C.

is essentially unknown. Many of these resins are solids that undergo cross-linking reactions at the melting point; they are therefore, not as readily adaptable to the preparation of simple tests for radiation curability at room temperature as liquids. Since it was not feasible to visually observe for radiation-induced gellation or cross-linking in these solid materials, thermal analysis methods were applied to determine whether cross-linking by radiation occurred.

The materials were irradiated to appropriate doses by exposures to gamma-rays in the NRL Cobalt-60 Source Facility. Testing by Differential Scanning Calorimetry (DSC) and Thermal Mechanical Analysis, penetration mode (TMA/P), was carried out to determine if crosslinking occurred, indicated by an increase in glass transition temperature ($T_g$) or melting point. With other resins which were obtained in a fluid or soft solid form, a radiation-induced reaction was observable as a change in viscosity or conversion to a solid form. Table IV presents a summary of those examined to date and the resulting qualitative observations.

Formulating High Temperature Resins

Many of the high temperature resins listed above are solids or semi-solid, such as the F-178. If they are to be applied as spreadable liquid or paste adhesives, they must be formulated with a reactive monomer diluent. A study was conducted to determine the solubilities of these resins in several functional monomers. The resins and monomers evaluated are listed in Table V along with qualitative estimates of their solubilities. Proportions of 1:1 by weight were used primarily. Where solubility was low, greater amounts of monomers were tried; finally, each mixture was heated to 65°C as a last resort to increase the probability of obtaining complete solubility. Only the three mixtures in the lower right of the table formed clear solutions, although the HR-600:VP reached an almost clear mixture at the elevated temperature.

N-vinyl-2-pyrrolidone (VP), whose structure is shown below, was chosen as a reactive solvent because of its chemical similarity to N-methyl-2-pyrrolidone (NMP), one of the few solvents known for the polyimide prepolymers.

With these indications that 30 Mrad cures would produce materials with a high glass transition temperature, the solutions of the above polyimide resins in VP were evaluated as adhesives by single lap-shear tests. Electron-beam curing was performed in the NRL 2 MeV Van de Graaff accelerator to doses of 30 Mrad. This accelerator does not have a beam scanner, so irradiation was performed one specimen at a time at a dose rate of 0.1 Mrad/sec. with a beam current of 35 μa. By a thermocouple experiment on a dummy specimen it was determined that the adhesive in the specimens reached a temperature of approximately 54°C during the irradiation. Cured specimens were tested at room temperature and at 150°C. The values reported in Table VI are averaged from five specimens each. Results confirm the high softening points of these materials. However, the low shear strength values and the brittle nature of the adhesive bond lines suggested that they were overcured at 30 Mrad. Further studies will be conducted to maximize the desired properties of the high-temperature resin formulations.

Radiation-Cured Vinyl Pyrrolidone

One of the many advantages of radiation curing is the capability to induce partial cures in either the monomer or the monomer-resin formulation. Such cure advancement steps can be conducted at room temperature. No further reaction occurs until additional radiation is applied during processing. Thus, the viscosity of an adhesive formulation can be modified by pre-irradiation to obtain optimum spreading characteristics on the adherend surfaces without the need for raising temperature or pressure. A demonstration experiment of this capability was conducted with vinyl pyrrolidone. A cylindrical container of the fluid monomer was irradiated in the NRL cobalt-60 source in increments of dose until the viscosity reached the desired spreading consistency at a dose of 0.65 Mrad.

Vinyl pyrrolidone solidifies when irradiated to 1 Mrad and continues to harden with increased doses. Solidification is accompanied by a slight expansion of the material, which was measured to be approximately 4%. Post-cure heating for 2 hours at 177°C then produced only about 1% net shrinkage in the specimen cured with a 30 Mrad dose. Compared to the fact that heat/peroxide curing produces a 16% shrinkage, this characteristic adds significantly to the advantages of radiation curing over conventional procedures. Radiation curing should also make it possible

to produce relatively strain-free bonding in adhesive joints and in fiber-reinforced composites.

## FUTURE PLANS

1. Studies of the radiation curing potential of the materials described here, as well as other commercially available products that are described as radiation curable, will be continued.

2. The most promising candidates will be studied more extensively to optimize the formulations and irradiation conditions for maximum bond strength and high temperature performance, and to minimize interfacial stresses.

3. The application of these materials for joining aluminum, titanium and composite materials will be demonstrated.

4. These resins and others will be evaluated for suitability as the matrix in fiber-reinforced composites.

5. The experimental program will be directed toward the selection and processing of materials to withstand severe environments typical of service conditions. Laboratory tests will be performed to demonstrate the improvements that can be achieved by radiation curing processes.

## REFERENCES

1. K. H. Morganstern, "Processing With Radiation," Chemtech, 612-615, Oct. 1974.

2. A. B. Hoefelmeyer and M. S. Howeth, "Radiation Curing in the Aerospace Industry," General Dynamics Report No. SMD-005, 1 Sept. 1968.

Table I

ADVANTAGES OF RADIATION CURING

Room Temperature Cure

- Stress-Free Joints.
- No Thermal Distortion

Saves Energy

- Eliminates need for Autoclave.

Avoids Air Pollution

- Solvent is Cured as Part of Resin.
- No Volatile By-Products.

Spot-Bonding Capability

Ideal for Weld-Bonding

Table II

Single Lap-Shear Strength versus Radiation Dose*
Al to Al (alloy 7075), Epocryl 12 Formulations

| Formulation | Test Temp. °C | Lap-Shear Strength (MPa)** | | | |
|---|---|---|---|---|---|
| | | 8 Mrad | 10 Mrad | 20 Mrad | 30 Mrad |
| Epocryl 12/DVB | 25 | - | 12.1 | 11.9 | 12.0 |
| | 115 | 11.4 | 11.8 | 11.6 | 11.8 |
| | 150 | 11.1 | 11.2 | 11.4 | 11.4 |
| Epocryl 12/TAC | 25 | - | 11.4 | 10.9 | 11.0 |
| | 115 | 10.8 | 10.8 | 10.7 | 11.0 |
| | 150 | 10.4 | 10.3 | 10.0 | 10.2 |
| Epocryl 12/Styrene | 25 | - | - | - | - |
| | 115 | - | 9.6 | - | 9.7 |
| | 150 | - | 8.5 | - | - |

*Electron beam irradiation at ambient temperature

** [psi] = 145 x [MPa]

Table III

Comparison of Radiation Cured and Heat Cured Formulations of Epocryl 12 (Shell)

Comparison of Single Lap-Shear Strength at Elevated Temperatures

| Formulation | Cure* | Single Lap-Shear Strength (MPa) | | | | |
|---|---|---|---|---|---|---|
| | | 25°C | 115°C | 150°C | 200°C | 260°C |
| Epocryl 12/DVB | Radiation | 12.1 | 11.8 | 11.2 | 6.3 | 5.0 |
| | heat/peroxide | | 11.3 | 10.9 | 5.4 | 3.5 |
| Epocryl 12/TAC | Radiation | 11.4 | 10.8 | 10.3 | 6.0 | 4.8 |
| | heat/peroxide | 10.2 | 10.5 | 9.9 | 5.2 | 3.1 |
| Epocryl 12/Styrene | Radiation | 9.2 | 9.6 | 8.4 | 4.1 | 1.7 |
| | heat/peroxide | 9.4 | 9.5 | 8.0 | 1.5 | |

*Cure Processes:

Radiation - Electron beam, 3-MeV Dynamitron, 10 Mrad

Heat/peroxide - 0.5% benzoyl peroxide, 2 hours at 80°C under pressure

Table IV

Radiation Effects on High Temperature Resins

| Trade Name | Manufacturer | Resin Type | Dose,(Mrad)* | Obervations |
|---|---|---|---|---|
| HR-600C | Hughes | acetylene-terminated polyimide | 30,90 | no change in DSC of powdered resin |
| Kerimid 601 | Rhodia | addition polyimide | 30 | change in DSC indicates reaction occurred |
| F-178 | Hexcel | addition polyimide | 30 | crosslinked to a hard piece, high $T_g$ |
| SR 5208 | Narmco | epoxy | 30 | no change in hardness of specimen |
| EKKCEL I-2000 | Carborundum | aromatic polyester | 30 | no change in DSC |
| Astrel | 3 M Co. | polyarylsulfone | 30 | no change in DSC |
| 200 P | ICI | polyethersulfone | 30 | no change in DSC |
| Plastilok 608 | Goodrich | thermosetting acrylic | 20 | tougher, less elongation |
| Montac 1349 | Monsanto | hot-melt adhesive | 5,10,20 | no change in DSC |
| Ricon 159 | Colorado Chem. Spec. | 1,2-polybutadiene in heptane | 20 | tough crosslinked solid. irradiated after solvent removed |

Table IV (continued)

| Trade Name | Manufacturer | Resin Type | Dose,(Mrad)* | Observations |
|---|---|---|---|---|
| Ricon 1595 | Colorado Chem. Spec. | 1,2-polybutadiene in vinyl toluene | 3,6,9,12 | crosslinking increases with dose from sticky gel to hard, tough solid |
| Ricon - 150 | Colorado Chem. Spec. | 70% 1,2 PBD, 30% 1,4 PBD | 20 | soft gum |
| Ricon - 157 | Colorado Chem. Spec. | Same, with lower viscosity | 20 | sticky, high viscosity fluid |
| Phthalocyanine | NRL | $C_{10}$ Diamide | 20 | no change (DSC) straw color |
| Fluoropolymer | NRL | fluorinated polyurethane | 16 | hard, tough film |

*Cobalt-60 source

Table V

Solubility of High Temperature Resins
in Vinyl Functional Monomers
(1:1 Mixtures)

| Resin | Type | Triallyl Cyanurate | Divinyl Benzene | Vinyl Pyrrolidone |
|---|---|---|---|---|
| I-2000 | aromatic polyester | insol | insol | insol |
| ASTREL | polyarylsulfone | slightly | slightly | slightly |
| HR-600 | acetylene terminated polyimide | insol | slightly | partly |
| K-601 | addition polyimide | partly | partly | very soluble |
| F-178 | addition polyimide | partly | partly | very soluble |
| $C_{10}$ Diamide | phthalocyanine | slightly | partly | very soluble |

Table VI

High Temperature Strength of
Radiation-Cured Polyimide Formulations

100 parts polyimide

50 parts vinyl pyrrolidone

Dose: 30 megarads

| Polyimide | single lap-shear strength, MPa* 25°C | 150°C |
|---|---|---|
| Kerimid 601 | 4.1 | 5.2 |
| Hexcel F-178 | 5.2 | 4.6 |

* [psi] = 145 x [MPa]

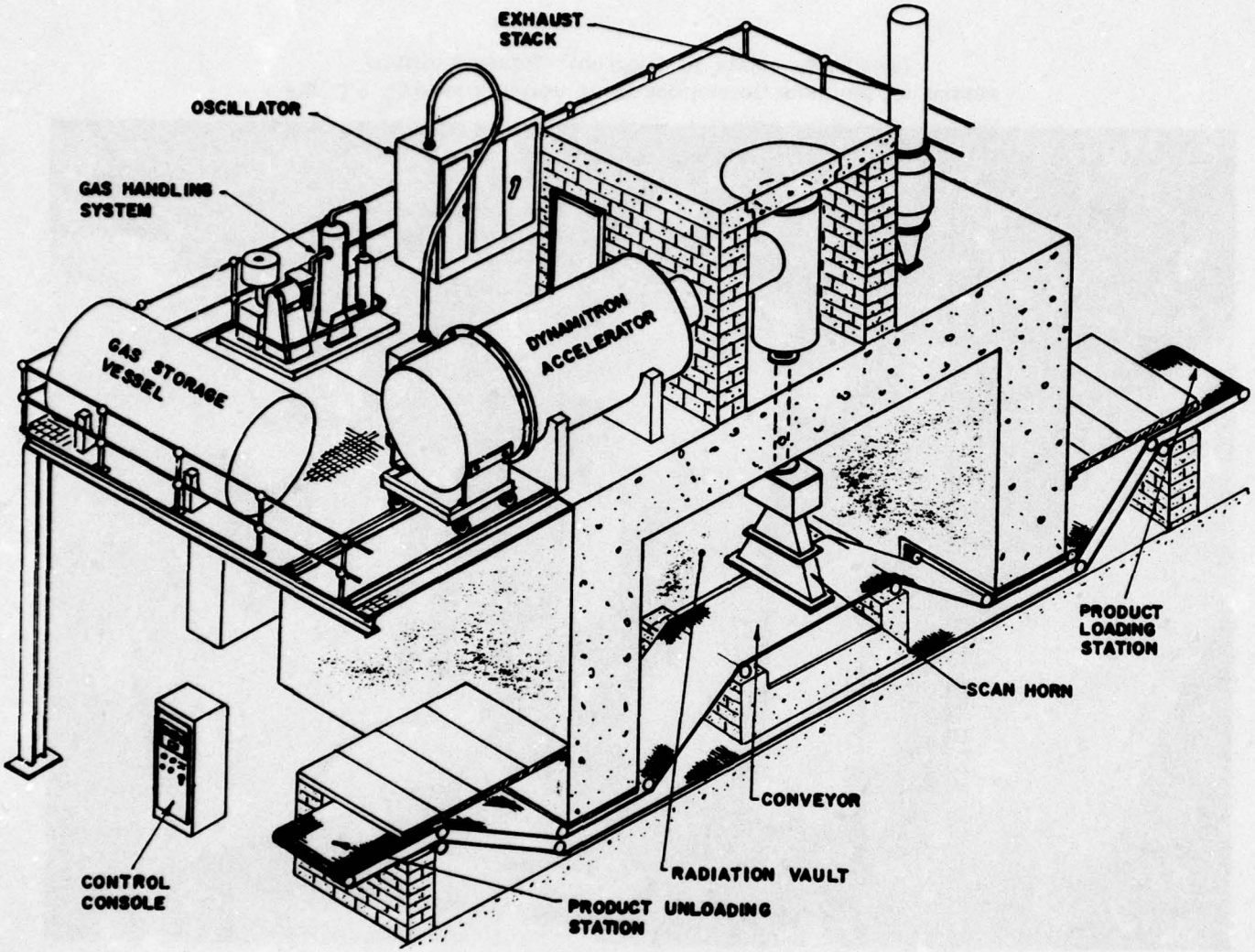


Fig. 1 — Typical Dynamitron electron beam processing facility
(courtesy of Radiation Dynamics, Inc.)

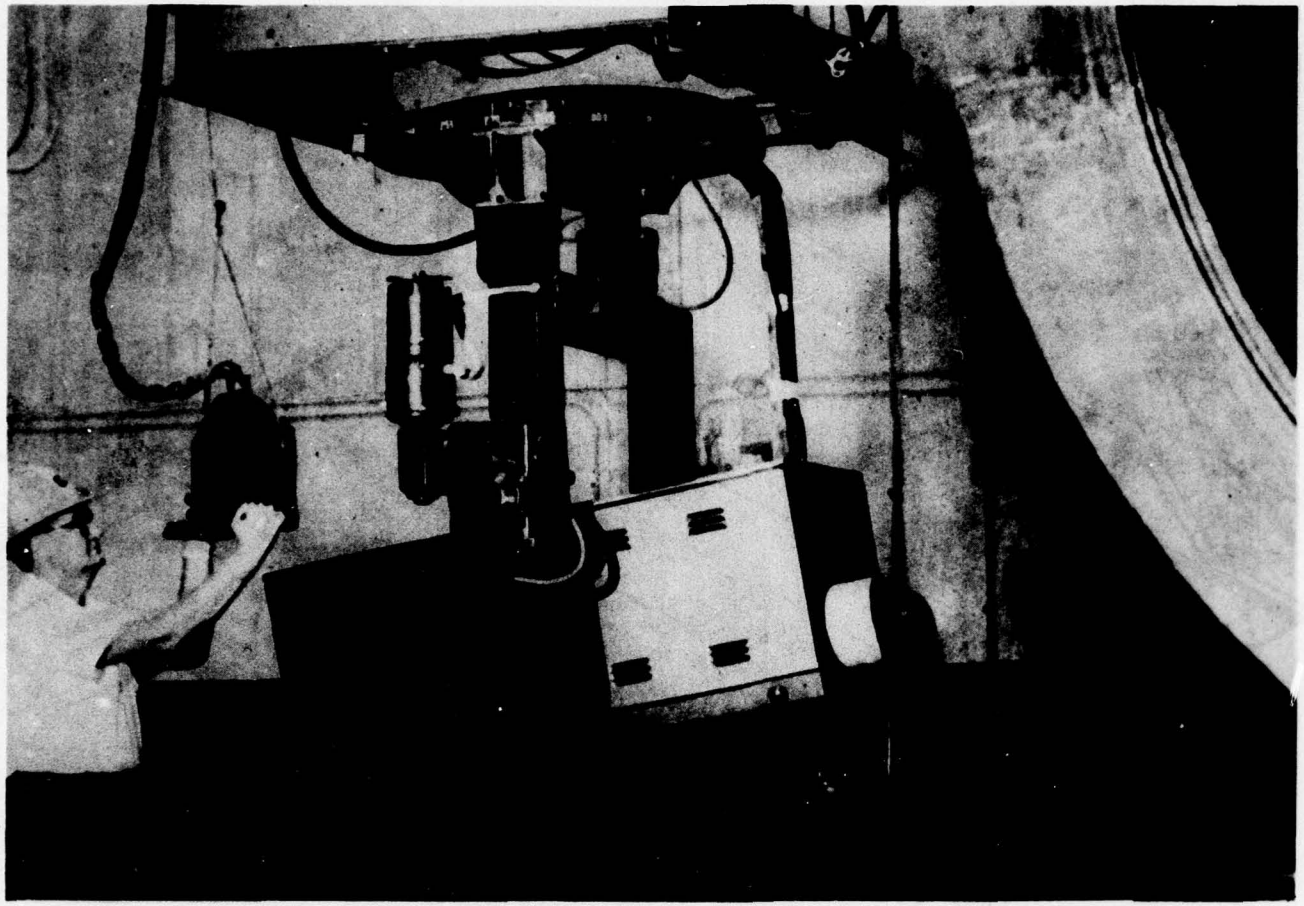

Fig. 2 — Typical Linatron linear accelerator, mounted for remote control scanning. (courtesy of Varian Associates)

TRIALLYL CYANURATE

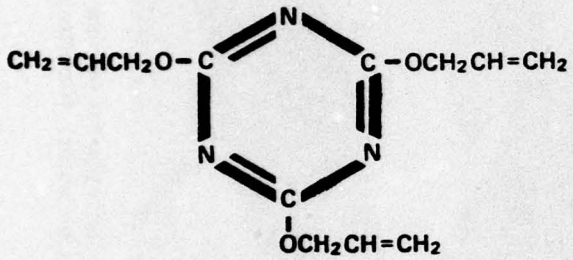


DIVINYL BENZENE

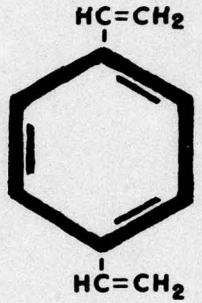


STYRENE

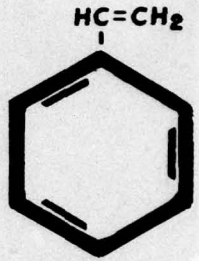


Fig. 3 — Vinyl functional monomers

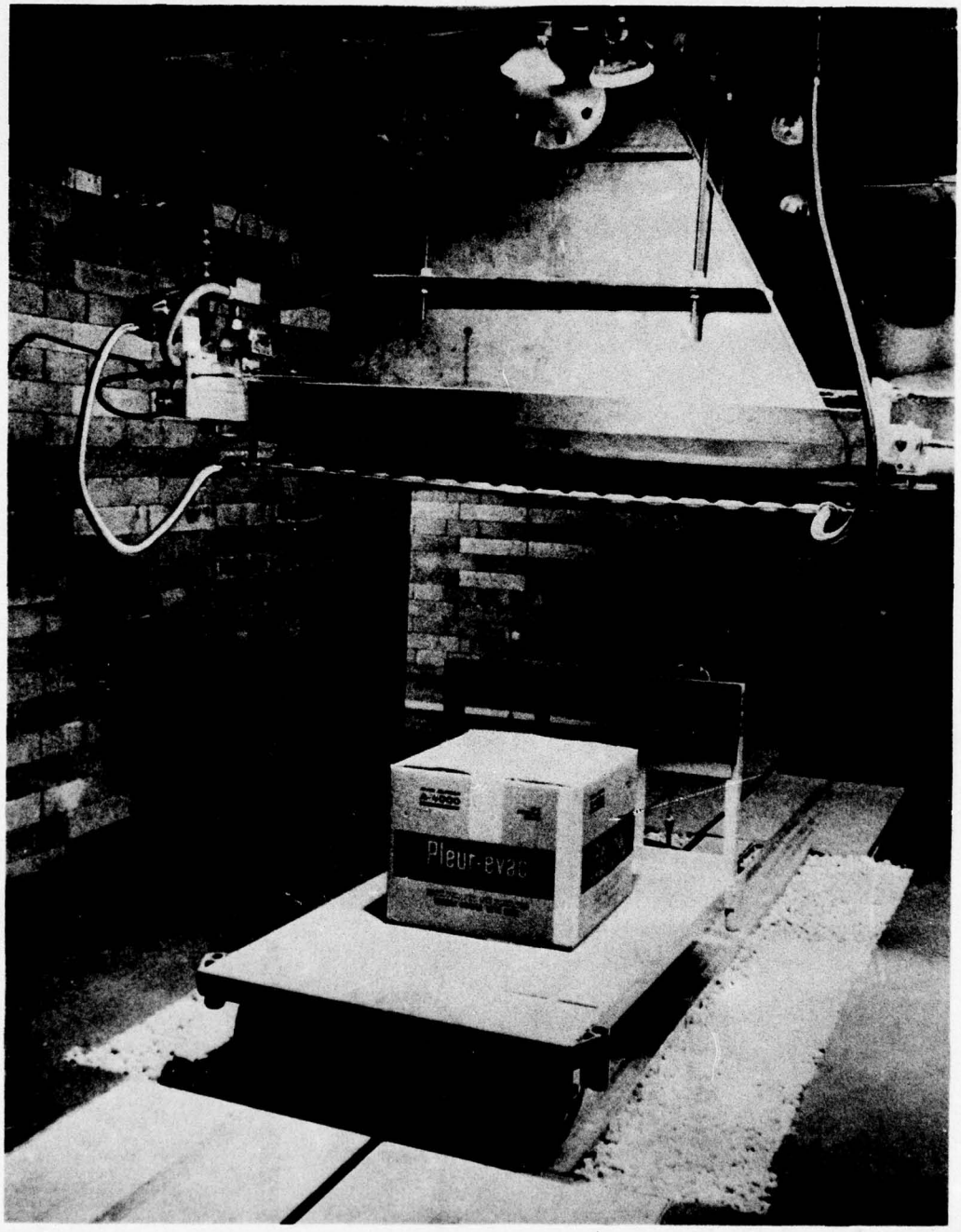


Fig. 4 — View of conveyor car passing under the electron beam scanner at the RDI Service Center. (Courtesy of Radiation Dynamics, Inc.)

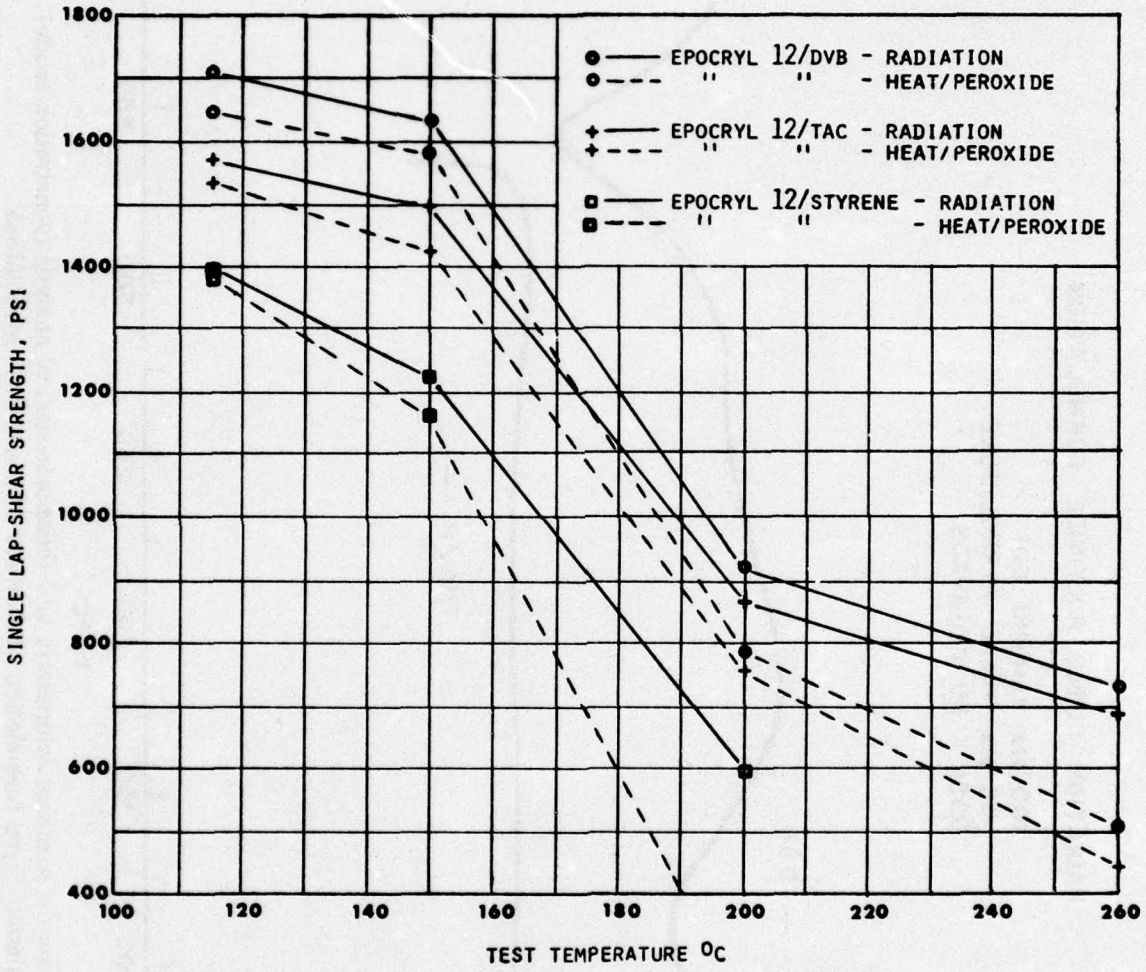


Fig. 5 — Radiation-cured versus heat-cured formulations of Epocryl 12 (Shell). Comparisons of single lap shear strength at elevated temperatures.

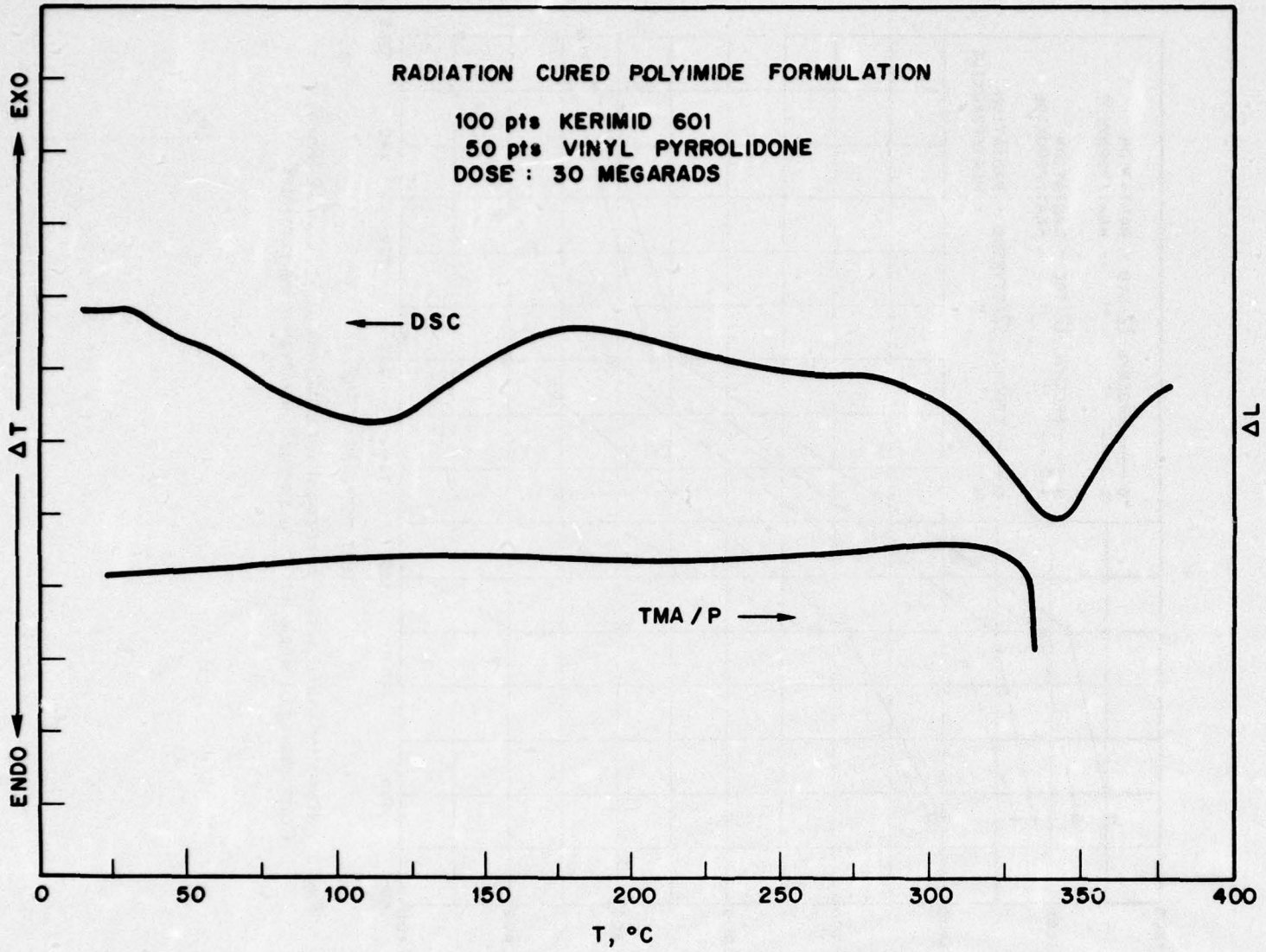


Fig. 6 — Curves of differential scanning calorimetry and thermomechanical analysis (penetration mode) of radiation cured formulation of Kerimid 601 and vinyl pyrrolidone

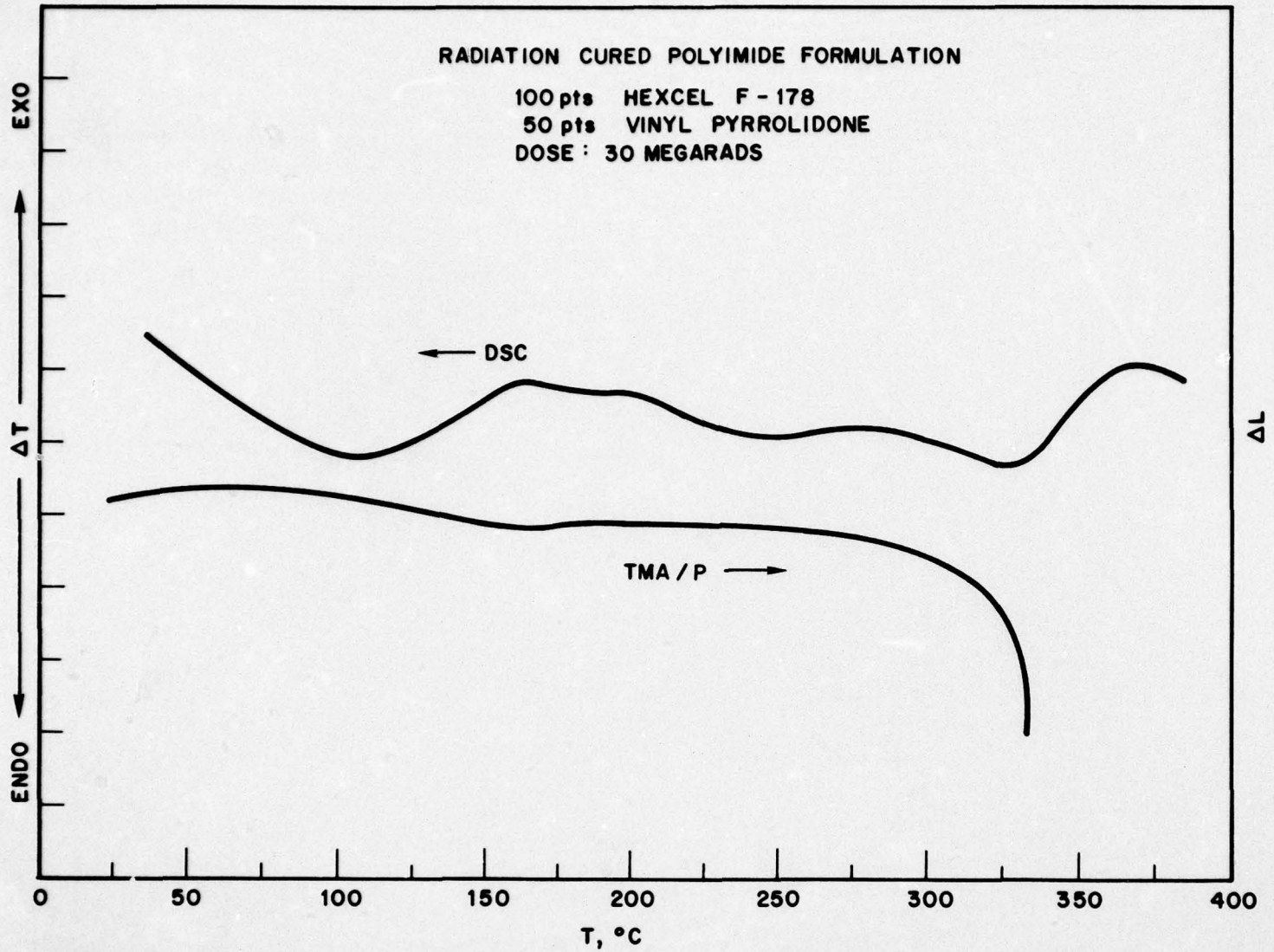


Fig. 7 — Curves of differential scanning calorimetry and thermomechanical analysis (penetration mode) of radiation cured formulation of Hexcel F-178 and vinyl pyrrolidone

# TASK E. COMPOSITES FABRICATION

J. V. Gauchel and H. C. Nash
Organic Chemistry Branch
Chemistry Division

## INTRODUCTION

The fabrication process for fiber-reinforced resin-matrix composites involves a complex combination of physical and chemical processes. The objective of this task is to study the interaction of these processes as the parameters of the fabrication cycle are varied. From this investigation, the parameters which optimize the mechanical properties of cured laminates are evaluated for each material system of interest to the V/STOL Program. Once these values are determined, samples are manufactured for testing in the Design Optimization Task of the program.

The parameters of the fabrication cycle can be divided into two categories: those which affect the curing process and those which affect the consolidation process. Of the parameters affecting the curing process, the temperature cycle is the most important. The cure cycle may be defined as the time-temperature history that the laminate is subjected during the fabrication process. This includes such information as heating rates, dwell times and temperatures, maximum cure temperatures, cooling rates, and post-cure conditions. Other variables critical to the curing process are aging of the prepreg in storage prior to processing and the amount of contaminants (e.g., water or solvents) incorporated into the prepreg. The main parameter affecting the consolidation process is pressure, particularly its relation to viscosity at various stages of the cure process. Both the amount of pressure and the point in the cycle at which the pressure is applied are important considerations. Lay-up parameters such as type and amount of bleeder material, vacuum bag design, and dam design also are considerations in the consolidation process.

It is evident that to optimize all the parameters of the fabrication process would be an immense task. Since the program is both time and manpower limited, it has

been necessary to choose certain parameters for investigation. For commercial systems such as Narmco's 5208/T300 the manufacturer's recommended cure cycle was accepted as a reasonable starting point. Variations from these conditions were made to adjust for available process equipment capabilities. The cure cycle parameters of dwell time and temperature, and the time in the cure cycle when pressure was applied, were varied until high quality, reproducible laminates could be fabricated. For non-commercial systems the process would be more complex. First, an initial fabrication cycle based on the kinetics of the resin cure reaction would be developed. Using this cycle as a baseline, the paramters of the cycle are systematically varied. After each variation, the laminate's properties are reevaluated. If the variation improves the laminate, it would be incorporated into the baseline fabrication cycle. Thus, the fabrication cycle can be continuously modified until a tentative fabrication cycle is established.

To date, this process has been extremely tedious. The recent aquisition of an Audrey Dielectric Analyzer System to monitor the resin cure directly in the laminate should ease the work of this Task.

PROGRESS

During the course of the past year the major emphasis of the Composites Fabrication Task has been the optimization and evaluation of the Narmco 5208/Thornel 300 baseline system. The C-10 polyphthalocyanine system has also been investigated and a tentative cure cycle developed.

Narmco 5208/T300 System

The initial task of this program was to adjust the fabrication cycle of the Narmco 5208/T300 system so that reproducible laminates could be manufactured with the equipment available - a 50-ton Wabash Press. The first attempt using an autoclave lay-up without a vacuum bag proved unsuccessful. When the vacuum bag was included, the test laminates began to improve; however, they were still not satisfactory due to overbleeding. This problem was traced to an overload pressure applied by the press during closure. The pressure overload was eliminated by using steel parallels as load-bearing members during the vacuum portion of the cure cycle. Before high pressure was to be applied, the press was opened, the parallels removed, and the press reclosed. Because the high

pressure setting was greater than the minimum closure pressure and could be pre-set, the second closure developed no overload in the laminate.

After the overloading was eliminated, another problem became evident - resin build-up on the edges of the laminate. This problem was solved by replacing the chloroprene edge dams with dams of porous felt. The porous felt dam allowed resin to flow freely from the preformed laminate during the cure cycle while restricting the flow of fibers. It also increased the area of continuous path for air to escape from the laminate. The lay-up sequence used in all subsequent tests is shown in Figure 1.

The cure-temperature cycle supplied by the Narmco Materials Inc. proved to be very satisfactory in most respects. Sample dwell times and dwell temperatures were monitored using Chromel-Alumel thermoucouples embedded in a test laminate. This technique allowed changing the platen conditions so that the sample actually followed the cure cycle, rather than assuming the sample was in temperature equilibrium with the platens.

Table 1 lists the fabrication cycle developed for the Narmco 5208/T300 laminates. The dwell times and temperatures are unchanged from the recommended cycle. An additional 50 minutes of vacuum bag exposure at room temperature was added to remove any excess moisture which the laminate might have absorbed during the course of the lay-up procedure.

The test of any fabrication cycle is the quality of the laminates produced. Thirteen 25 cm x 25 cm x 16 ply laminates ranging in orientation from $[\pm 15]$ to quasi-isotropic were laminated for testing in the Design Optimization Task. Each plate was characterized as to specific gravity, volume fraction fiber, volume fraction matrix, and volume fraction voids. The plates were also ultrasonically scanned for defects. Table 2 lists the results of the physical characterization tests. Volume fraction fibers ranged from 0.685 to 0.70. Void fraction varied from 0.011 to 0.024.

One comment about void fraction analysis is necessary at this point. The technique used in this program was digestion with concentrated nitric acid. Because this technique requires extremely accurate measurements of the densities of the fiber and the matrix, it is not uncommon to see negative void contents or zero void contents reported. Since it was felt that a negative void count

has no physical significance, the density of the fiber and of the matrix were chosen within the manufacturers' specified tolerances so as to maximize the measured volume fraction voids. This explains the relatively high values of the volume fraction voids reported.

The ultrasonic inspection provided a convenient check on the uniformity of the laminates. Of the thirteen plates fabricated, nine were uniformally free of defects, three had minor scattered defects, and one contained large areas of defects. Samples from areas containing defects and samples from areas free of defects were analyzed for void content. The results are shown in Table 3. All areas with a void fraction greater than 0.0151 showed as defects in the ultrasonic examination. Areas where the void fraction was evaluated to be less than or equal to 0.0151 showed as defect-free in the ultrasonic test. This "quantitative" relationship between void content and ultrasonic response is being investigated further.

The mechanical response of each laminate was also evaluated. Test specimens 10 cm x 1.25 cm x 0.2 cm were machined such that the included angle $2\theta$ between fiber orientations ranged from $30^{o}$ to $150^{o}$ (see Figure 2). All test were performed in tension at an extension rate of 0.125 cm/min with the loading direction bisecting the included angle. Strain measurements were made parallel and perpendicular to the loading direction. From these experiments, tensile strength, $\sigma$, (Figure 3) tensile modulus, $E_{11}$, (Figure 4) and Poisson's ratio, $\nu_{12}$, (Figure 5) were evaluated as a function of angle. This information was supplied to the Design Optimization Task as input data to the design computer code. The data was also used to evaluate the quality of the fabrication cycle. The small degree of scatter in both tensile strength and tensile modulus indicates the relative uniformity of the test specimens. The specimen uniformity is further demonstrated by the results reported by the Design Optimization Task in the next section of this report.

An aspect of quality control sometimes overlooked on laminate systems is the fiber angle. In Figures 3, 4, and 5 the large angular dependency of the mechanical response of an angle ply laminate is shown. In order to fabricate test specimens with known fiber angle, it is necessary to develop not only a uniform lay-up technique but also a controlled specimen machining technique.

The methodology to reproducibly lay-up specimens of known fiber angle is not new: it requires attention to

detail and skillful operators. However, this job can be simplified by "kitting" the laminates prior to lay-up. In the kitting operation the 12 in.-wide unidirectional strips of prepreg were assembled into a pattern from which a 100 in. by 100 in. square was cut. The angle which the side of the square made with the fiber in the prepreg was set to $\theta$. After the square was cut, it could be divided into 16 individual 25 cm x 25 cm square lamina, each with fibers running in the $\theta$ direction. It was then a simple task to match the square corners of the individual lamina in assembling a $\pm\ \theta$ laminate. Results of the kitting operation for the Narmco 5208/T300 laminate show that the included angle, $2\theta$, could be held reproducible to $\pm$ 0.5 degrees.

Exact geometric control of the machining of the test coupons prior to testing is also important. Unless the samples are cut so that the loading direction and the bisector of the included angle are identical, the test is not valid. Fortunately, there are checks to see that the tests specimens have been aligned properly. If one measures $E_{12}$, (the stress in the loading direction divided by the strain perpendicular to the loading direction) as a function of included angle, from symmetry considerations:

$$E_{12}\ (2\theta) = E_{12}\ (180\text{-}2\theta) = E_{21}\ (2\theta)$$

Figure 6 depicts the results of such an experiment for the 5208/T300 laminates fabricated in this task. Likewise, if one measures Poisson's ratio as a function of included angle, lamination theory states that:

$$\frac{\nu_{12}\ (2\theta)}{E_{12}\ (2\theta)} = \frac{\nu_{12}\ (180\text{-}2\theta)}{E_{11}\ (180\text{-}2\theta)} = \frac{\nu_{21}\ (2\theta)}{E_{22}\ (2\theta)}$$

where $\nu_{12}\ (2\theta)$ = Major Poisson's ratio

$\nu_{11}\ (2\theta)$ = Tensile Modulus in the loading direction

$\nu_{22}\ (2\theta)$ = Transverse Tensile Modulus

$\nu_{21}\ (2\theta)$ = Transverse Poisson's ratio

$2\theta$ = Included Angle

Figure 7 shows the results for the 5208/T300 laminates tested. The geometric uniformity of the specimen is again apparent.

C-10 Polyphthalocyanine/Thornel 300 (24 x 26 Fabric)

Establishing the fabrication cycle of a new matrix material, such as the C-10 polyphthalocyanine, requires more information than just the resin cure kinetics. The type and content of impurities, the resin compatibility with reinforcing fibers, the method by which it is preimpregnated, and the prepreg flow characteristics are all necessary to the development of a reasonable cycle. In the past year, emphasis has been placed on developing a tentative cure cycle for the C-10 system from limited information on the above parameters. The amount of information available has been restricted because of lack of sufficient quantities of C-10 resin.

The cure kinetics of the C-10 resin still have not been quantitatively defined. The pure resin melts sharply to a low viscosity liquid at 185°C, but at this temperature the polymerization reaction proceeds extremely slowly. At 220°C the reaction proceeds at a faster, more practical rate. If the resin is "staged" at 220°C for 45 minutes under vacuum, the melting point can be reduced to 90°C. Some viscosity increase is associated with this operation but the material remains sufficiently fluid for proper hot-melt impregnation. This "staging", if continued too long, can increase the viscosity past the point at which hot-melt prepreging is possible.

Fibers and fabrics were impregnated by hot-melt processing. The reinforcements were heated to 200°C before applying a measured amount of the B-staged resin. Having the fibers hot, promoted uniform impregnation and limited the time for reaction to take place during the impregnation process.

Cure of C-10 matrix graphite-fabric laminates was achieved using a short press cycle in conjunction with a post cure (Table 4). The cycle consists of 1 hour at 200°C under vacuum plus 1 hour at 200°C under 100 psi pressure followed by 1 hour at 260°C under 100 psi pressure. When processing a tape system, pressures may be reduced to ~50 psi. The C-10 system showed good flow characteristics during processing. The sample was allowed to cool below 100°C under pressure. Post cure was 54 hours at 260°C. The post cure can be shortened by raising the temperature, but this may require an inert atmosphere to prevent thermal oxidation.

Preliminary test results on the C-10 laminates are shown in Table 5 in comparison with CPI 2214, a typical

addition polyimide based on Kerimid 601. Given the similar moduli of the two systems, the higher flexure strength for the C-10/graphite fabric system at room temperature indicates that this system has larger flexure strain-to-failure than the polyimide system.

## FUTURE WORK

The immediate goals of the Composites Fabrication Task are to optimize the C-10 polyphthalocyanine fabrication cycle and to produce laminates for extensive mechanical evaluation. Another important variable to be considered is the degree to which resin purity requirements can be relaxed without sacrifice of thermal and mechanical properties. For the Narmco 5208/T300 system, special emphasis will be placed on prepreg ageing studies (in conjunction with the Chemical Characterization Task) and on elevated temperature mechanical evaluation (with the Design Optimization Task). The effects of exposure to water and/or water-solvent combinations will also be considered. Polyimide systems such as Kerimid 601 and Hexcel's F-178 will also be examined during this fiscal year.

Table 1

Fabrication Cycle for Narmco 5208/T300 Prepreg

1. Place lay-up in press.
2. Put spacer bars in place so that press may be closed without applying pressure to the sample.
3. Close press.
4. Apply full vacuum, hold 50 minutes.
5. Heat Platens to 135°C at 2-3°C/min.
6. Hold at 135°C for 1 hr.
7. Remove spacer bars and apply 100 psi pressure to the laminate and release vacuum.
8. Heat to 177°C at 3°C/min.
9. Hold at 177°C for 2 hrs.
10. Slow cool under pressure to $< 100^{\circ}C$.
11. Post cure for 4 hrs at 205°C.

Table 2

Physical Properties of Narmco 5208/T300 Laminates

| SAMPLE | ORIENTATION* | VOLUME FRACTION FIBER | VOLUME FRACTION VOIDS |
|---|---|---|---|
| 1-5B | $\pm 22.5^{o}$ | .694 | .0160 |
| 1-2H | $\pm 22.5^{o}$ | .695 | .0210 |
| 2-5B | $\pm 22.5^{o}$ | .697 | .0120 |
| 2-2H | $\pm 22.5^{o}$ | .700 | .0120 |
| 3-5B | $\pm 30^{o}$ | .696 | .0190 |
| 3-2H | $\pm 30^{o}$ | .696 | .0240 |
| 4-5B | $\pm 30^{o}$ | .698 | .0120 |
| 4-2H | $\pm 30^{o}$ | .700 | .0130 |
| 5-5B | $\pm 15^{o}$ | .695 | .0110 |
| 5-2H | $\pm 15^{o}$ | .698 | .0140 |

| SAMPLE | ORIENTATION* | VOLUME FRACTION FIBER | VOLUME FRACTION VOIDS |
|---|---|---|---|
| 6-5B | $\pm 15^{o}$ | .694 | .0110 |
| 6-2H | $\pm 15^{o}$ | .700 | .0130 |
| 7-5B | $\pm 37.5^{o}$ | .694 | .0130 |
| 7-2H | $\pm 37.5^{o}$ | .696 | .0140 |
| 8-5B | $\pm 37.5^{o}$ | .695 | .0130 |
| 8-2H | $\pm 37.5^{o}$ | .697 | .0130 |
| 9-5B | $\pm 30^{o}$ | .692 | .0135 |
| 9-2H | $\pm 30^{o}$ | .688 | .0157 |
| 10-5B | $\pm 45^{o}$ | .691 | .0161 |
| 10-2H | $\pm 45^{o}$ | .687 | .0126 |
| 11-5B | $\pm 45^{o}$ | .685 | .0151 |
| 11-2H | $\pm 45^{o}$ | .697 | .0145 |

| SAMPLE | ORIENTATION* | VOLUME FRACTION FIBER | VOLUME FRACTION VOIDS |
|---|---|---|---|
| 12-5B | Q.I. | .693 | .0135 |
| 12-2H | Q.I. | .685 | .0145 |
| 13-5B | Q.I. | .694 | .0134 |
| 13-2H | Q.I. | .686 | .0132 |

*All Plates 16 Ply

Table 3

Volume Fraction Void Threshold For Defect Detection
By The Current Ultrasonic Inspection Technique

| SAMPLE | VOID VOLUME FRACTION | DEFECTS REPORTED BY ULTRASONIC INSPECTION |
|---|---|---|
| 6-5B | .0110 | No |
| 2-2H | .0120 | No |
| 4-2H | .0130 | No |
| 5-2H | .0140 | No |
| 11-5B | .0151 | No |
| 9-2H | .0157 | Yes |
| 1-5B | .0160 | Yes |
| 10-5B | .0161 | Yes |
| 3-5B | .0190 | Yes |
| 1-2H | .0210 | Yes |
| 3-2H | .0240 | Yes |

Table 4

Tentative Fabrication Cycle For
C-10 Phthalocyanine/T300 Fabric

1. Place lay-up in press.
2. Put spacer bars in place so that press may be closed without applying pressure to the sample.
3. Close press.
4. Apply full vacuum.
5. Heat platens to 205°C at 3-5°C/min.
6. Hold at 205°C for 1 hr.
7. Remove spacer bars and apply 100 psi pressure*
8. Release vacuum.
9. Heat to 260°C at 3-5°C/min.
10. Hold at 260°C for 1 hr.
11. Cool under pressure to less than 100°C.
12. Post cure for 54 hrs. at 260°C.

*Pressure may be reduced to 50 psi for a Thornel 300 tape system.

Table 5

Preliminary Mechanical Properties of
C-10 Polyphthalocyanine-Graphite Fabric System

| | C-10 Phthalocyanine 2426* | CPI 2214** 2426* |
|---|---|---|
| Flexure Strength, Warp - R.T. ($GN/m^2$) | 0.65 | 0.44 |
| Flexure Modulus, Warp - R.T. ($GN/m^2$) | 51.7 | 54.5 |
| Volume Fraction Fiber | 0.66 | 0.65 |

*Thornel 300 3K tow woven into a 24 x 26 fabric

**An addition polyimide based on Kerimid 601

AD-A035 928 NAVAL RESEARCH LAB WASHINGTON D C F/G 11/4
HIGH PERFORMANCE COMPOSITES AND ADHESIVES FOR V/STOL AIRCRAFT.(U)
DEC 76 W D BASCOM, L B LOCKHART

UNCLASSIFIED NRL-MR-3433 NL

2 OF 2
AD
A035928

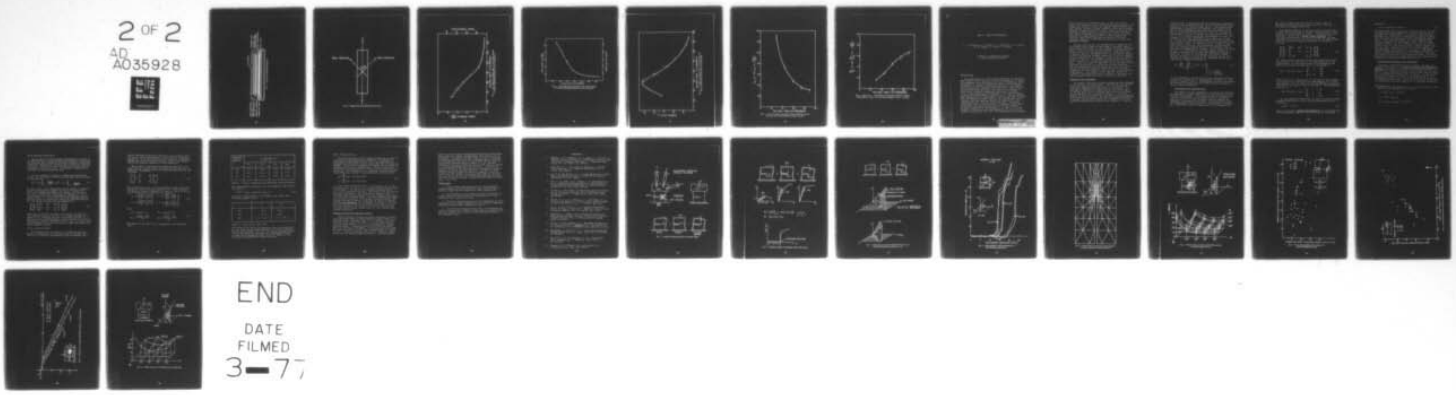

END

DATE
FILMED
3-77

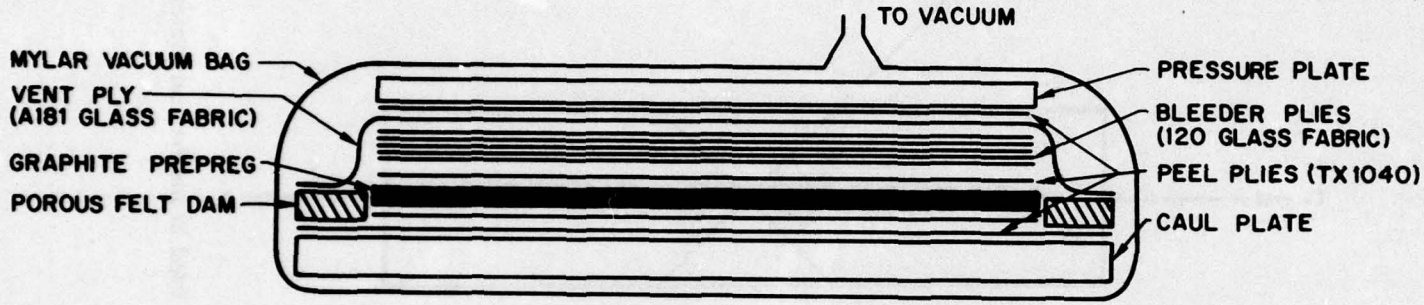


Fig. 1 — Lay-up for 5208/T300 laminates

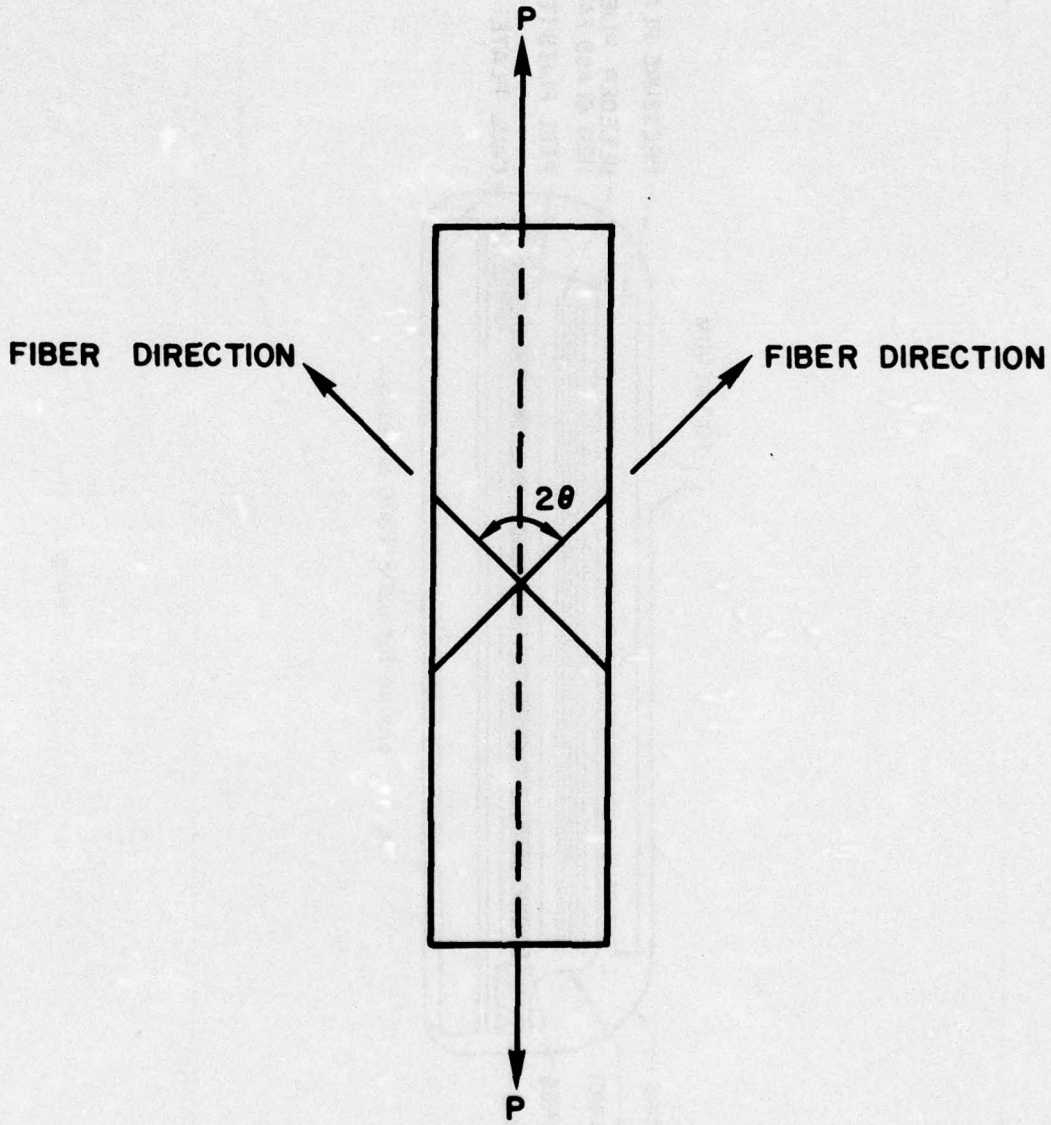


Fig. 2 — Sample used in mechanical evaluation tests

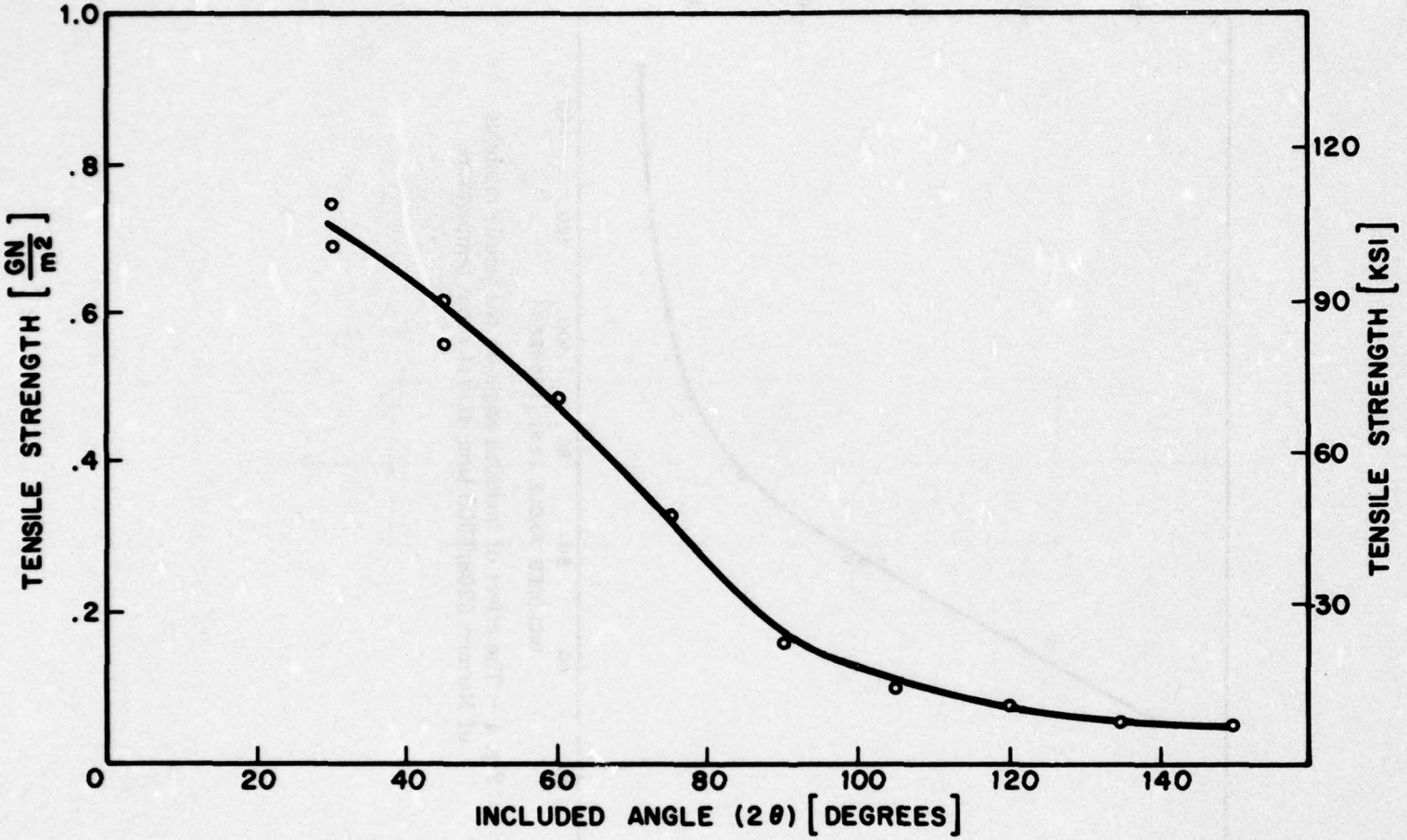


Fig. 3 — The effect of included angle on the tensile strength of Narmco 5208/T300 laminates at room temperature

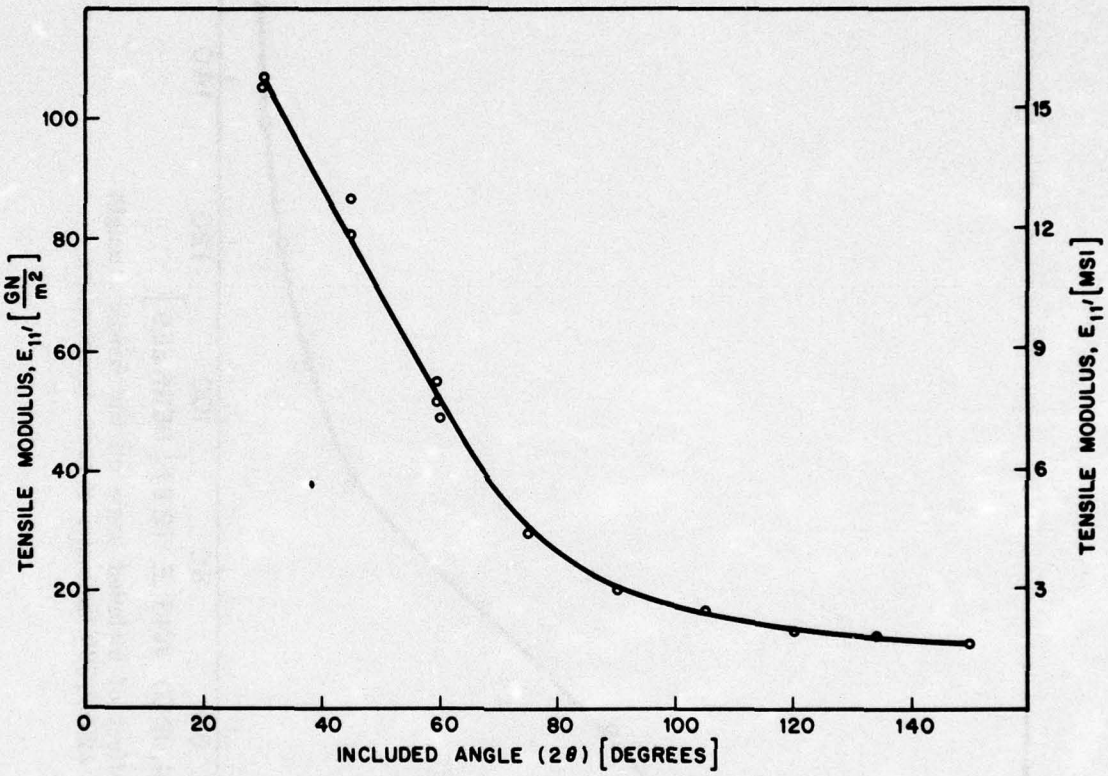


Fig. 4 — The effect of included angle on the tensile modulus of Narmco 5208/T300 laminates at room temperature

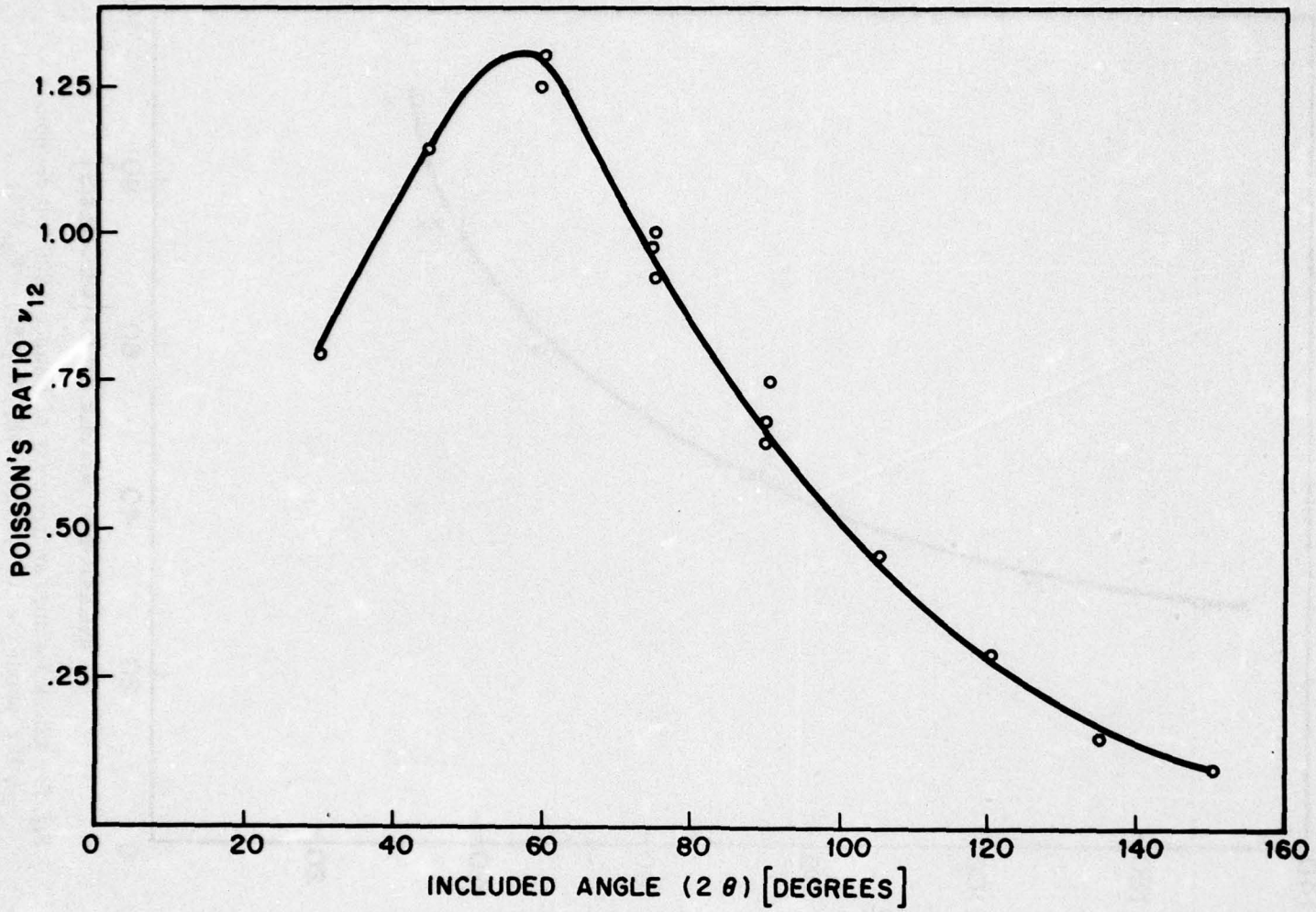


Fig. 5 — The effect of included angle on Poisson's ratio for Narmco 5208/T300 laminates at room temperature

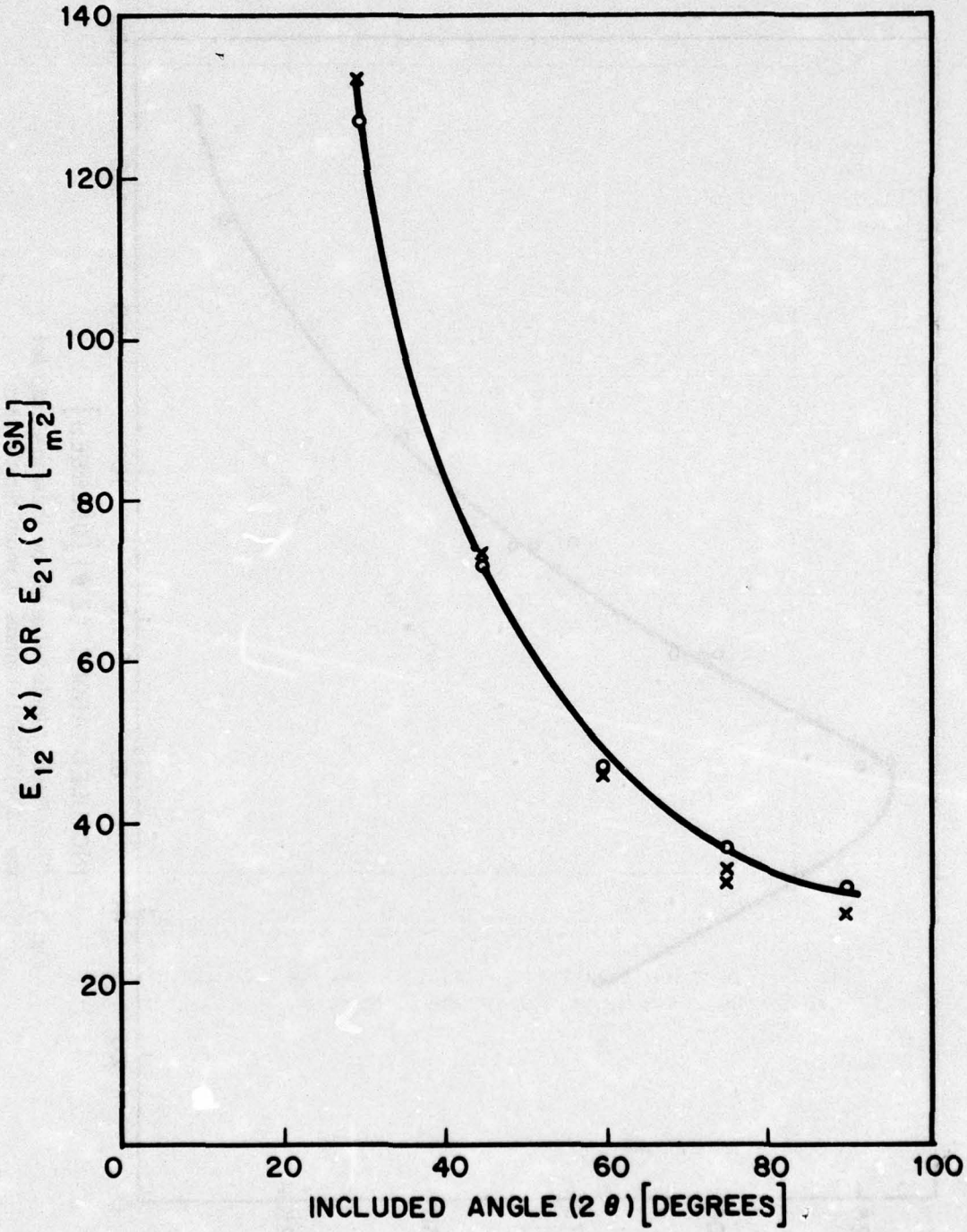


Fig. 6 — Check for angular symmetry of Narmco 5208 test coupons.
If coupons are cut symmetrically, $E_{12}(2\theta) = E_{21}(2\theta)$

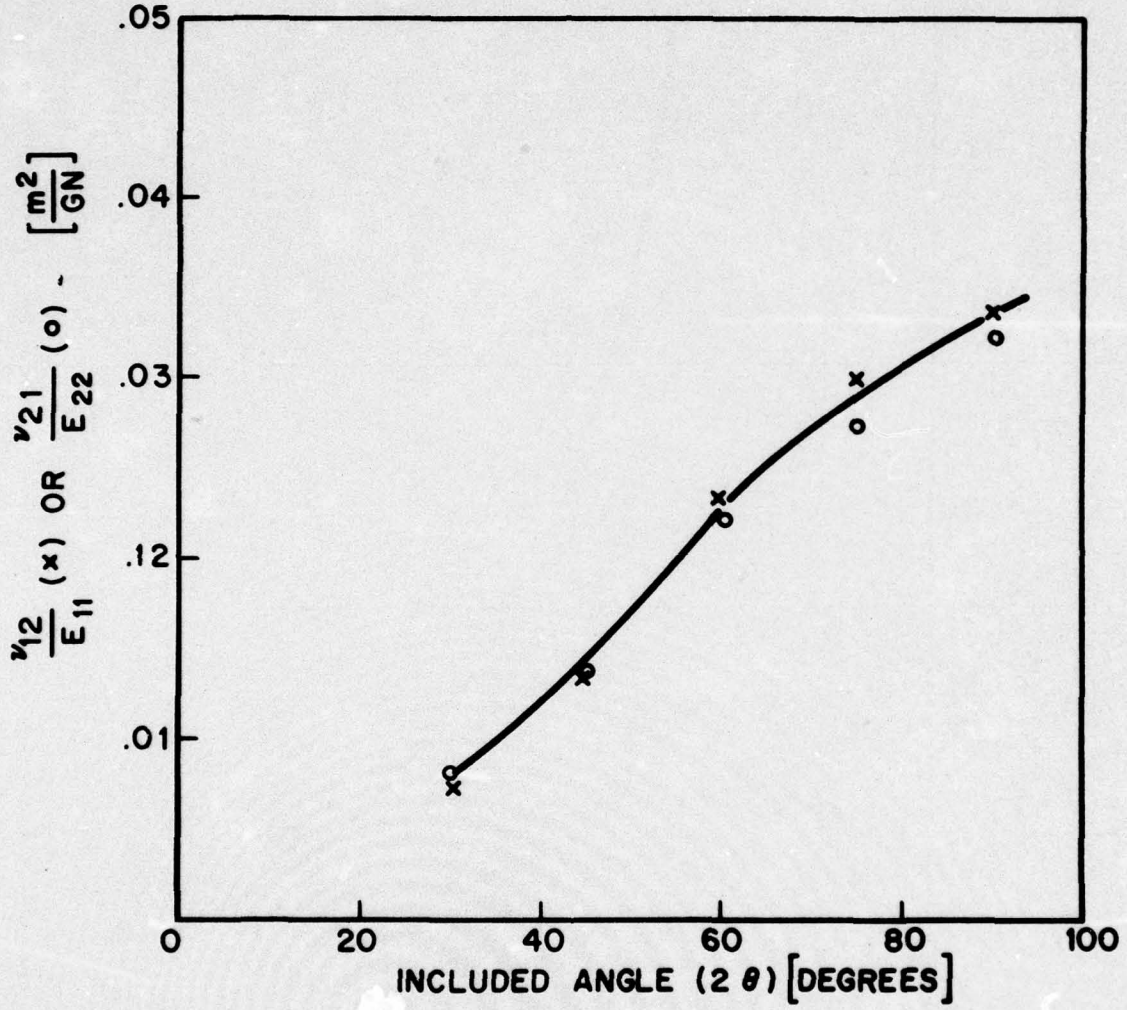


Fig. 7 — Check for strain gage alignment and angular symmetry on Narmco 5208/T300 test coupons. For symmetric laminates, $\nu_{12}/E_{11} = \nu_{21}/E_{22}$.

# TASK F DESIGN OPTIMIZATION

L. A. Beaubien, P. W. Mast, D. R. Mulville, S. A. Sutton
R. W. Thomas, J. Tirosh, I. Wolock

Mechanics of Materials Branch
Ocean Technology Division

## INTRODUCTION

The applicability of structural materials is limited in many cases by their ability to resist propagation of flaws. The toughness value associated with such a property, widely documented in isotropic materials, has not been obtained similarly for fibrous reinforced composites. The reasons are not merely the technical difficulties of observing and controlling crack extension, but also that the modes of fracture in a general angle-ply laminate are coupled (i.e., both opening and sliding modes take place simultaneously under pure tensile loading, etc.). Neither analytical expressions nor experimental observations have yet been able to relate the remote load to the conventional stress intensity factors when the process of fracture is more complex than just colinear crack extension. There are particular cases in the fracture of composites where modes of fracture are separated so that the linear fracture mechanics approach is transferable (i.e., Ref. [1], [2]), notably in unidirectional reinforcement [3], [4], but not without restrictions [5], [6]. By recognizing the coupling

effect between the different modes it was felt that a useful yet practical start for obtaining fracture data is by conducting studies in which one applies simultaneously the most general in-plane loading: tension, shear and rotation. Fracture of composites which results from a variety of such combined loadings applied to various cross-ply laminates will better describe the situation that occurs in service. Therefore the experimental effort on this program was directed toward producing fracture data on cross-ply laminates subjected to different proportions of the three combined loadings.

Failure criteria will be determined for composites and for bonded joints under a broad range of in-plane loads, using resins of interest to the program and being characterized in the other tasks of this program. The validity of these criteria will be demonstrated in a laboratory test, in which a typical subcomponent will be selected as well as a defect and typical loading conditions. A finite element stress analysis will be conducted to determine the stresses around the defect. The failure criteria derived will be used to predict the conditions under which the defect will grow. Tests will then be conducted and the failure criteria modified as necessary to provide an accurate predictor. The data obtained on various layups will then be used in a design optimization procedure with respect to fracture toughness, over the range of materials and stress variables investigated. The results of the fracture studies on composites and adhesives will be related to the resin properties again within the range of variables examined.

Composite Test Procedure

A computer controlled in-plane loader has been designed at NRL to meet this requirement. This machine was used to test small edge-notched coupons (1" x 1.5" x 0.1") of cross-ply laminates of graphite/epoxy (T300/5208). The specimen is clamped by a fixed grip at one end and by a "floating" grip, free to displace and rotate (in a plane) at the opposite end, as shown in Figure 1. The three degrees of freedom of this floating grip are controlled by three hydraulic actuators such that any desired combination of shear, tension and rotation can be applied via a computerized program which controls the actuators. Once the

combined load is preselected the test proceeds by maintaining the proportionality between the three loads until total separation of the specimen takes place. This proportional displacement loading path is described as a radius vector ($\vec{r}$) in the displacement space with the coordinates $d_0$, $d_1$ and $d_2$ originating at the crack tip (Fig. 2). During the displacement controlled loading, the associated forces ($t_0$, $t_1$, $t_2$) are recorded versus the displacements so that the changes in the three compliances ($c_0 = d_0/t_0$, $c_1 = d_1/t_1$, $c_2 = d_2/t_2$) are simultaneously obtained as shown in Fig. 2. It was observed that the three forces do not decrease at the same instant. When the composite starts to fail it doesn't necessarily decrease all the compliances simultaneously, and load carrying capacity may still be sustained even if some kind of damage starts to grow. After a while, as shown in Fig. 3, the increase in the displacement results in gradual relaxation of the loads and substantial damage is observed. A method to discriminate the point at which failure initiates is to follow the variation in the total dissipative energy consumed by the specimens monitored on-line by the computer according to

$$D_E = \sum_{i=1}^{3} \left( \int_{d=0}^{d_j} t_j \, \delta d_j - t_j d_j \right) \qquad (1)$$

$i = 1 \rightarrow$ shear
$i = 2 \rightarrow$ tension
$i = 3 \rightarrow$ rotation

In our experiments the sum of the three contributions show a distinct increase as the displacement increases, as indicated in Figures 2 and 4. Consequently we define this point as fracture initiation and the fracture data obtained is based on this definition.

Presentation of Fracture Data

The subject of this paragraph is to recast the fracture data gathered on small coupons into several forms more conceivable by designers. The computational procedures which follow are based upon the recorded forces at incipient fracture ($f^c_0$, $f^c_1$, $f^c_2$) resulting from the imposed displacement as explained previously. The associated stress and displacement field throughout the specimen is resolved by a structural analysis program derived by Beaubien [8].

The finite element mesh used here is shown in Fig. 5. The above critical forces at fracture - $f^c_0$, $f^c_1$, $f^c_2$ - were used as boundary conditions.

The laminate appears to initiate failure without substantial non-linearities as revealed from the rather abrupt increase in the dissipative energy. Consequently one can establish a priori (by a linear stress analysis) the 'influence coefficients' [E] for each angle-ply laminate representing the various stiffnesses of the notched coupons under the 3 possible loading conditions Ux, Uy and W. It reads

$$\begin{Bmatrix} f_o \\ f_1 \\ f_2 \end{Bmatrix} = \begin{bmatrix} E_{0x} & E_{0y} & E_{0z} \\ & E_{1y} & E_{1z} \\ \text{sym} & & E_{2z} \end{bmatrix} \begin{Bmatrix} U_x \\ U_y \\ W_z \end{Bmatrix} \tag{2}$$

For simplification and convenience the generalized forces {f}, acting at the midcenter of the edge along which the displacements {u} are prescribed, are transformed to the notch tip location and denoted by {t} according to

$$\{f\} = [T_f]\{t\}, \quad [T_f] = \begin{bmatrix} 1 & 0 & 0 \\ 0 & 1 & 0 \\ c_1 & -c_0 & 1 \end{bmatrix} \tag{3}$$

where $c(c_0, c_1)$ is the location of the load {f} with respect to the notch tip. Similarly the displacement {u} is also transformed by $[T_u]$ to the notch tip coordinate and denoted there by {d} as shown in Fig. 1 and Fig. 2. The geometrical relation is

$$\{u\} = [T_u]\{d\}, \quad [T_u] = \begin{bmatrix} 1 & 0 & -c_1 \\ 0 & 1 & c_0 \\ 0 & 0 & 1 \end{bmatrix} \tag{4}$$

It can readily be shown from [3] and [4] that the transformation matrices for forces and displacements are connected by

$$[T_u]^{-1} = [T_f]^T \tag{5}$$

Hence, the general CONSTITUTIVE EQUATION for the coupon test specimen emerges from (2), (3) and (4) by the following

expression

$$\{d\} = [T_f]^T [E]^{-1} [T_f]\{t\} \qquad (6)$$

The experiments are continuously monitored by {t} and {d}. At present the displacements {d} are not measured on the specimen but rather given by the motion of the actuator. Therefore Eq. 6 serves as a computational device to determine the relative compliances (three independent compliances) of the testing machine so vitally important for precise evaluation of experimental data. The so called 'failure surfaces' on the d space are plotted in a polar form* in Fig. 6. The fracture data on these surfaces compose the tests performed on 30°, 45° and 60° degrees of included angle (with respect to the notch). The smooth curves between fracture points at different proportions of shear, tension and rotation are quite obvious. This can partially be attributed to the automated nature of the test procedure as well as the high quality of the laminates furnished by the Composites Fabrication Task.

Data Reduction Methods for Composites

The goal in applying fracture mechanics concepts in composite materials is to reduce the numbers of independent parameters required to characterize their fracture properties. The experimental tests which depend on three different loading conditions convey fracture data (Fig. 6) which are inherently three-dimensional in nature. In the following we will attempt to reduce the dimensionality of the experimental data in Fig. 6 from three to two by considering approaches which have been used successfully in the past to characterize fracture properties of isotropic materials.

---

* In polar form the variables $d_0$, $d_1$, $d_1$ are related to the three polar coordinates r, $\theta_1$, $\theta_2$ by

$$r = (d_0^2 + d_1^2 + d_2^2)^{1/2}$$

$$\theta_1 = \tan^{-1} (d_1/d_0)$$

$$\theta_2 = \tan^{-1} [d_2/(d_0^2 + d_1^2)^{1/2}]$$

## Crack Opening Displacement

The concept of 'crack opening displacement' is based on the premise that the displacement associated with the notch (or with the whole flank) at incipient fracture constitutes a material property and therefore can be used as a fracture criterion. The question as to whether this holds true in composites subjected to combined loading is considered in the light of our experimental data.

For this purpose we define a normalized displacement vector (Dx, Dy) along N discrete points along the two flanks of the notch by

$$D_x^{(j)} = \frac{1}{N} \sum_{i=1}^{N} \frac{U_x(r_i)}{\sqrt{r_i}}, \quad D_y^{(j)} = \frac{1}{N} \sum_{i=1}^{N} \frac{U_y(r_i)}{\sqrt{r_i}} \tag{7}$$

As seen in Eq. 7 the displacement of the flank is weighted by the corresponding distance $(1/\sqrt{r_i})$ to the tip of the notch and averaged throughout the flanks. Evaluation of Eq. (7) is repeated for each mode of loading (j = 0,1,2 corresponds to the three displacement loadings Ux, Uy, W, shown in Fig. 1). As a result the total opening displacement Dx and Dy is resolved by adding the contributions of all the acting loading modes as expressed by

$$\begin{Bmatrix} D_x \\ D_y \end{Bmatrix} = \begin{bmatrix} D_x^{(0)} & D_x^{(1)} & D_x^{(2)} \\ D_y^{(0)} & D_y^{(1)} & D_y^{(2)} \end{bmatrix} \begin{Bmatrix} U_x \\ U_y \\ W_z \end{Bmatrix} \tag{8}$$

where {u} in Eq. 8 is related to (t) by Eq. (4) and (6). The numerical evaluation of Eq. (8) at each combination of loads {t} at incipient fracture is presented in Fig. 7. The results do not demonstrate a clear topological structure required for fracture characterization. Eq. 7 is not a well suited parameter for data reduction of angle ply composites under combined loading.

## Stress Intensity Factor

By assuming that the notch tip is sharp and the composite is homogeneous, an analytical near-tip elastic solution [9] is valid and consequently used to evaluate the

stress intensity factors ($K_1$ and $K_2$) at the critical loads {f} in all tested combinations for the various cross-ply laminates. It is the purpose of this analysis to determine whether the critical stress intensity factors can characterize the fracture behaviors of our composites.

The relation connecting the normalized opening of the crack (Dx, Dy) to the stress intensity factors ($K_1$, $K_2$) in composites is coupled and can be generally described by the following

$$\begin{Bmatrix} D_x \\ D_y \end{Bmatrix} = \begin{bmatrix} A & B \\ C & E \end{bmatrix} \begin{Bmatrix} K_1 \\ K_2 \end{Bmatrix} \tag{9}$$

The coefficients A, B, C, E are readily inferred from the analytical work of Sih and Leibowitz [9]. They consist of the material elastic properties Aij and the roots $S_1$ and $S_2$ of the characteristic equation as follows:

$$\left.\begin{aligned} A &= \mathrm{Im}\left\{\frac{S_1P_2 - S_2P_1}{S_1 - S_2}\right\}, \quad B = \mathrm{Im}\left\{\frac{P_2 - P_1}{S_1 - S_2}\right\} \\ C &= \mathrm{Im}\left\{\frac{S_1Q_2 - S_2Q_1}{S_1 - S_2}\right\}, \quad E = \mathrm{Im}\left\{\frac{Q_2 - Q_1}{S_1 - S_2}\right\} \end{aligned}\right\} \tag{10}$$

Where

$$\left.\begin{aligned} P_1 &= a_{11}S_1^2 + a_{12} & P_2 &= a_{11}S_2^2 + a_{12} \\ Q_1 &= \frac{a_{12}S_1^2 + a_{22}}{S_1} & Q_2 &= \frac{a_{12}S_2^2 + a_{22}}{S_2} \end{aligned}\right. \tag{11}$$

The values of $a_{ij}$ used in the experiments are tabulated below.

| T300/5208 included angle α | $a_{ij}\ [10^{-7}]\ psi^{-1}$ | | | |
|---|---|---|---|---|
| | $a_{11}$ | $a_{12}$ | $a_{22}$ | $a_{66}$ |
| 30° | 48.7 | -23.4 | 3.20 | 6.45 |
| 45° | 60.3 | -43.0 | 2.96 | 4.74 |
| 60° | 82.1 | -65.2 | 2.60 | 3.73 |

TABLE I. Elastic compliances of T300/5208 cross-ply angles.

The characteristic equation, for the symmetric case used in our tests is,

$$a_{11}S^4 + (2a_{12} + a_{66})\,S^2 + a_{22} = 0 \qquad (12)$$

Using the coefficients $a_{ij}$ from Table 1 we obtain the following complex roots:

| α | $S_1$ | $S_2$ |
|---|---|---|
| 30° | .75 i | 3.42 i |
| 45° | .94 i | 2.36 i |
| 60° | 1.7 + .52 i | -1.7 - .52 i |

TABLE II. The roots of Eq. (12).

The values of $K_1$ and $K_2$ are obtained from the inversion of Eq. (9) where $(D_x, D_y)$ are evaluated at incipient fracture. Results are plotted in Fig. 8. The data is grouped along a preferred direction but there is considerable scatter so that stress intensity factor does not appear to be a satisfactory parameter for data reduction.

The J Integral Vector

The two components of the energy release rate Jx and Jy in a form of path independent integrals, elaborated and profounded by Budiansky and Rice [10], are applicable to homogeneous bodies which can be anisotropic and nonlinear in general. Their values represent the amount of the potential energy which would be relaxed when a traction free crack would extend (differentially) in the x and y directions respectively. The integrals to be evaluated counterclockwise along arbitrary contour $\Gamma$ surrounding the notch are [10]:

$$J_x = \int_\Gamma (\omega_{n_x} - T_i \, \partial u_i/\partial_x)ds$$
$$J_y = \int_\Gamma (\omega_{n_y} - T_i \, \partial u_i/\partial_y)ds. \qquad (13)$$

$\omega$ is the strain energy density (i.e., $\int \sigma_{ij} d\varepsilon_{ij}$), $T_i$ is the traction vector on $\Gamma$ (i.e., $T_i = \sigma_{ij} n_j$) and ds is an element of the path $\Gamma$. $J_x$ and $J_y$ are evaluated numerically by Eq. (13) at incipient fracture. The results for the various cross-ply laminates in Jx, Jy plane are shown in Fig. 9. The data points align themselves along straight lines, each line for each cross-ply angle. Thus the distinction between the fracture properties of different cross-ply angles (and probably between different composites as well) is reduced to just <u>two parameters</u> as for example the slope of the line and the value of Jx at the intersection with Jy = 0 line. This last parameter (Jx value at Jy = 0) is strictly the critical strain energy release rate $G_{Ic}$ for a notch which extends colinearly.

<u>Failure Criteria for Adhesive Joints</u>

Initial fracture studies have been completed for adhesive joint specimens of rubber-modified epoxy bonded to an aluminum plate. Specimens were 1.5" in length, 1.0" wide and 0.1" thick with 0.75" long x 1.0" wide epoxy plates cast and cured along a 0.1" x 1.0" side against a similar aluminum plate. Aluminum plates were milled and etched prior to casting of the epoxy. A notch was machined along the bond line with a 0.050" thick diamond wheel to a depth of 0.6". A razor blade was then used to initiate a small crack near the epoxy-aluminum interface. Specimens were

placed in the in-plane loading system previously described, and a range of in-plane displacements were applied to the specimens. The failure surface shown in Fig. 11 is based on fracture initiation for those specimens which exhibited brittle behavior and onset of significant plastic flow for those which exhibited ductile behavior, i.e., general yielding of the resin along the entire bond line as opposed to localized yielding near the crack tip. A brittle to ductile transition was observed as the proportion of shear loading to tension loading increased. In cases of high tension loading relative to shear or bending, it was observed that the initial crack grew away from the interface into the epoxy, whereas for increasing proportion of shear loading to tension loading, failure occurred near the interface. [11], [12].

## FUTURE WORK

1. The fracture characterization of the T300/5208 graphite/epoxy cross-ply laminates under a broad range of in-plane loads will be completed at room temperatures.

2. The validity of the failure criteria determined in predicting defect growth will be demonstrated in a sub-component test, using a box beam.

3. Fracture characteristics will be determined at room temperature and elevated temperature for graphite composites made with several high temperature resins.

4. The fracture characteristics will be determined for adhesive bonded joints under a broad range of in-plane loads and the validity of the failure criteria demonstrated in sub-component tests.

## REFERENCES


1. Mandell, J. F., McGarry, E. J., Wang, S. S. and Im. J., "Stress Intensity Factors for Anisotropic Fracture Test Specimens of Several Geometries," J. Composite Materials, Vol. 8, (1974), pp. 106-116.

2. Phillips, D. C., "The Fracture Mechanics of Carbon Fibre Laminates," J. Composite Materials, Vol. 8, (1974), pp. 130-141.

3. Wu, E. M. and Reuter, R. C., "Crack Extension in Fiberglass Reinforced Plastics," University of Illinois TAM Report No. 275, (1965).

4. Sih, G. C., Chen, E. P., Huang, S. L. and McQuillen, E. J., "Material Characterization on the Fracture of Filament-Reinforced Composites," J. Composite Materials, Vol. 9, (1975), pp. 167-185.

5. Tirosh, J., "The Effect of Plasticity and Crack Blunting on the Stress Distribution in Orthotropic Composite Materials," J. Appl. Mech., Vol. 40, (1973), pp.785-790.

6. Konish, H. J., Jr., Swedlow, J. L. and Cruse, T. A., "Fracture Phenomena in Advanced Fiber Composite Materials," AIAA Journal, Vol. 11, (1973), pp. 40-43.

7. Wu, E. M. and Jerina, K. L., "Computer Aided Mechanical Testing of Composites," Materials Research and Standards, MTRSTA, Vol. 12, (1972), pp. 13-18.

8. Beaubien, L., "TOTAL," Two Dimensional Orthotropic Time Sharing Analysis Library, "Structural Mechanics Software Series," Vol. I, University of Virginia Press (in press).

9. Sih, G. C. and Leibowitz, H., "Mathematical Theories of Brittle Fracture," Fracture, Vol. II, Chapter II, (H. Leibowitz, ed.), Academic Press (1969) pp. 67-190.

10. Budiansky, B. and Rice, J. R., Conservation Laws and Energy Release Rates, J. Appl. Mech. Vol. 40, (1973), pp. 201-203.

11. Mulville, D. R. and Vaishnav, R. N., "Interfacial Crack Propagation," J. Adhesion, 1975, Vol. 7, pp. 215-233.

12. Bascom, W. D., Timmons, C. O. and Jones, R. L, J. Materials Sci., 10, 1037 (1975).

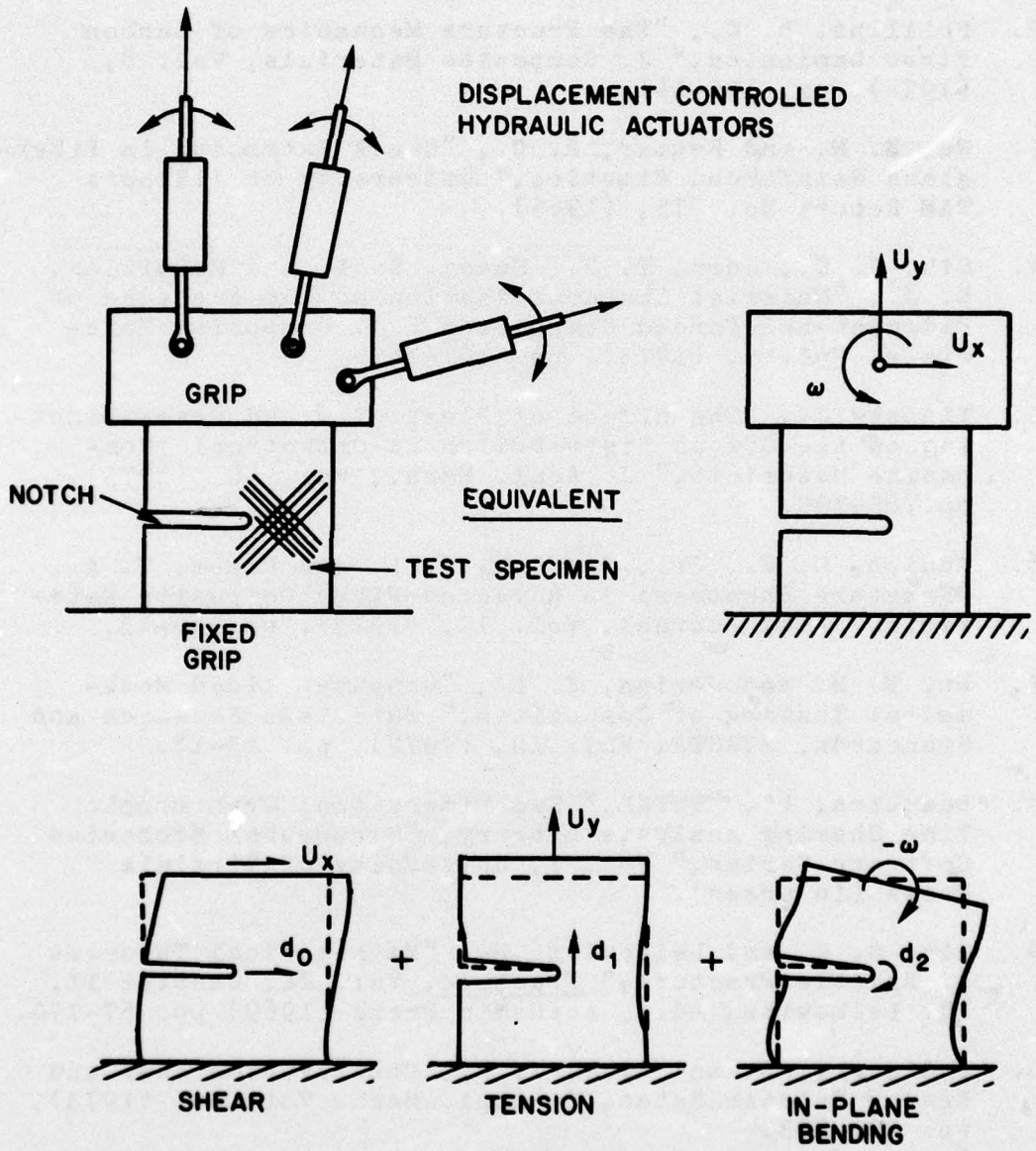


Fig. 1 — Loading conditions produced by in-plane loaders

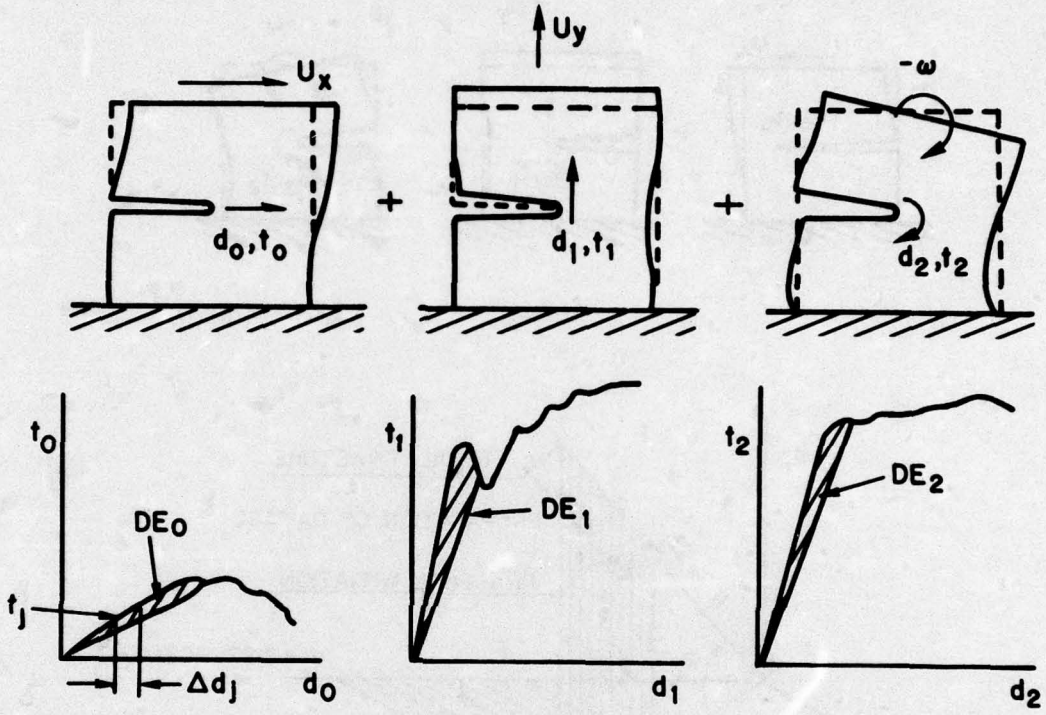


$$DE_i = \frac{1}{2}\left\{\left[\sum_{j=0}^{n} t_j \, \Delta d_j\right] - \left[d_j \, t_j\right]\right\} \qquad \begin{matrix} i = 0,1,2 \\ j = 1,2,\ldots n \end{matrix}$$

$$DE = DE_0 + DE_1 + DE_2$$

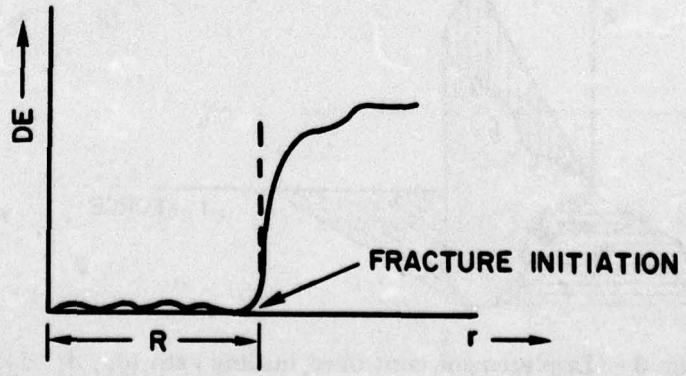


Fig. 2 — Dissipative energy of composites under in-plane loads

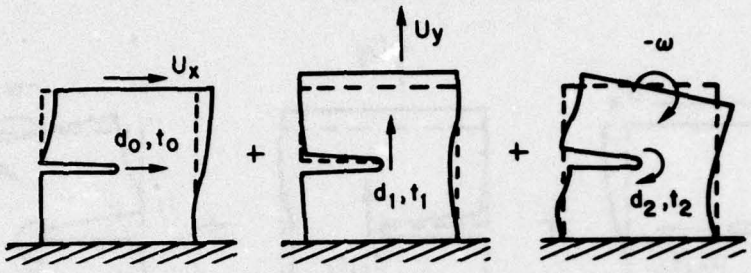


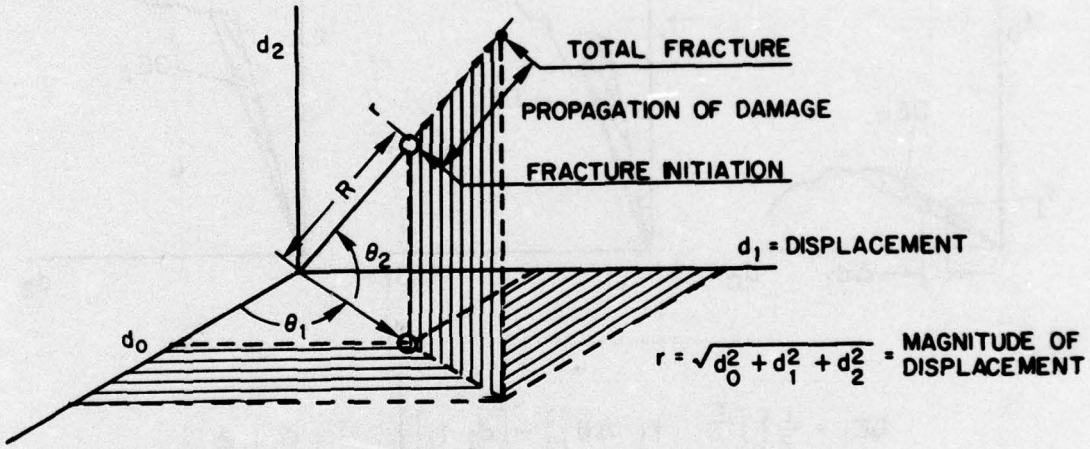


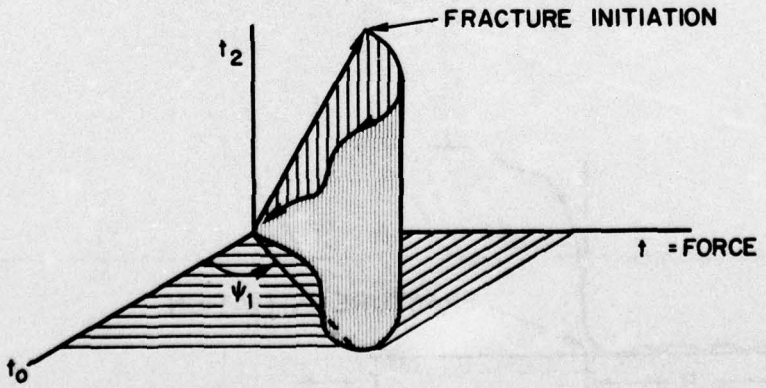


Fig. 3 — Displacement controlled loading path ($d_0$, $d_1$, $d_2$) and the associated force path ($t_0$, $t_1$, $t_2$)

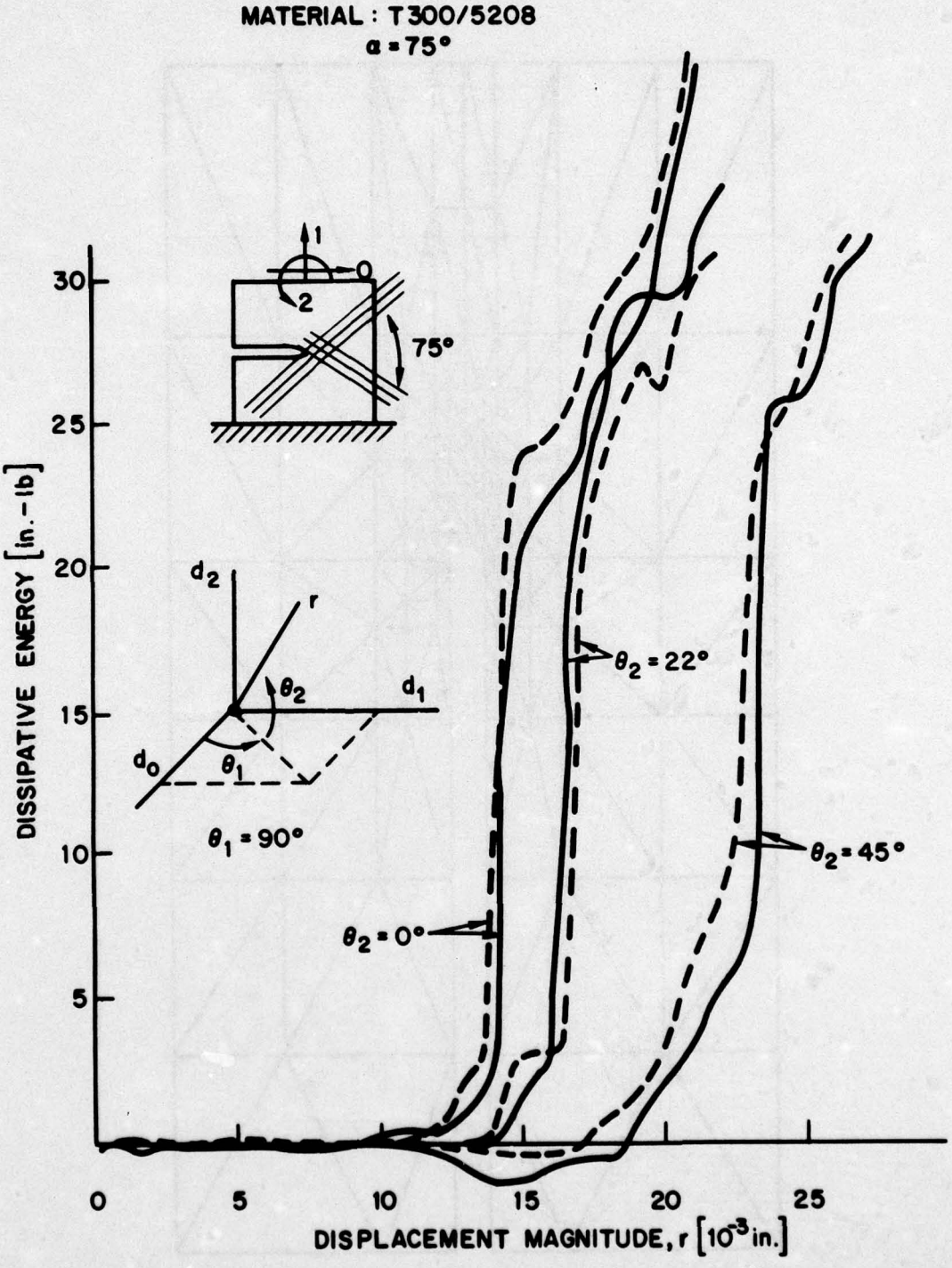


Fig. 4 — Reproducibility of fracture initiation for three different loading paths

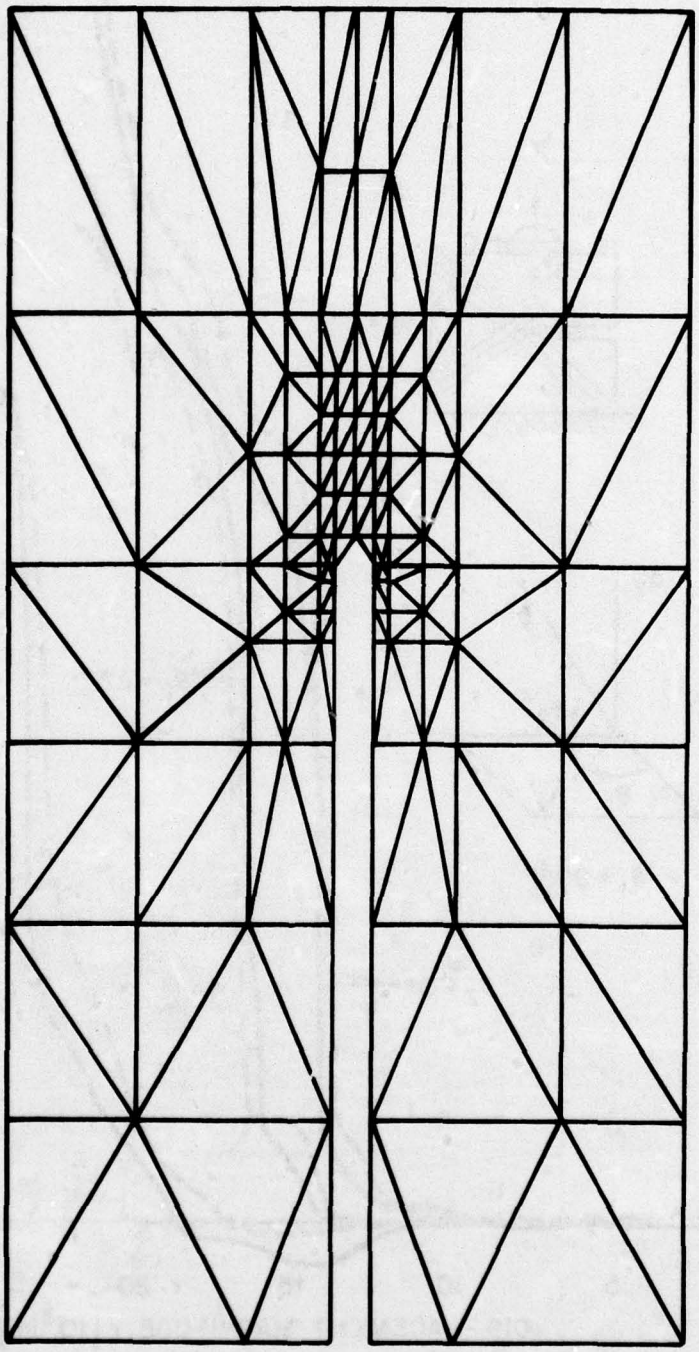

Fig. 5 — Finite element mesh used for stress analysis of composite specimens at fracture initiation

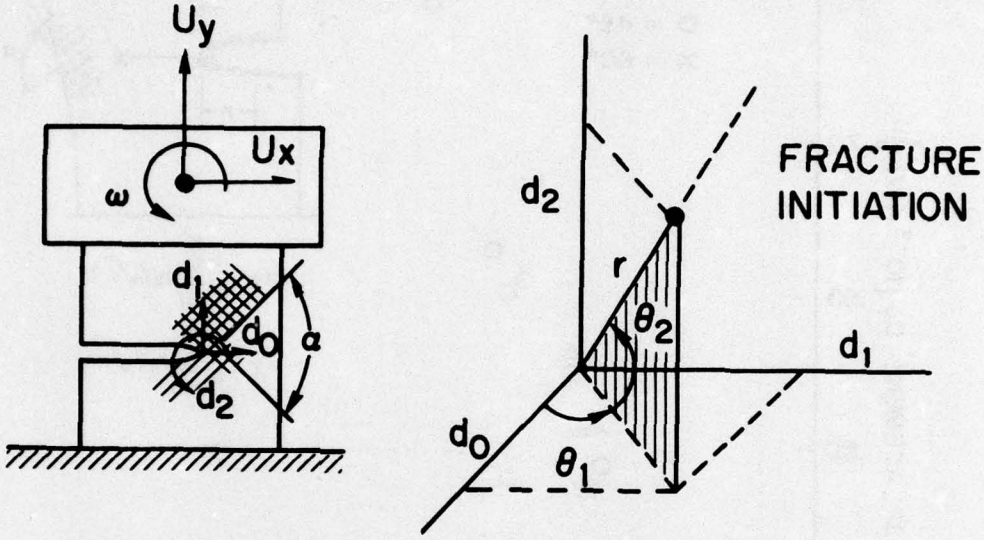


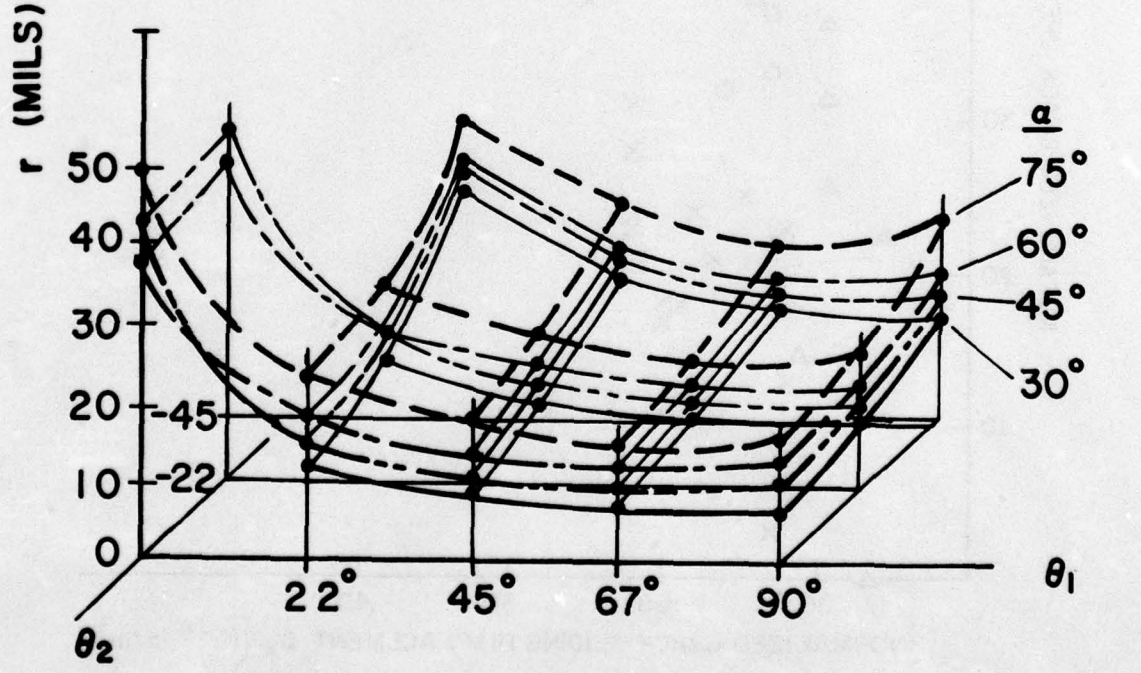


Fig. 6 — Failure surfaces for Thornel 300/5208 composite for several angles of lay-up

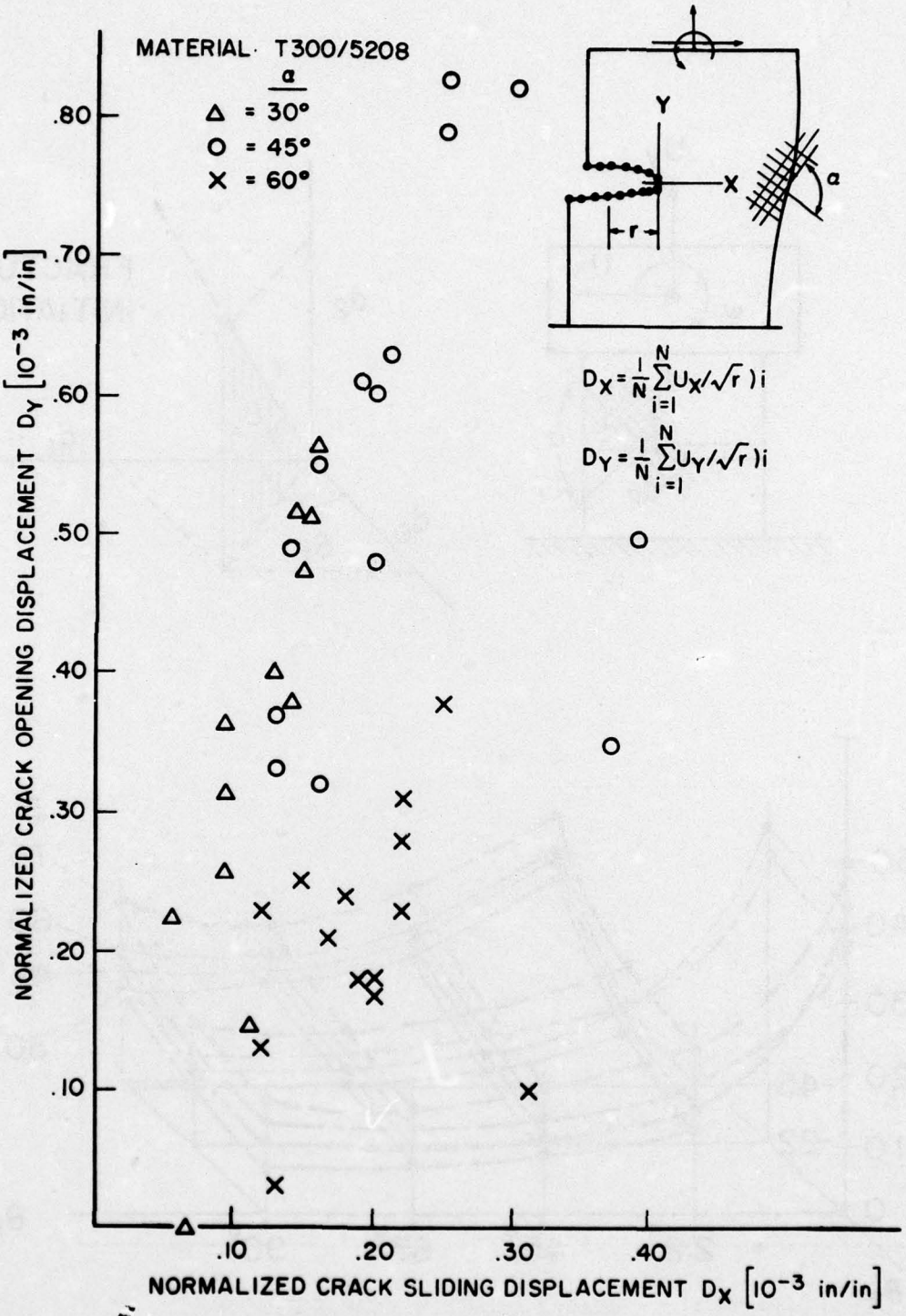


Fig. 7 — Crack opening displacement criterion for Thornel 300/5208 composite

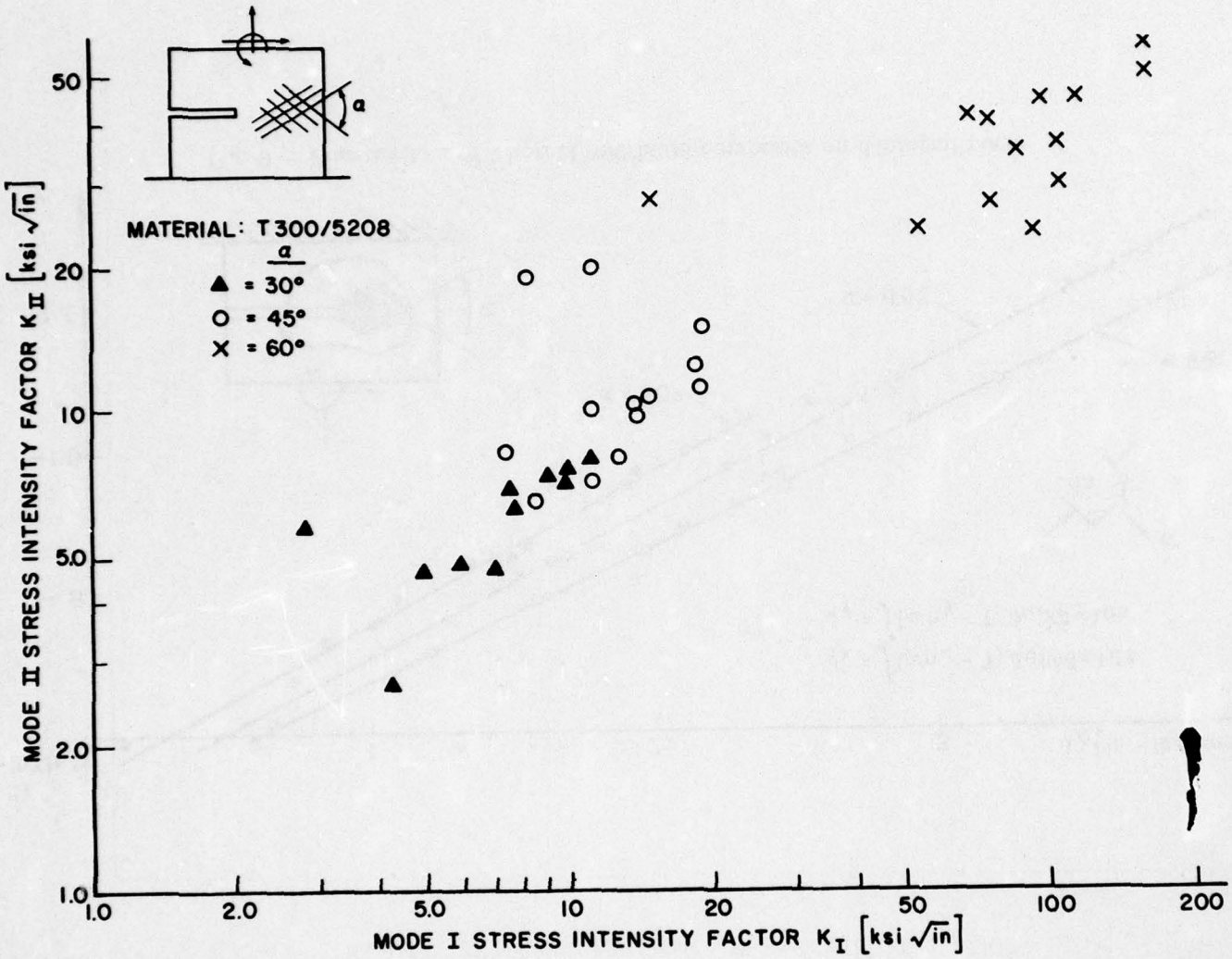


Fig. 8 — Stress intensity factor criterion for Thornel 300/5208 composite

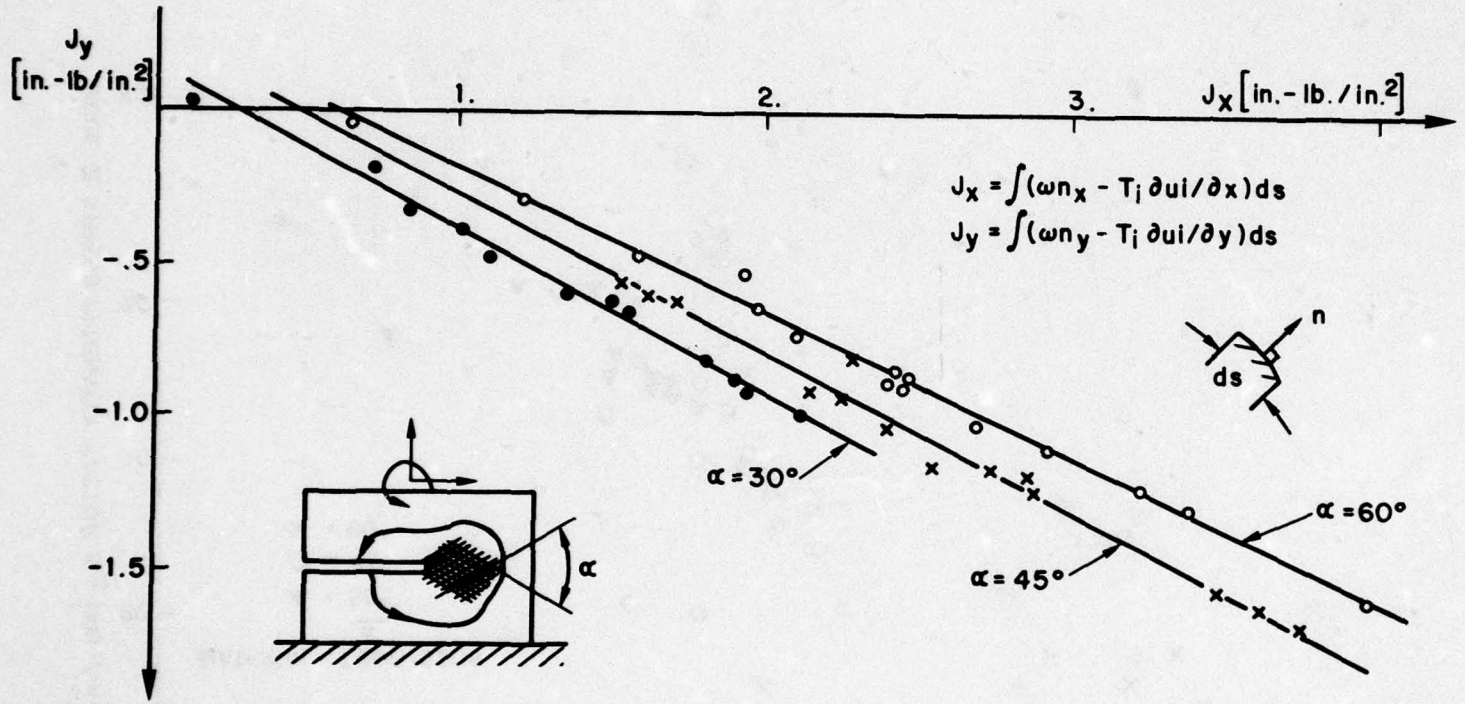


Fig. 9 — Fracture loci of Thornel 300/5208 composite on J-integral plane

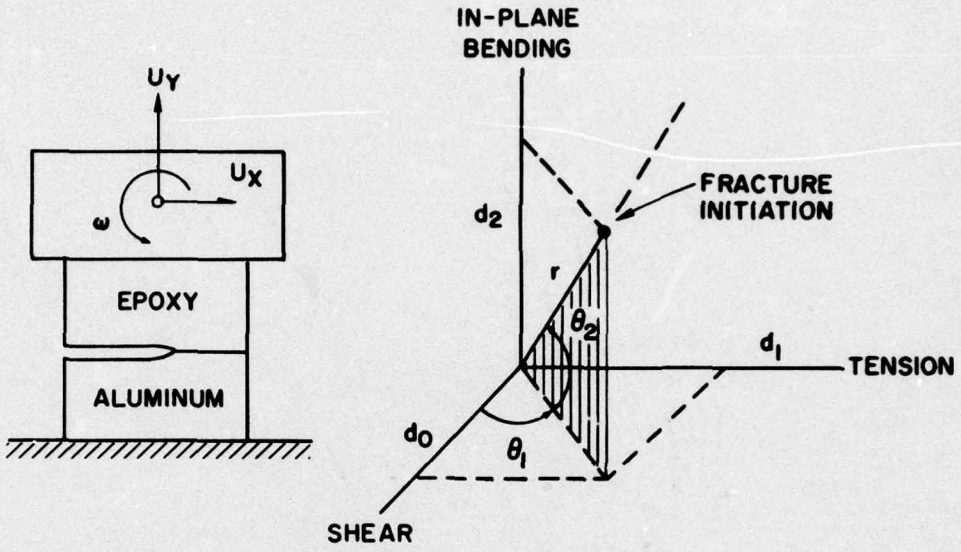


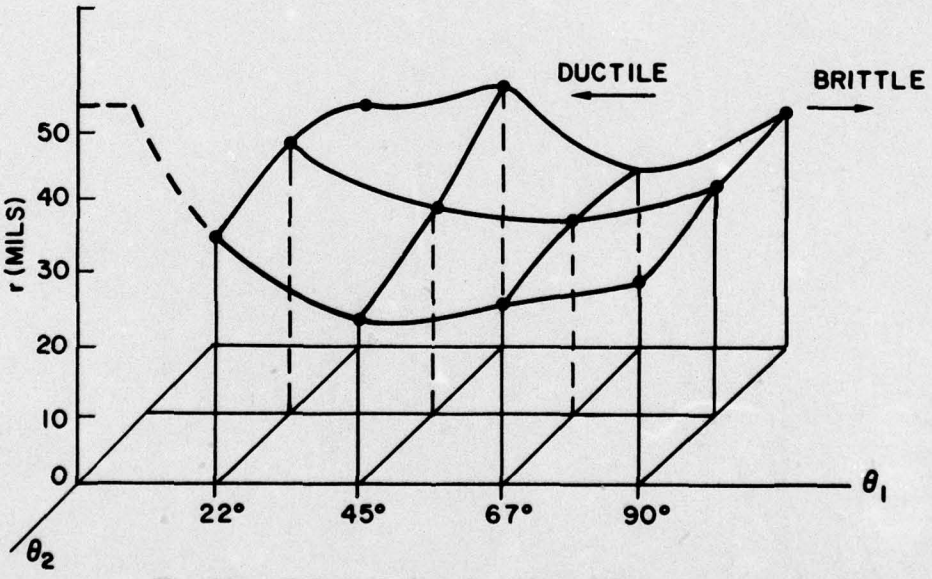


Fig. 10 — Failure surface for Al/modified-epoxy bonded joints